ADS-B and Mode S Data for Aviation Meteorology and Aircraft Performance Modelling

Master of Science Thesis - Aerospace Engineering

Q.H. Vû

Delft University of Technology

TU Delft Delft University of Technology

Cover page: FlightRadar24 with wind barbs

ADS-B and Mode S Data for Aviation Meteorology and Aircraft Performance Modelling

Master of Science Thesis

For obtaining the degree of Master of Science in Aerospace Engineering
at Delft University of Technology

Q.H. Vû

October 1, 2018

Faculty of Aerospace Engineering · Delft University of Technology

Delft University of Technology

Delft University Of Technology
Department Of
Control and Simulation

The undersigned hereby certify that they have read and recommend to the Faculty of Aerospace Engineering for acceptance a thesis entitled **"ADS-B and Mode S Data for Aviation Meteorology and Aircraft Performance Modelling"** by **Q.H. Vû** in partial fulfillment of the requirements for the degree of **Master of Science**.

Dated: October 1, 2018

Readers:

Prof.dr.ir. J.M. Hoekstra

Dr.ir. J. Ellerbroek

J. Sun, MSc.

Dr.ir. C.J. Simao Ferreira

Contents

List of Figures

List of Tables

List of Abbreviations

AC	Altitude code
ACARS	Aircraft Communications Addressing and Reporting System
ADS-B	Automatic Dependent Surveillance - Broadcast
AMDAR	Aircraft Meteorological Data Relay
AP	Address parity
ASAS	Airborne Separation Assurance Systems
ATC	Air Traffic Control
ATM	Air Traffic Management
BDS	Comm-B Data Selector
CAS	Calibrated airspeed
DAP	Downlink Aircraft Parameters
DF	Downlink formats
DP	Data parity
DR	Downlink request
EAS	Equivalent airspeed
ECMWF	European Centre for Medium-Range Weather Forecasts
EHS	Enhanced Surveillance
ELS	Elementary Surveillance
FAA	Federal Aviation Administration
FS	Flight status
GFS	Global Forecast System
GNSS	Global Navigation Satellite System
GS	Ground speed
IAS	Indicated airspeed
IC	Interrogator code
ICAO	International Civil Aviation Organization
ID	Identity code
II	Interrogator identifier
ISA	International Standard Atmosphere
KNMI	Royal Netherlands Meteorological Institute
LVNL	Air Traffic Control the Netherlands
METAR	Meteorological Aerodrome Report
MRAR	Meteorological Routine Air Report
NWP	Numerical Weather Prediction

PI Interrogator parity
PR Primary Surveillance Radar
PRT Pulse repetition frequencies
RR Reply request
RRS Reply request subfield
SI Surveillance identifier
SLS Sidelobe suppression
SSR Secondary Surveillance Radar
TAS True airspeed
UM Utility message

Part I

Scientific Paper

ADS-B and Mode S Data for Aviation Meteorology and Aircraft Performance Modelling

Huy Vû, Junzi Sun, Joost Ellerbroek, Jacco Hoekstra
Control and Simulation, Faculty of Aerospace Engineering
Delft University of Technology, Delft, The Netherlands

***Abstract*—With the increase in air traffic volume, aircraft are required to be equipped with a transponder by aviation authorities to increase the surveillance in air traffic control. These transponders transmit periodically Automatic Dependent Surveillance-Broadcast (ADS-B) signals and by interrogation the Mode S signals. These signals can be received by anyone with a simple receiver and are a new source for aviation research. It contains flight trajectories and aircraft states which were previously only available for air traffic control and aircraft operators. This paper uses ADS-B and Mode S data to derive an accurate meteorological model and uses this model to determine aircraft performance parameters, which are usually not publicly available. A Meteo-Particle model is used and validated with the European Centre for Medium-Range Weather Forecasts (ECMWF) model. For wind speed, wind direction and temperature the mean absolute error are 2.73 m/s, 7.73 degrees and 1.32 K respectively. The true airspeed is the actual airspeed that the aircraft experiences. It is required to determine aircraft performances. The true airspeed can be obtained with the wind derived in the Meteo-Particle model and ADS-B ground speed. Using the true airspeed information, aircraft performance parameters for climb, cruise and descend phase are determined for 16 aircraft types. These derived aircraft performance parameters, based on a large quantity of ADS-B and Mode S data, are a good alternative to the close-sourced performance parameters.**

I. Introduction

Air traffic has increased over the past years, Airbus and Boeing are expecting a growth in air traffic of almost five percent per year for the coming twenty years [1], [2]. To increase efficiency in Air Traffic Management (ATM), EUROCONTROL and the Federal Aviation Administration (FAA) have set up the programs SESAR and NextGen respectively. To increase surveillance, all commercial aircraft are required to have transponders onboard in Europe and the United States by 2020 [3], [4]. With the transponder, aircraft can transmit information, periodically via Automatic Dependent Surveillance - Broadcast (ADS-B) or on request (interrogation) by Air Traffic Control (ATC) with the Secondary Surveillance Radar (SSR) via Mode A/C/S. ADS-B is nowadays already implemented in the majority of aircraft. Via ADS-B, position, altitude, ground speed, heading and vertical velocity are broadcasted. Via Mode S (selective), the SSR can interrogate Downlink Aircraft Parameters (DAP) from individual aircraft [5]. These DAPs contain, for example, aircraft state and intent data, which are part of Mode S Enhanced Surveillance (EHS). It is also possible to obtain direct weather information measured on-board of an aircraft via Mode S Meteorological Routine Air Report (MRAR).

ADS-B and Mode S signals transmitted by aircraft can be received by everyone within line-of-sight with low-cost hardware receivers and can, therefore, be considered as 'open data' [6]. Popular online flight trackers, like *FlightRadar24* and *FlightAware*, use these signals to show real-time aircraft location and related information. In this paper, for decoding ADS-B and Mode S signals, the Python library *pyModeS* [7] is used and further developed.

Since aircraft performance parameters are usually kept confidential by aircraft manufacturers and airlines, the goal of this paper is to improve aircraft performance modelling parameters, that already have been obtained in earlier research for the *BlueSky* open air traffic simulator [8]. The goal is to use additional Mode S data to construct a meteorological model, as well as using the results to derive the true airspeed of aircraft.

The remainder of this paper is structured as follows: section II presents previous research, followed by an explanation and decoding of ADS-B and Mode S signals in section III. In section IV, meteorological derivations will be shown, the usage of a Meteo-Particle model and how aircraft performance parameters can be obtained. In section V, the results and validations of section IV are shown. The paper concludes with a discussion and conclusion in sections VI and VII.

II. Background

To improve efficiency in air traffic and to reduce emission by aircraft, accurate trajectory predictions are required. For these predictions, meteorological conditions (wind and temperature), aircraft performance (weight and thrust, aerodynamics) and navigation performance (aircraft intent, pilot skills) are important variables [9], [10]. Ground speed and cumulative along-track errors can occur when no accurate wind estimations are available [9].

A. Aircraft Performance Parameters from ADS-B

For the *BlueSky* open air traffic simulator [8], developed by C&S/ATM department of the Aerospace Engineering of the Delft University of Technology, previously ADS-B data has been used to build a database with aircraft performance parameters.

Sun [11] extracted a set of more than thirty aircraft performance parameters from seven distinct flight phases for common commercial aircraft. Using machine learning methods, it is possible to identify flight phases [12] and to extract relevant properties in ADS-B data. All parametric models were

combined to describe a complete flight that includes take-off, initial climb, climb, cruise, descent, final approach and landing. However, wind effects are ignored in this research [11]. In [13], meteorological data from the Global Forecast System is integrated to estimate the true airspeed of an aircraft at any given location.

The lift, thrust, fuel consumption and climb/descent rates are influenced by the aircraft mass. ADS-B data was used by Sun et al. [14] to infer the mass of an aircraft during its take-off phase with two methods. Aggregated Meteorological Aerodrome Report (METAR) data at observed airports and ground speed is used to estimate the true airspeed of aircraft during take-off.

Gloudemans [15] used ADS-B data to determine the operational flight envelope (operational limits like maximum altitude, minimum and maximum rate of climbs and minimum turn radius) and obtained estimations for lift and drag coefficients for seven flight phases. However, in this research, strong assumptions were made in terms of wind and flight strategies. In the end, the true airspeed was set equal to the ground speed.

B. Obtaining meteorological conditions

In the research listed above, true airspeed is ignored or estimated with additional data sources. There are different methods to obtain meteorological conditions. The first method is using a numerical weather prediction (NWP) model, which uses mathematical models to predict weather based on current conditions (data from satellites, ground stations, weather balloons, etc.). Starting with current conditions, a forecast is generated by integration in time. Two commonly used global NWP models are the United States' National Weather Service Global Forecast System (GFS) and the European Centre for Medium-Range Weather Forecasts (ECMWF).

The second method uses the aircraft as a 'meteorological sensor'. The Aircraft Meteorological Data Relay (AMDAR) system is reporting meteorological information to ground stations via the Aircraft Communications Addressing and Reporting System (ACARS). However, this information is not publicly available. The frequency of AMDAR observations depends on the flight phase (climb, level or descent) [16] and therefore has a typical resolution of few tens of kilometers [17]. In AMDAR, data from different aircraft sensors are smoothed over a period of ten seconds during climb/descent phase and 30 seconds during level flight above FL200. Smoothing is applied to ensure consistency between observations from different sensors and different onboard computer systems [16].

In Mode S Enhanced Surveillance (EHS), selected altitude, indicated airspeed, roll/track angle/rate and airspeeds are transmitted. With this information, it is possible to derive the wind vector (speed and direction) and temperature information by using atmospheric relationships. Mode S can also contain direct meteorological observations (wind, temperature and humidity) in Meteorological Routine Air Report (MRAR), which is publicly available like other Mode S signals, in contrast to AMDAR. Despite information for AMDAR and Mode S are coming from the same instruments, Mode S has a much higher frequency because it is transmitted upon interrogation, which is only limited by the rotation frequency of the SSR.

The third method to obtain wind is using aircraft track/flight information to derive meteorological information. This information is available from the primary radar or from ADS-B data, which contain aircraft's position information (latitude, longitude and altitude), ground speed and track angle.

The fourth and last method uses radiosondes or weather balloons. Radiosondes are equipped with a temperature sensor and humidity sensor. To determine the geopotential altitude, a pressure sensor and/or GPS receiver is used. The wind speed is derived from the ground track of the balloon during its climb.

C. Meteorological conditions from Mode S

1) Mode S Enhanced Surveillance: De Haan from the Royal Netherlands Meteorological Institute (KNMI) conducted a lot of research on Mode S EHS meteorological observations between 2009 and 2014 [18], [19], [20], [21], with data provided by the Air Traffic Control the Netherlands (LVNL) from the tracking and ranging (TAR) radar at Schiphol. In other researches, the KNMI [22] and the Meteorological Office (Met Office) [23] in the United Kingdom, used their own receivers to obtain ADS-B and Mode S signals.

To compute wind, it is important to have the true north heading instead of the magnetic heading for aircraft, so a heading correction is applied (declination) to Mode S data. De Haan concluded that after correction of the magnetic declination, aircraft still have a heading error of several degrees. An additional heading correction is determined with landing aircraft at Amsterdam Airport Schiphol, whereby the runway heading is used as a correction factor over a period of twelve months. The disadvantage of this method is that many aircraft are en-route over The Netherlands instead of landing. In 2013, an improved method for deriving wind and temperature was proposed [24]. For temperature within a certain flight phase, time-dependent and aircraft specific temperature corrections were applied. A lookup table with corrections was built with the differences between Mode S EHS derived temperature and NWP model temperature. An additional heading correction was determined by using additional wind information from an NWP model or AMDAR.

As mentioned by De Haan [20], the resolution of Mode S has an influence on the precision of the derived meteorological values. Mode S EHS reduces the precision of the state vector from 16-bit to 10-bit binary representation (quantization error). Mirza et al. [25] investigated the observation errors due to the reduced precision of Mode S EHS signals by comparing it to on-board measurements from a research aircraft.

2) Mode S Meteorological Routine Air report: Part of Mode S is MRAR and this register contains wind, temperature, static pressure, turbulence and humidity information. MRAR is not interrogated much by ATC in Europe. Only a few ATC organisations have been reported to interrogate this: by a radar at Ljubljana airport in Slovenia [17], [26], three Czech

radars, one German radar and one Slovakian radar [27]. In the Maastricht Upper Area Control (MUAC), only aircraft in range of Copenhagen ATC interrogated MRAR [28]. Since MRAR is not a mandatory Mode S register, MRAR messages are only sent by a small number of aircraft and these do not or barely include aircraft of Airbus and Boeing [17], [26], [27], [28].

D. Meteorological conditions from flight trajectories

Meteorological parameters can also be obtained from flight trajectories. Hollister et al. [29] proposed a method to derive wind speed from aircraft tracks during a turn. Delahaye [30] used the same method including downlinked true airspeed data to estimate wind. When onboard true airspeed measurements are available, wind estimations are obtained from a linear model solved with a Kalman filter. However, when only aircraft tracks are available, wind is estimated from one or two turns, depending on the number of aircraft in a certain airspace. In case one track is available, wind is derived after two asymmetric turns (three straight lines separated by two turns). When two aircraft are available, one turn of both trajectories is enough to estimate wind. Finally, vector spline interpolations are used to generate wind maps from these local wind estimations.

Hurter et al. [31] used aircraft trajectories of aircraft flying in different directions to estimate the wind speed and direction with a least squares approximation. The idea is that when ground speeds are plotted from equal aircraft sizes, sinusoidal shapes will emerge, which is a result of wind. For location, head and tailwind will have a phase difference of 180 degrees in a sine. The wind direction can be obtained from the sine angle shift (headwind results in a lower ground speed) and wind direction from the amplitude.

ADS-B contains similar data as primary radar data. De Leege et al. [22] used ADS-B data for estimating wind, air pressure and temperature. From single or multiple aircraft, the ground speed vector information was used. The wind is recursively estimated, using a modified Kalman filter, from an aircraft in a turn, assuming that the aircraft flies at a constant altitude with constant true airspeed. With a constant wind vector, this results in a non-linear least-square problem that is solved using an extended Kalman filter. Pressure is estimated by the difference between the pressure altitude and the GNSS altitude. The temperature can then be assumed from the International Standard Atmosphere.

III. ADS-B and Mode S data

Nowadays air traffic surveillance is done with a Primary Surveillance Radar (PR) and a Secondary Surveillance Radar (SSR). A primary radar works with passive echoes: the radar transmits an electromagnetic wave and measures the direction and the time between the transmitted and the reflected signal from aircraft. Primary radars determine the presence, slant distance and azimuth of aircraft, but are not able to obtain the identity.

A. Automatic Dependent Surveillance-Broadcast

An alternative for the primary radar is ADS-B. ADS-B is a technology in which an aircraft periodically transmits its position, ground speed, altitude, vertical speed and call-sign, as well as other status parameters.

B. Mode S

To obtain the identity of the aircraft, the SSR is used. The SSR is a cooperative surveillance method, which requires aircraft to be equipped with a transponder (transmitter and responder). In contrast to the SSR, the PR is no-cooperative (independent) and does not require the installation of aircraft transponders. The SSR can interrogate aircraft by three modes: Mode A for the identity code (squawk code), Mode C for altitude code and Mode S. In Mode S, the SSR selectively interrogates an aircraft by its 24-bit ICAO address and requests aircraft downlink parameters.

Mode S replies from aircraft are downlinked using frequency 1090 MHz. Below, the format of the Mode S reply is shown. The first field contains the downlink format (DF). For Mode S, DF20 and DF21 are used. The flight status (FS) indicates whether the aircraft is airborne or on-ground, indicates if the squawk code has changed or on request of ATC a special position indication (SPI). The downlink request (DR) and utility message (UM) contain downlink information and transponder communication status. In the following 13 bits, the encoded pressure altitude (AC) is included in DF20 and the identity code (ID) is included in DF21. The message field (MB) is a 56-bit field that contains the downlinked aircraft parameters. The last 24 bits contain an overlaid parity that can be used to check whether the signal contains transmission errors. This parity contains (partly) the ICAO address of the aircraft.

Number of bits	5	3	5	6	13	56	24
Content	DF	FS	DR	UM	AC/ID	MB	AP/DP

The Mode S transponder can maintain 255 different 56-bit wide Comm-B Data Selector (BDS) registers that can be interrogated by ATC [32]. These BDS registers contain a variety of aircraft states and intent information, as well as Airborne Separation Assurance Systems (ASAS), and is transmitted in the message field of the signal. BDS registers will be updated with a minimum interval specified in the *Technical Provisions for Mode S Services and Extended Squitter* (ICAO Doc 9871 [33]) and will be cleared by the transponder if the register is not updated within this interval. BDS registers are indicated by two hexadecimal characters. Commonly interrogated BDS registers and its content are shown in table I. BDS register 1,0, 1,7, 2,0 and 3,0 are part of Mode S Elementary Surveillance (ELS). BDS register 4,0, 5,0 and 6,0 are part of Mode S Enhanced Surveillance (EHS).

All uplink and downlink signals contain an overlaid parity of 24 bits at the end. This parity is used to check whether the signal contains transmission errors. The parity is generated by a modulo-2 division of the message $M(x)$ by the generator

TABLE I
BDS REGISTERS AND CONTENT

BDS	Register	Content
1,0	Data link capability report	Transponder capability
1,7	GICB capability report	Supported Mode S registers
2,0	Aircraft identification	Call-sign
3,0	ACAS active resolution advisory	Resolution advisories
4,0	Selected vertical intention	Selected altitude Barometric pressure setting
4,4	Meteorological routine air report (MRAR)	Wind speed Wind direction Static air temperature Average static pressure Humidity
5,0	Track and turn report	Roll angle True track angle Ground speed Track angle rate True airspeed
6,0	Heading and speed report	Magnetic heading Indicated airspeed Mach number Vertical speed

$G(x)$ in equation 1. The parity $P(x)$ is overlaid by modulo-2 addition with additional information: the aircraft ICAO address (Address parity (AP)), AA field information (Data parity (DP)) or the interrogator code (IC) (Interrogator parity (PI)). Interrogator parity is only used for DF11 (all-call replies). DF20 and DF21 contain either an address parity or data parity, while all other downlink formats use address parity.

- In address parity, the parity is overlaid with the ICAO address of the aircraft.
- In data parity, a modulo-2 addition is applied with the most significant 8 bits of the ICAO address and the two characters of the BDS register. Hence, the first two hexadecimal characters will be changed in data parity and in the case of a correct signal, the last four characters should always result in the last four characters of the ICAO address.

The transmitted signal $T(x)$ will be $M(x)$ appended with the overlaid parity $P'(x)$ as shown in equation 2.

$$\begin{aligned} G(x) = {} & x^{24} + x^{23} + x^{22} + x^{21} + x^{20} + x^{19} \\ & + x^{18} + x^{17} + x^{16} + x^{15} + x^{14} \\ & + x^{13} + x^{12} + x^{10} + x^{3} + 1 \end{aligned} \tag{1}$$

$$\begin{aligned} P(x) &= M(x)/G(x) \\ P'(x) &= P(x) \oplus \{\text{ICAO, AA, IC}\} \\ T(x) &= M(x) + P'(x) \end{aligned} \tag{2}$$

C. Decoding Mode S signals

Decoding Mode S signals is a challenging task. Since the SSR knows which aircraft and which downlink parameters are interrogated, the Mode S reply does not contain this information. Unlike the SSR that knows which aircraft is interrogated and which parity is used, we do not know which aircraft is interrogated or whether the signal contains transmission errors. Except for BDS registers 1,0, 2,0 and 3,0, no information is included about which BDS register is included in the message field. Since the SSR interrogates for a specific BDS register, this would not be a problem for the SSR itself.

1) ICAO address retrieval: Since it is not known whether address parity or data parity is used in the signal, a signal without transmission errors shall result in a full ICAO address in case of address parity or the last four hexadecimal characters of the ICAO address in case of data parity.

Retrieval of the ICAO address is done as follows and is illustrated in figure 1.

1) The parity of the first 88 bits (without overlay) is calculated with the generator in equation 1.
2) A modulo-2 addition is applied on the parity with the last 24 bits of the received signal (the overlaid parity). This will result in the ICAO address or the modified AA field. This method is referred to as the 'reversed parity' in this paper.

When reversed parity is applied, this results in two cases:

- A possible ICAO address[1], and the signal is
  - correct
  - corrupt
- An impossible ICAO address, which indicates that the signal is
  - overlaid by data parity (last four hexadecimal characters should be correct)
  - corrupt

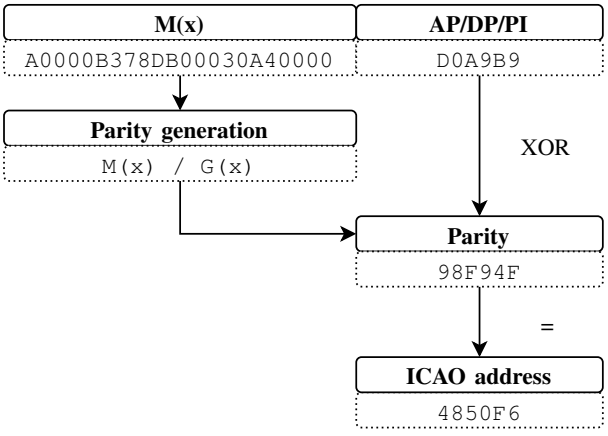

Fig. 1. ICAO address retrieval with reversed parity

2) Detecting the correctness of Mode S signals: A small error in the signal can result in another possible ICAO address. If, for example, a single bit flipped, the parity may result in a slightly different ICAO address. Since ICAO addresses are usually allocated in sequence (within the allocated country

[1]A possible ICAO address is defined when it is in a block of allocated addresses for countries (blocks in sizes of 2^{10}, 2^{12}, 2^{15}, 2^{18} or 2^{20} addresses) as stated in ICAO Annex 10 Aeronautical Telecommunications [32]

block), this error can result in an existing ICAO address of a subsequent aircraft. Checking an ICAO address with a list of ICAO addresses that occurred in ADS-B is because of this not reliable. The SSR expects a specific type of reply from a certain aircraft. Hence, the SSR can determine the correctness of Mode S signals. In this paper, it is not known which aircraft is interrogated. Another method will be used to check whether the signal contains errors.

a) The correctness of downlink format 21 signals: For determining the correctness of DF21 signals, the squawk code is used. For each squawk code, the ICAO addresses are linked which results in a list of addresses that are found for each squawk code. Addresses that occurs more than a certain time for a given squawk code are assumed to be correct. Once the correct ICAO address is known for a given squawk code, it is possible to correct slightly different ICAO addresses for this squawk code to the correct address[2]. When the correct ICAO address is known, error correction can be applied for corrupt signals, but this will not be considered in this paper. In this paper, only signals will be used that are overlaid by address parity. This is because for data parity it cannot be determined whether the message is correct and also first the BDS register should be identified.

With this method, a list of airborne aircraft addresses will be built. This could be used to identify aircraft that do not transmit ADS-B signals. However, for meteorological derivations, the position of an aircraft is required. Therefore Mode S signals from aircraft that do not transmit ADS-B, cannot be used and will be discarded for analysis in this paper.

In The Netherlands, squawk codes 1000 (general code for IFR) and 7000 (general code for VFR) are not unique. Since squawk codes will be re-used/changed, the number of ICAO addresses per squawk code increases over time. With additional flight status information in the Mode S signal, it can be determined when an aircraft changes its squawk code.

b) The correctness of downlink format 20 signals: Determining the correctness signals with DF20 is more difficult than signals with DF21 since DF20 does not contain a unique parameter like the squawk code. DF20 contains the encoded pressure altitude, which is not unique. These signals are combined with ADS-B data that have the same ICAO address and same timestamp. The correctness of DF20 is determined by comparing the Mode S altitude with ADS-B altitude. If the difference is below a certain threshold, the message is considered as correct. This method is not possible for aircraft on-ground since an ADS-B ground message does not report altitude, while Mode S signals still contain the pressure altitude.

D. Mode S BDS register identification

To identify the BDS register, the following method is applied. Each BDS register has a specific format and contains status bits and content bits (and in some cases a sign bit, for example, for vertical rate). If the status bit is set to zero (register field not available), the sign bits and all content bits of that field should contain zeros. If the status bit is set to one, the content bits will contain a value. All reserved fields should contain zeros. After examining the status bits, it is possible that signals will match with multiple BDS registers with this approach. For example, except for the first two register fields in BDS 5,0 and BDS 6,0, other register fields have the status, sign and content bits on exactly the same position. To identify the most probable BDS register between BDS 5,0 and 6,0, a probabilistic approach is used.

1) BDS 4,0: In BDS 4,0 the selected MCP/FCU/FMS altitude and/or the barometric pressure setting is transmitted. Analysis with data from our receiver showed that if a signal is identified as BDS 4,0, it will be almost certain BDS 4,0, irrespectively matches with other BDS registers. However, a small additional check is applied. The modulo 100 is calculated of the MCP/FCU or FMS selected altitude. Modulo 100 is chosen because usually the selected altitude can be changed by increments of 100 ft or 1000 ft. Due to the Mode S resolution of the MCP/FCU or FMS selected altitude (which is 16 ft), precision errors can occur (for example, 33,008 ft instead of 33,000 ft). If the remainder is smaller than 8 ft or larger than 92 ft, it will be accepted as BDS 4,0. When MCP/FCU or FMS selective altitude is not available, a check is done on the barometric pressure setting (QNH, atmospheric pressure adjusted to mean sea level). If the barometric pressure setting is in range of 1013.25 ± 25 hPa, it will also be accepted as BDS 4,0. The barometric pressure setting ranges between 800 and 1210 hPa.

2) Probabilistic identification of BDS 5,0 and BDS 6,0: To identify whether BDS 5,0 or BDS 6,0 is included in Mode S, the ground speed in BDS 5,0 is decomposed in a V_x and V_y component with the track angle χ_g. For BDS 6,0, the Mach number is converted to true airspeed (with the international standard atmosphere) and decomposed in a V_x and V_y component with the magnetic heading χ_a (converted to true north). The difference between track angle and heading angle is usually small and can, therefore, be considered as comparable. Decomposing a vector into a west-east component V_x and a south-north component V_y with angle χ is done as in equations 3 and 4 respectively.

$$V_x = \boldsymbol{V} \sin(\chi) \tag{3}$$

$$V_y = \boldsymbol{V} \cos(\chi) \tag{4}$$

To identify the most likely BDS register between BDS 5,0 and BDS 6,0, a multivariate normal distribution $\mathcal{N}(\boldsymbol{\mu}, \boldsymbol{\Sigma})$ is used with the mean $\boldsymbol{\mu}$ (equation 5) and variance $\boldsymbol{\Sigma}$ (equation 6) of the decomposed ground speed vector from reference information (ADS-B).

$$\boldsymbol{\mu} = \begin{bmatrix} \mu_{V_x} & \mu_{V_y} \end{bmatrix} \tag{5}$$

Since there is no correlation assumed between V_x and V_y, the covariance matrix will be as given in equation 6 where $\sigma \in \mathbb{R}$.

[2]For example, if the first two characters of an ICAO address are different, it can be overlaid by data parity

$$\mathbf{\Sigma} = \begin{bmatrix} \sigma^2_{V_x} & 0 \\ 0 & \sigma^2_{V_y} \end{bmatrix} \tag{6}$$

The BDS register is identified by the highest probability density function as given in equation 7. An example probability density function of a signal that could be either BDS 5,0 or BDS 6,0 is shown in figure 2. In this figure, the cross indicates the decomposed ground speed from ADS-B. The decomposed ground speed of BDS 5,0 and BDS 6,0 are shown as dots. BDS 5,0 has the highest probability (closest to the reference value) and the signal is therefore identified as BDS 5,0.

$$f(\boldsymbol{x}) = \frac{1}{\sqrt{(2\pi)^k \det \mathbf{\Sigma}}} \exp\left(-\frac{1}{2}(\boldsymbol{x}-\boldsymbol{\mu})^T \mathbf{\Sigma}^{-1}(\boldsymbol{x}-\boldsymbol{\mu})\right) \tag{7}$$

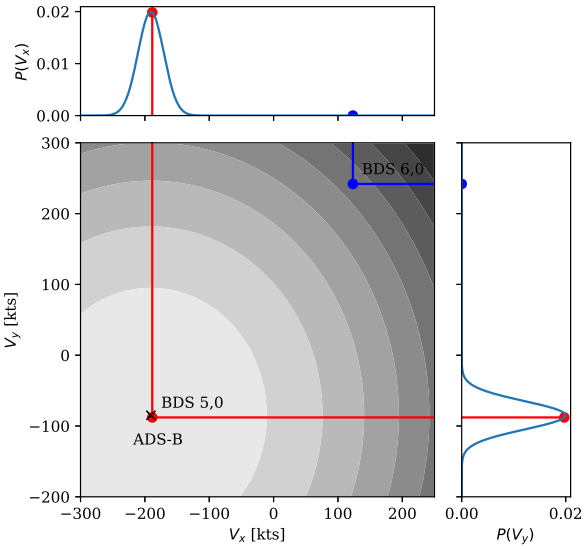

Fig. 2. Probability density function of a signal

E. ADS-B/Mode S receiver set-up & Statistics

At the Faculty of Aerospace Engineering at the Delft University of Technology, an ADS-B/Mode S receiver is installed. ADS-B and Mode S replies are logged from aircraft within line-of-sight, up to a distance of 400 km from aircraft at cruise altitude. In figure 3, a map is shown with the received Mode S signals (combined with ADS-B position) by this receiver on 5 January 2018. It can be seen that Mode S interrogations are very concentrated along flight paths and around airports (Amsterdam and Brussels). In total, 33.4 million Mode S signals are received, from which 19.6 million are linked with an ADS-B position. Signals without ADS-B positions are from aircraft without ADS-B or contain transmission errors. With the DF21 squawk code check, it turned out that 2 million signals are from aircraft that do not transmit ADS-B. The majority of these signals are received above the Netherlands, Belgium and the North Sea. In figure 4, a distribution per hour is shown with the total number of Mode S signals. Also, the number of signals that contain errors with the proposed error detection is also shown. The ratio of corrupted signals is 35%.

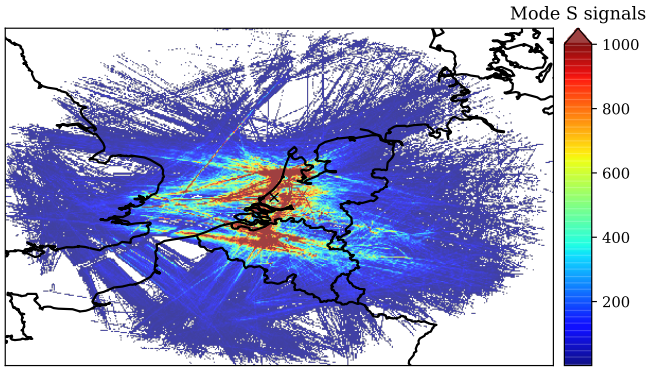

Fig. 3. Received Mode S signals on 5 January 2018

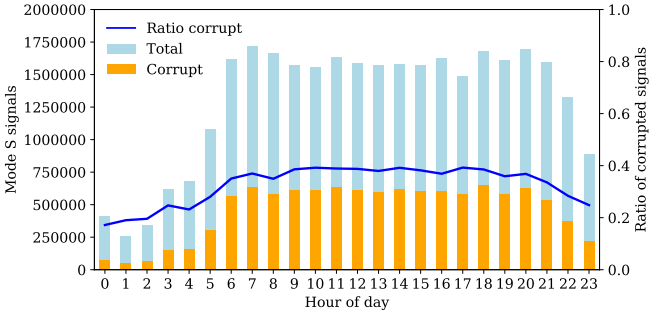

Fig. 4. Distribution of Mode S signals per hour on 5 January 2018

F. Modelling the Mode S magnetic heading bias

In Mode S signals, the magnetic heading is transmitted in the heading and speed report (BDS 6,0). Earlier researches with radar data from LVNL by De Haan [18], [24], showed that there is a deviation in the transmitted value of the magnetic heading due to outdated magnetic declination tables on-board. De Haan [18] used landing aircraft and runway headings to determine the magnetic deviation. In 2013, De Haan [24] proposed a method to determine the heading correction by using external wind data. However, this paper proposes an alternative, possibly more accurate approach.

The magnetic declination (variance) is the difference between the true north and the magnetic north, and is a function of time, latitude, longitude and altitude, which is illustrated in figure 5. The magnetic deviation is the error due to device measurement inaccuracies or local magnetic fields. Aircraft use magnetic declination look-up tables to convert the true heading from the inertial reference unit (IRU) to magnetic heading [34]. EASA Certification Specifications for Large Aeroplanes (CS-25 Amendment 12) states that acceptable accuracy values for the magnetic heading derived from true and magnetic declination tables are 3 degrees for latitudes between 60 °S and 70 °N.

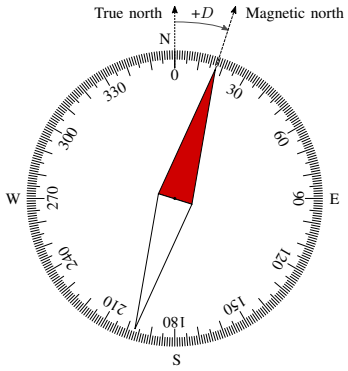

Fig. 5. Magnetic north = True north + Declination (D) + Deviation

In this paper, ADS-B and Mode S data from on-ground aircraft (taking-off, landing and taxiing) will be used to determine the magnetic deviation. Aircraft on-ground are not influenced by wind and therefore the heading of the aircraft will be equal to the ground track. The disadvantage of this approach is that only aircraft that have landed at an airport can be used for analysis.

Amsterdam Airport Schiphol is equipped with an Advanced Surface Movement Guidance & Control System (A-SMGCS) for surveillance, routing, guidance and control. As part of this system, an SSR (TAR-1 radar) has been installed at the airport to interrogate aircraft, including ground traffic (mainly for identification purposes).

For this analysis, an ADS-B/Mode S receiver has been installed at the Schiphol Group head office, with a clear view on runway 18C/36C. However, the receiver is capable of receiving signals from aircraft that are not in line-of-sight due to multipath effects. Mode S signals with a flight status indicating that the aircraft is on-ground and an ADS-B speed lower than 100 kts are used. This threshold is chosen because during landing, aircraft can experience crosswind and a heading correction is used to compensate for the drift while being on-ground. At speeds lower than 100 kts, it is assumed that the aircraft has aligned with the runway.

Due to the low resolution of ground track angle in ADS-B from on-ground aircraft (2.97 degrees), the track angle from ADS-B will not be used to determine the magnetic deviation. Instead, the true north track angle of the runways and taxiways will be used that is obtained from the Aeronautical Information Publication (AIP) published by LVNL [35].

A set of runways and taxiways from where Mode S signals are received is used with its true track angle. By converting the ADS-B position to a Cartesian reference system, the distance to each centerline of the runway/taxiway is calculated. The received Mode S signal is assigned to a runway/taxiway when the distance is less than 15 meters from the centerline and the ADS-B track angle is not more than 10 degrees different than the runway track angle.

Assuming that aircraft are aligned with the centerline, runway/taxiway track angles are used to derive the magnetic deviation in BDS 6,0. The transmitted track angle in BDS 5,0 and magnetic heading in BDS 6,0 have a resolution of 0.18 degrees (90/512 degrees), rounded to the nearest multiple. For comparison with the runway/taxiway track, the same resolution of 0.18 degrees is used, rounded to the nearest multiple.

IV. Modelling

A. Meteorological derivations

To obtain the actual air temperature, the Mach number and the true airspeed should be known. To determine the wind, the true airspeed vector and ground speed vector should be known. These parameters can be obtained from ADS-B and Mode S data. In table II, the relevant parameters from ADS-B and Mode S are shown for meteorological derivations. As shown in table II, parameters in ADS-B and BDS 5,0 are comparable, except that ADS-B contains position and altitude information. BDS 6,0 contains the magnetic heading and Mach number, which are essential in calculating wind and temperature.

TABLE II
USABLE INFORMATION FROM ADS-B AND MODE S

ADS-B	BDS 5,0	BDS 6,0
True track angle	True track angle	Magnetic heading
Ground speed	Ground speed	Indicated airspeed
Position (lat, lon)	True airspeed	Mach number
Pressure altitude		

1) Air pressure and air density: With the pressure altitude from ADS-B, the local air pressure and air density can be calculated with the International Standard Atmosphere (ISA). Air pressure p is an exponential function of altitude h and can be calculated with equation 8. h_b and p_b are the base altitude and air pressure respectively of an atmospheric layer and are shown in table III. Other ISA constants are shown in table IV.

$$\begin{aligned} p &= p_b \left[1 + \frac{\lambda(h-h_b)}{T_b}\right]^{\frac{-g}{\lambda R}} & \lambda \neq 0 \\ p &= p_b \exp\left[-\frac{g(h-h_b)}{RT_b}\right] & \lambda = 0 \end{aligned} \tag{8}$$

The air density ρ can be calculated with the perfect gas law given in equation 9, knowing the air pressure p from equation 8, the local air temperature T and the specific gas constant R.

$$\rho = \frac{p}{RT} \tag{9}$$

2) Temperature: Equation 10 shows the calculation of the temperature T with the true airspeed V_{TAS} and indicated airspeed V_{IAS} or Mach number M. These parameters are available in BDS 5,0 and BDS 6,0.

$$\begin{aligned} T &= \frac{V_{TAS} \cdot p}{V_{IAS} \cdot \rho \cdot R} & M < 0.3 \\ T &= \frac{V_{TAS} \cdot T_0}{M^2 \cdot a_0^2} & M \geq 0.3 \end{aligned} \tag{10}$$

TABLE III
INTERNATIONAL STANDARD ATMOSPHERE LAYERS

	h_b [m]	T_b [K]	λ [K/km]	p_b [Pa]	ρ [kg/m^3]
Troposphere	0	288.15	-6.5	101,325	1.225
Tropopause	11,000	216.65	0.0	22,632	0.364
Stratosphere	20,000	216.65	1.0	5,475	0.088

3) Wind: In figure 6, the relation between true airspeed, ground speed and wind is shown. The ground speed vector $\boldsymbol{V_{GS}}$ is the sum of the true airspeed vector $\boldsymbol{V_{TAS}}$ and wind vector $\boldsymbol{W}$ as shown in equation 11. χ_g, χ_a and χ_w are the ground speed vector angle (track angle), airspeed vector angle (heading) and wind vector angle with respect to true north respectively.

$$\boldsymbol{V_g} = \boldsymbol{V_{TAS}} + \boldsymbol{W} \tag{11}$$

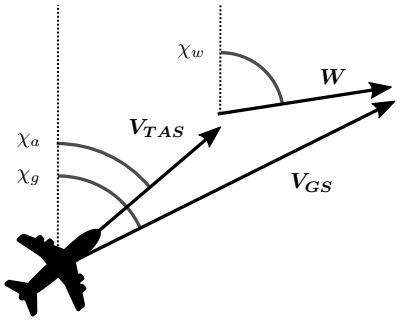

Fig. 6. Relation between true airspeed, ground speed and wind

To simplify calculations in equation 11, the vectors $\boldsymbol{V_{GS}}$, $\boldsymbol{V_{TAS}}$ and $\boldsymbol{W}$ will be decomposed into a west-east component V_x and a south-north component V_y. Decomposing a vector in x and y components can be done with equations 3 and 4 respectively. Wind components can then be calculated with equations 12 and 13.

$$W_x = V_{x,GS} - V_{x,TAS} \tag{12}$$

$$W_y = V_{y,GS} - V_{y,TAS} \tag{13}$$

The ground speed vector can be obtained from ADS-B using reported ground speed and track angle. The true airspeed can be obtained directly from BDS 5,0 or can be calculated with the indicated airspeed or Mach number from BDS 6,0 as shown in equation 14. With the magnetic heading in BDS 6,0, converted to true north, the airspeed vector can be derived.

$$\begin{aligned} V_{TAS} &= V_{IAS}\sqrt{\frac{\rho_0}{\rho}} \quad M < 0.3 \\ V_{TAS} &= M\sqrt{\gamma RT} \quad M \geq 0.3 \end{aligned} \tag{14}$$

TABLE IV
INTERNATIONAL STANDARD ATMOSPHERE CONSTANTS

Symbol	Description	Value	Unit
a_0	Sea level speed of sound	340.3	m/s
g	Gravitational acceleration	9.81	m/s^2
p_0	Sea level air pressure	101 325	Pa
R	Specific gas constant	287.05	J/(kg·K)
T_0	Sea level temperature	288.15	K
ρ_0	Sea level air density	1.225	kg/m^3

B. Meteo-Partical Model

The meteorological derivations in subsection IV-A are incorporated in the Meteo-Partical model (MP model) [36]. A flow diagram of how ADS-B and Mode S signals are used in the MP model is shown in figure 7. For each wind and temperature derivation obtained from ADS-B and Mode S data, the MP model creates particles that can be considered as point objects with the state of the wind and temperature. These particles propagate and decay over time according to a Gaussian random walk model, where the particle age increases at each time step. Wind particles can propagate in 3D, but wind speed and direction are only computed in the horizontal plane. Temperature particles propagate in 2D at the same altitude. At each time step, the particles are re-sampled: particles that have propagated outside of the horizontal and vertical boundaries are removed and remaining particles will be sampled by age.

Advantages of using the MP model is that meteorological conditions can be computed in less dense areas, in areas with less aircraft. Historic information is used without the need of storing historical measurements. Wind and temperature are reconstructed by using the weighted state values from surrounding particles. The confidence of wind and temperature derivations depends on the number, mean distance, homogeneity and strength of the particles. New meteorological derivations that are not consistent with the current wind and temperature field will be rejected according to a probabilistic acceptance mechanism. An example wind field with wind barbs and confidence interval is shown in figure 8.

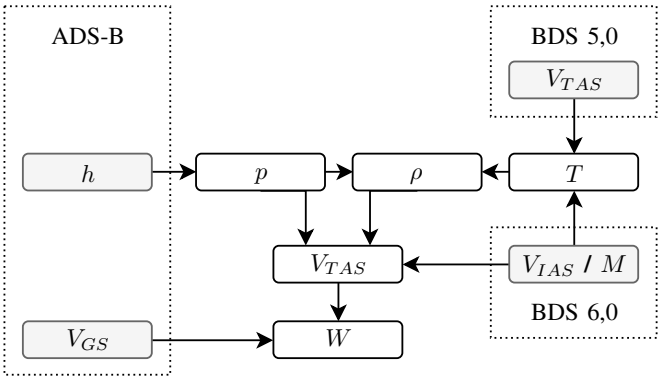

Fig. 7. Flow diagram meteorological derivations

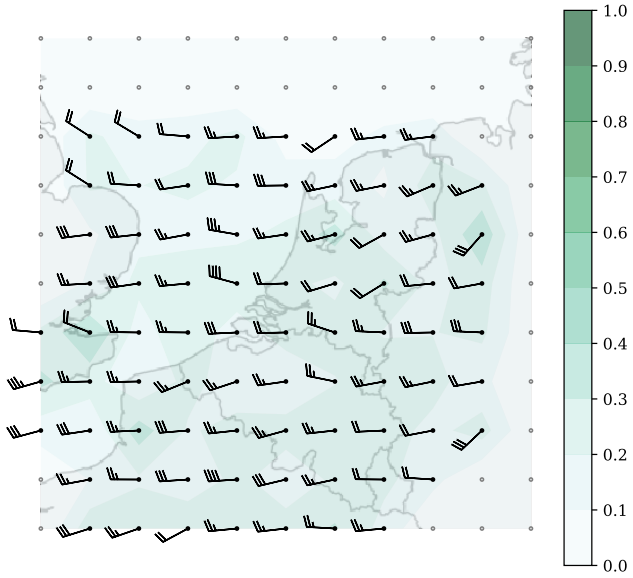

Fig. 8. Wind field construction with confidence contour

C. Improving aircraft performance parameters

With the obtained wind and temperature conditions from the MP model, operational performance and limitations of aircraft can be estimated. Although indicated airspeed, true airspeed and Mach number are transmitted in Mode S, the use of the MP model has its advantages. Mode S parameters have a certain resolution. For some parameters this resolution is low, for example, true airspeed has a resolution of 2 kts. Due to the fusion of inputs from multiple aircraft, derivation errors due to the low resolution of Mode S will be averaged out. Mode S parameters are only updated when interrogated by an SSR, while with the MP model it is possible to determine the wind and temperature at any time due to the propagation and decay. Further, the MP model gives a complete state of the atmosphere instead of a local measurement (aircraft position), which can useful for other applications, not limited to aviation.

1) Flight extraction and flight phase identification: From large amounts of ADS-B data, individual flights need to be extracted. To deal with unsorted flight-data, the unsupervised machine learning clustering method (DBSCAN) is used to cluster and sort the data per flight. A minimum number of 100 data points is used to construct a (partial) flight. Since ADS-B data can be scattered and noisy; smoothing, filtering and interpolation are applied per flight.

For aircraft performance, it is important to identify the flight phase. This is identified by fuzzy logic with the inputs altitude (h), ground speed (GS) and vertical speed (VS) as explained in [12]. It uses membership functions to define the degree of truth for the inputs. For example, during climb, the altitude will be low, with a medium ground speed and positive vertical speed. Cruise will have a high ground speed and altitude, with a vertical speed close to zero. The following estimators are used to identify the flight phase:

$$\begin{array}{ccccccc} h_{low} & \wedge & GS_{medium} & \wedge & VS_{+} & \Rightarrow & \text{Climb} \\ h_{high} & \wedge & GS_{high} & \wedge & VS_{0} & \Rightarrow & \text{Cruise} \\ h_{low} & \wedge & GS_{medium} & \wedge & VS_{-} & \Rightarrow & \text{Descent} \end{array}$$

In this paper, only the flight phases climb, cruise and descent will be analysed since the installed ADS-B/Mode S receiver has a limited reception for low altitudes due to line-of-sight characteristics. Therefore take-off, initial climb, final approach and landing are not considered.

The calibrated airspeed and Mach number are important parameters during climb and descent. During the climb, the first part will be performed with a constant calibrated airspeed, followed by a climb with a constant Mach number. During the descent, the first part will be performed with a constant Mach number, followed by a descent with a constant calibrated airspeed. The altitude where the constant calibrated airspeed becomes constant Mach number (or vice-versa), is called the crossover altitude. Due to limited complete climbs and descents from our receiver, the crossover altitude is obtained from earlier research [11].

The following aircraft performance parameters will be derived for climb (CL), cruise (CR) and descent (DE):

- Climb / descent:
  - Constant calibrated airspeed climb / descent:
    - Ground speed (GS) and true airspeed (TAS)
    - Calibrated airspeed (CAS)
    - Vertical speed
  - Constant Mach number climb / descent:
    - Ground speed and true airspeed
    - Mach number
    - Vertical speed
- Cruise:
  - Ground speed and true airspeed
  - Calibrated airspeed
  - Mach number

2) Aircraft performance parameter estimation: Using ADS-B and Mode S data with the MP model, the true airspeed of an aircraft at any given point can be determined with ground speed from ADS-B and estimated wind from the MP model. With the estimated temperature and true airspeed, the Mach number and the indicated airspeed can be calculated as given in equations 15 and 16 respectively. The difference between indicated and calibrated is assumed to be small and therefore considered as equal.

$$M = \frac{V_{TAS}}{\gamma R T} \tag{15}$$

With the aircraft altitude, the air pressure can be calculated from the ISA as given in equation 9. The indicated airspeed can be derived with the air density, the dynamic pressure and the ISA constants as given in equation 16:

$$
\begin{aligned}
q_{dyn} &= p\left(\left(1+\frac{\rho\cdot V_{TAS}^2}{7p}\right)^{3.5}-1\right)\\
V_{CAS} = V_{IAS} &= \sqrt{\frac{7p_0}{\rho_0}\cdot\left(1+\frac{q_{dyn}}{p_0}\right)^{2/7}-1}
\end{aligned}
\tag{16}
$$

For each aircraft type, phase and performance parameter, a probability distribution is fitted on the data. The used distributions are a normal distribution ($\mathcal{N}$), a gamma distribution (Γ) and a beta distribution (B). To estimate the best unbiased model parameters for the distributions, a maximum likelihood is used. After this, the one-sample Kolmogorov-Smirnov (KS) test is applied to select the best distribution.

Using the same notation of [11], each aircraft performance parameter will be described by equation 17:

$$
\left\{\hat{\psi} \mid \psi_{min}, \psi_{max} \mid \text{*pdf}\right\} \tag{17}
$$

The first part, $\hat{\psi}$, is the optimal performance value, followed by the minimum and maximum values that are obtained from a 90% confidence interval. The last part is the distribution that is obtained from the KS test with the distribution parameters as shown in equation 18:

$$
\text{*pdf} = \begin{cases} ['norm', \mu, \sigma] & \text{for } x \sim \mathcal{N} \\ ['gamma', \alpha, \mu, k] & \text{for } x \sim \Gamma \\ ['beta', \alpha, \beta, \mu, k] & \text{for } x \sim B \end{cases} \tag{18}
$$

Where μ is the mean parameter, σ the deviation and α, β, k are shape parameters for the gamma and beta distribution.

V. Experiments & Results

Before using Mode S signals, identifying the correct Mode S BDS register is crucial for obtaining the correct parameters. In this section, the BDS register identification will be validated with ATC data. Earlier research showed that the magnetic heading in BDS 6,0 contains deviations and these deviations will be determined with an analysis of on-ground aircraft. When correct Mode S parameters are obtained, the MP model can be used for wind and temperature derivations. The results of the MP model will be validated with on-board data from an aircraft and a numerical weather prediction model. When the meteorological derivations have been validated, aircraft performance parameters can be derived.

A. Validation of BDS register identification with ATC radar data

To validate the BDS register identification method, a one-hour dataset from LVNL's TAR-1 SSR located at Amsterdam Airport Schiphol is used. The dataset is formatted in EUROCONTROL's ASTERIX CAT048 format (All Purpose STructured EUROCONTROL SuRveillance Information EXchange) [37]. This dataset is decoded using the Python library Asterix developed by Croatia Control [38].

The dataset contains 273,336 observations on 7 September 2017 between 13h and 14h UTC. From this dataset, the aircraft ICAO address, altitude (flight level), calculated ground speed, calculated track angle and Mode S message field are used. In these observations, there are 253,059 raw Mode S messages, but with the indication which BDS register is interrogated (BDS 4,0, 5,0 or 6,0).

For the probabilistic identification of the BDS register, reference information for altitude, ground speed and track angle is required. As reference information, the included flight altitude (level), calculated ground speed and calculated track angle in the ASTERIX dataset are used. The BDS register of Mode S messages in the LVNL dataset is identified with and without the probabilistic method and the success rates are shown in table V.

In table V, it can be seen that the number with wrong BDS register identification increases with the probabilistic method. However, further analysis showed that one aircraft, a Beech 200 Super King Air (ICAO address `399675`), transmitted BDS 6,0 with only magnetic heading (44 signals), which was incorrectly identified as BDS 4,0. When this aircraft is filtered out, the BDS register of 19 Mode S signals (0.0075%) were identified incorrectly. Wrong BDS identification only occurred between BDS 5,0 and BDS 6,0.

In some cases, the BDS register could not be identified. This is because not all fields in BDS 5,0 or BDS 6,0 are available to build a multivariate distribution. All BDS 4,0 signals are identified correctly as BDS 4,0.

TABLE V
Results BDS register identification

Probabilistic identification	No	Yes
BDS identified correctly	221,652 (87.59%)	250,816 (99.11%)
BDS identified incorrectly	6 (0.002%)	63 (0.025%)
BDS could not be identified	31,401 (12.41%)	2180 (0.86%)

B. Magnetic heading deviation analysis at Schiphol

Over a period of 5 months, from 22 November 2017 to 19 April 2018 (with some outages), in total 6.8 million Mode S signals were obtained from 3833 unique aircraft with the status on-ground. On 12 January 2018, the receiver was moved to another position which improved the reception of Mode S signals from on-ground aircraft (mainly due to improved reception from runway 09/27 and the G/F-gates).

For the analysis, only aircraft types (ICAO aircraft type designators) with more than 1000 BDS 5,0 and BDS 6,0 signals with a distance less than 15 m to the centerline and a ground speed lower than 100 kts are used. This resulted in 27 aircraft types.

1) BDS 5,0 ground track and runway track angle: To verify the proposed methodology, first, the difference between the track angle from BDS 5,0 and the runway headings are compared (n = 784,302 signals). As mentioned earlier, the wind will not affect the ground track of an aircraft, and therefore the difference is expected to be zero degrees. For

24/27 aircraft types, the median is 0 degree, while for 3/27 aircraft types the median is -0.176 degrees. The A388 has the largest spread in BDS 5,0 track angle, but no explanation could be found for this. With this result, it can be concluded that the track angle in BDS 5,0 is equal to the runway headings.

2) BDS 6,0 magnetic heading and runway track angle: At Amsterdam Airport Schiphol, the magnetic declination is around +1.13 degrees (east) (World Magnetic Model 2015) in January 2018. By using the runway true track angle and magnetic heading in BDS 6,0, the difference between these parameters will be the magnetic declination and should be +1.05 degrees (due to the Mode S resolution of 0.18 degrees).

Figure 9 shows the boxplots of the differences between the runway track angle and the magnetic heading in BDS 6,0 (n = 678,189 signals). The dashed line indicates the magnetic declination of Amsterdam Airport Schiphol, and the difference between runway heading and magnetic heading is expected to be on this line.

Comparing different aircraft types, the median of the magnetic heading difference of the same aircraft type series are similar. For example, the Airbus A320 series (A318-A321) have a median close to each other. The same applies to the Boeing 737 series (B737-B739), the Boeing 747 (B744, B748), Boeing 777 (B772, B77L, B77W) and Boeing Dreamliner (B788 and B789). The median of the Boeing 737 series and the Embraer family (E190, E195 and E75), are the closest to magnetic declination as shown in table VI.

For some aircraft, the Airbus A330 series, Airbus A343 and the Boeing 787 series, the magnetic heading is nearly equal to the runway track (no magnetic declination) and some aircraft, like the Boeing 747 and 777 series, have a completely opposite magnetic declination.

Analysing more specifically the Boeing 747 (n = 41,263 signals), 69% of the B744 signals are from KLM aircraft, while none of the B748 signals are from KLM. For both aircraft types, the boxplots are similar and the medians are both -0.88 degrees. This behaviour is also visible for different airlines with a specific aircraft type. From this, it can be inferred that the magnetic deviation is aircraft type dependent, but not necessarily airline specific. While in BDS 5,0 the spread in track angle of the A388 was large, the spread in magnetic heading in BDS 6,0 is much smaller.

3) BDS 5,0 track angle and BDS 6,0 magnetic heading: Since many aircraft are interrogated for BDS 5,0 and BDS 6,0 closely after each other, a comparison between the transmitted aircraft track angle and magnetic heading is made. BDS 5,0 track angle and BDS 6,0 magnetic heading are compared if the received time difference between these signals is less than one second. The results are comparable to the comparison between BDS 6,0 and runway track angle: 18/27 aircraft types have the same difference, while 8/27 aircraft types have 0.18 degrees difference and one aircraft type (B763) has a difference of 0.35 degrees.

This indicates that the transmitted magnetic heading in BDS 6,0 is more accurate than the track angle in BDS 5,0 for the A388. Since this time no runway track angle is used in the comparison, the transmitted track angle in BDS 5,0 from the A388 seems to be inaccurate.

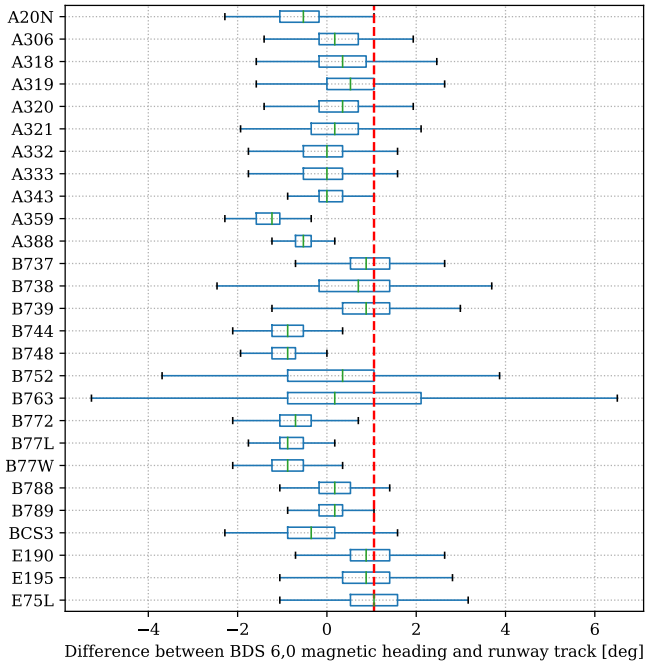

Fig. 9. Boxplots showing the difference between BDS 6,0 magnetic heading and runway/taxiway track per aircraft type

4) Aircraft type magnetic heading corrections: With the results obtained from figure 9, an aircraft type dependent heading correction can be derived which is the difference between the expected magnetic declination and the difference between transmitted BDS 6,0 magnetic heading and runway track. The correction values are given in table VI and these will be applied for further wind derivations as given in equation 19.

$$\text{True north} = \text{Magnetic north} - \text{Declination} + \text{Correction} \tag{19}$$

TABLE VI
CORRECTIONS FOR BDS 6,0 MAGNETIC HEADING

Aircraft type	Correction [deg]	Aircraft type	Correction [deg]
A20N	1.582	B744	1.934
A306	0.879	B748	1.934
A318	0.703	B752	0.703
A319	0.528	B763	0.879
A320	0.703	B772	1.758
A321	0.879	B77L	1.934
A332	1.055	B77W	1.934
A333	1.055	B788	0.879
A343	1.055	B789	0.879
A359	2.285	BCS3	1.406
A388	1.582	E190	0.176
B737	0.175	E195	0.176
B738	0.352	E75L	0.000
B739	0.175		

C. Validation of meteorological estimations

The results of the meteorological estimations are compared with on-board flight data from the research aircraft of the Delft University of Technology, a Cessna Citation II (C550) and a numerical weather prediction (NWP) model. First, the estimations without any post-processing are validated, that is only using the equations in subsection IV-A. Next, the estimations with post-processing in the MP model are validated.

The effect of additional corrections to Mode S on the MP model are analysed: filtering out corrupt Mode S signals based on the included altitude or squawk code, aircraft type magnetic heading corrections and filtering out measurements with a high roll angle ($\geq$ 5 degrees). The reason is that high roll angles affect the measured true airspeed.

To assess the accuracy, the Cessna on-board data and the NWP model are considered as true data source and used as reference. To determine the accuracy, the mean error (ME), mean absolute error (MAE), root mean squared error (RMSE) and the Pearson correlation coefficient[3] (R) are calculated.

1) Validation with on-board flight data: For validation with the Cessna, a total of 7 flights over 4 days are used. These flights were executed for research at an altitude of 16,000 ft and contain many turns. At this altitude, not many commercial aircraft fly, which results in a lower number of Mode S signals, except the signals from the Cessna itself. Also the effect of using Mode S signal from the Cessna itself will be analysed.

a) Raw weather derivations: From ADS-B and Mode S, the wind and temperature are derived as explained in subsection IV-A. These derived parameters are compared with the wind and temperature derived from data on-board of the Cessna and these results are shown in table VII.

In the temperature derivations, a lot of noise is observed. This noise is caused by the resolution of true airspeed and Mach number, which are 2 kts and 0.004 Mach respectively. Since the temperature is determined by equation 20, with C = 1/401.87. Small changes (and rounding errors) can cause temperature fluctuations, for example when case BDS 5,0 true airspeed and BDS 6,0 Mach number are not transmitted simultaneously and these parameters are not constant. An option to solve this is by smoothing the true airspeed and Mach number.

$$T = \frac{V^2}{\gamma R M^2} = C\left(\frac{V}{M}\right)^2 \tag{20}$$

b) MP model weather derivations: The wind and temperature estimations of the MP model are validated with the Cessna. For this, weather derivations from other aircraft will be included. However, when analysing the effect of the Cessna itself, the Mode S signals from the Cessna will be excluded from the input. The results are shown in table VIII.

When Mode S signals from the Cessna are included in the MP model, it can be seen that corrections have no influence on the MAE. This is because corrections do not have a large influence on the Cessna, since no heading correction is determined for the Cessna, and the Cessna was flying at a flight level that is not used by commercial aircraft for which heading corrections are determined. Therefore corrections will only affect other altitudes, while the wind and temperature are mainly derived from the Cessna itself.

[3]All mentioned correlation coefficients are significant at a level of $p < 0.01$

TABLE VII
ESTIMATION ERRORS IN RAW WIND AND TEMPERATURE CALCULATIONS WITH ON-BOARD DATA

	ME	MAE	RMSE	R
Wind speed w/o correction [m/s]	1.50	3.41	7.61	0.60
Wind speed w/ correction [m/s]	1.37	3.18	5.93	0.71
Wind direction w/o correction [deg]	1.77	12.00	18.62	0.84
Wind direction w/ correction [deg]	2.20	11.87	18.00	0.83
Temperature w/o correction [K]	0.62	3.30	8.63	0.58
Temperature w/ correction [K]	0.53	3.19	7.79	0.63

When Mode S signals from the Cessna are excluded an improvement can be seen in table VIII. This is because for other aircraft types heading corrections can be applied. The heading correction will only affect wind, the MAE for wind speed and direction improves up to 13% compared to the on-board data of the Cessna. Due to the roll limitation, some true airspeed measurements are filtered out that from being used for temperature estimation. This leads to a very small improvement.

Comparing the meteorological derivations in table VII with table VIII, it can be seen that the MP model improves the quality of wind and temperature estimations.

TABLE VIII
ESTIMATION ERRORS IN WIND AND TEMPERATURE CALCULATIONS

Including Cessna Citation II				
	ME	MAE	RMSE	R
Wind speed w/o correction [m/s]	0.79	2.24	3.01	0.88
Wind speed w/ correction [m/s]	0.92	2.28	3.00	0.88
Wind direction w/o correction [deg]	0.86	9.62	12.59	0.95
Wind direction w/ correction [deg]	0.98	9.16	11.47	0.94
Temperature w/o correction [K]	0.61	1.89	2.62	0.92
Temperature w/ correction [K]	0.59	1.86	2.51	0.93

Excluding Cessna Citation II				
	ME	MAE	RMSE	R
Wind speed w/o correction [m/s]	-0.31	3.31	4.05	0.63
Wind speed w/ correction [m/s]	0.02	2.95	3.64	0.70
Wind direction w/o correction [deg]	0.74	11.17	14.78	0.91
Wind direction w/ correction [deg]	-0.72	9.77	13.51	0.92
Temperature w/o correction [K]	0.05	1.58	2.06	0.94
Temperature w/ correction [K]	0.05	1.55	2.01	0.95

2) Validation with a numerical weather prediction model: The last validation is made with an NWP model. In contrast to the validation with the Cessna on-board data, the NWP model gives a total overview of the wind and temperature of the atmosphere. For this comparison, the hourly European Centre for Medium-Range Weather Forecasts (ECMWF) ERA5 reanalysis dataset is used with a latitudinal and longitudinal resolution of 0.28125 degrees (31 km).

Using historical data recorded from the installed ADS-B/Mode S receiver, the MP model derived the wind and temperature for each minute between 1 January 2018 00h UTC till 7 January 2018 23h UTC. These values are grouped by the closest hour and compared to the NWP model.

From a 7-day data input, the MP model estimated for in total 17,702,137 (without corrections) and 14,906,023 (with corrections) grid points the wind and temperature. These results are given in table IX. As can be seen in table IX, the MAE for wind speed decreases with 5% and wind direction with 10% when corrections are applied. Corrections have no effect on the MAE for temperature.

In figure 10, the statistics for wind and temperature estimated by the MP model for 5 January 2018 are shown. It can be seen that wind speed increases with altitude up to 30,000 ft and wind direction that day is mainly western wind. The temperature is decreasing with altitude till 33,000 ft and stays constant from that altitude, which is comparable to the international standard atmosphere. The vertical line is the median of the NWP model. For wind speed and direction, the MP model median is close to the NWP model median, while the MP model median for temperature is higher than the NWP model median.

TABLE IX
ESTIMATION ERRORS IN WIND AND TEMPERATURE CALCULATIONS

	ME	MAE	RMSE	R
Wind speed w/o correction [m/s]	0.17	2.87	4.18	0.97
Wind speed w/ correction [m/s]	0.16	2.73	4.03	0.97
Wind direction w/o correction [deg]	1.36	8.55	16.76	0.88
Wind direction w/ correction [deg]	0.47	7.73	15.82	0.90
Temperature w/o correction [K]	0.52	1.33	1.78	1.00
Temperature w/ correction [K]	0.49	1.32	1.75	1.00

At low wind speeds, the MAE of the wind direction increases since a small deviation in wind speed has a large effect on the wind direction as shown in figure 11. In this figure, it is clearly visible that wind speeds up to 5 m/s have a median of wind direction difference larger than 20 degrees and this median decreases when wind speeds increase.

In the case only wind speeds of the NWP model higher than 5 m/s are considered, the MAE for wind direction decreases to 6.07 degrees. When considering wind speeds higher than 10 m/s, the MAE for wind direction decreases to 5.39 degrees. The MAE for wind speed increases by 5% when only considering wind speeds higher than 10 m/s.

During this 7-day period, on 3 January, a severe storm raged over Western Europe, while on 7 January the wind was calm. During the storm, the MAE for wind speed and direction were similar to other days. Due to the calm wind on 7 January, the MAE in wind direction difference increased in table IX.

D. Aircraft performance parameter modelling

By using the MP model, for each aircraft, each time and location, the wind and temperature can be estimated. By knowing the wind vector, it is possible to determine the aircraft's true airspeed with ADS-B ground speed data. ADS-B and Mode S data of March 2018 from our receiver have been processed with the MP model. This resulted in 144 million positions from 8590 unique aircraft. From these positions, also a Mode S true airspeed message (BDS 5,0) was received within 5 seconds for 120 million positions. With the MP model, true airspeed was determined for 139 million positions.

From signals that contain BDS 5,0 true airspeed (assumed as correct, despite the low resolution), a comparison was made with the derived true airspeed from the MP model. The mean error, absolute mean error and root mean squared error for BDS 5,0 true airspeed and MP true airspeed are 0.15 kts, 1.70 kts and 2.11 kts respectively.

In this paper, aircraft performance parameters for 16 aircraft types have been analysed. Below, the results for climb, cruise and descent phase for the Airbus A320 are shown.

1) Climb phase Airbus A320: The altitude where constant CAS starts is at 5.0 km (FL160) and the crossover altitude between constant CAS and constant Mach number is set at an altitude of 9.6 km (FL310). During the constant CAS climb, the CAS is 148 m/s (288 kts), with a mean vertical speed of 7.37 m/s (1450 fpm). During constant Mach number climb, the Mach number is 0.77 with a mean vertical speed of 4.58 m/s (900 fpm).

It can be seen in figure 12 that using the true airspeed instead of the ground speed, the 90% confidence interval becomes narrower with 23 m/s for the constant CAS climb and 33 m/s for the constant Mach number climb. In both cases, the change of the mean is small.

2) Cruise phase Airbus A320: During cruise, the mean TAS is 229 m/s (445 kts), mean Mach number is 0.78. Using the true airspeed instead of the ground speed, narrows the 90% confidence interval by 29 m/s.

3) Descend phase Airbus A320: At an altitude of 9.5 km (FL310), the descent with constant Mach number starts with a Mach number of 0.77 and a mean vertical speed of -6.41 m/s (-1260 fpm). The crossover altitude between constant Mach number and constant CAS descend is set at 5.7 km (FL190). During constant CAS descent, the CAS is 143 m/s (278 kts) with a mean vertical speed of -7.93 m/s (-1600 fpm).

It can be seen in figure 14 that using the true airspeed instead of the ground speed, the 90% confidence interval becomes narrower with 31 m/s for the constant Mach descent and 21 m/s for the constant CAS descent. In both cases, the change of the mean is small.

4) Optimal performance parameters: The optimal performance parameters for other aircraft types are given in table X. It can be seen that for all aircraft types, the differences between the optimal ground speed and the optimal true airspeed are small. However, like with the Airbus A320, the confidence intervals become narrower when the true airspeed is used.

VI. DISCUSSION / RECOMMENDATIONS

In this paper, ADS-B and Mode S signals have been used to improve aircraft performance modelling parameters. With an

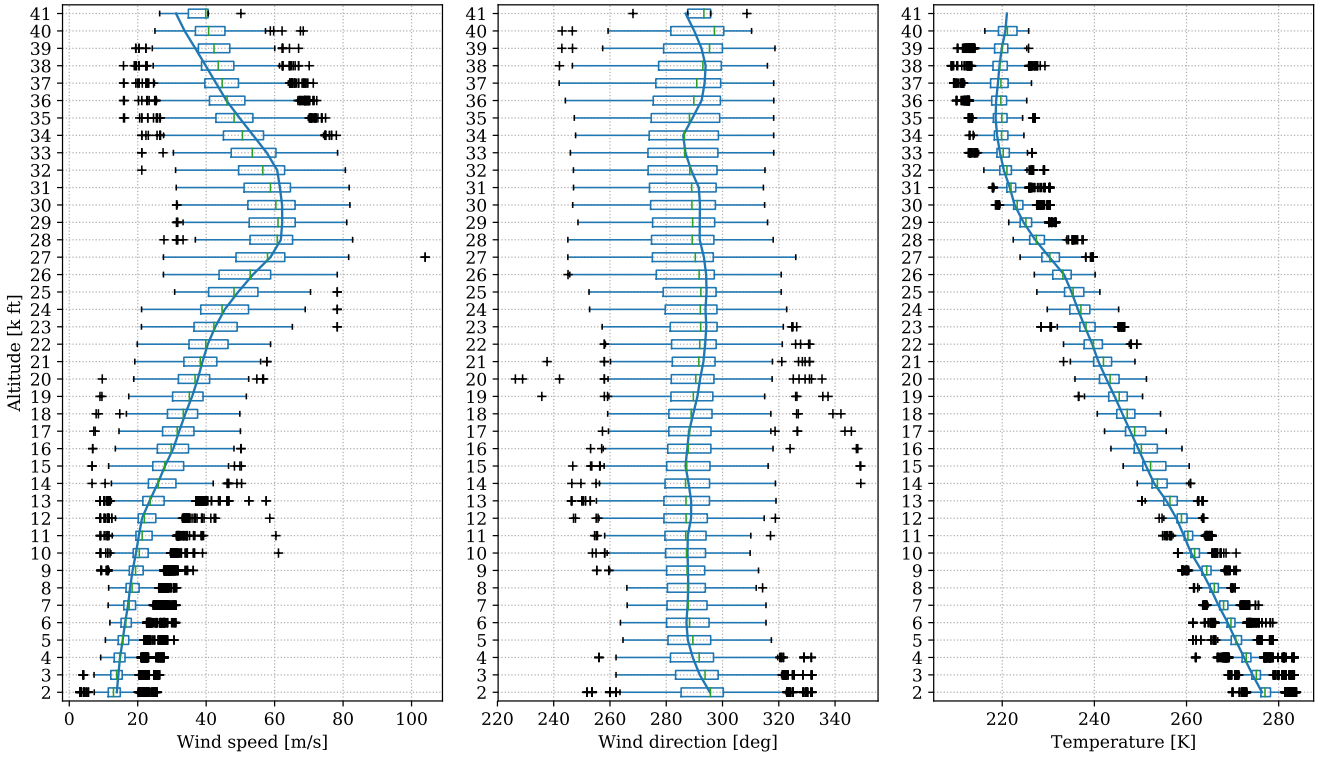

Fig. 10. Wind and temperature distribution per 1000 feet on 5 January 2018

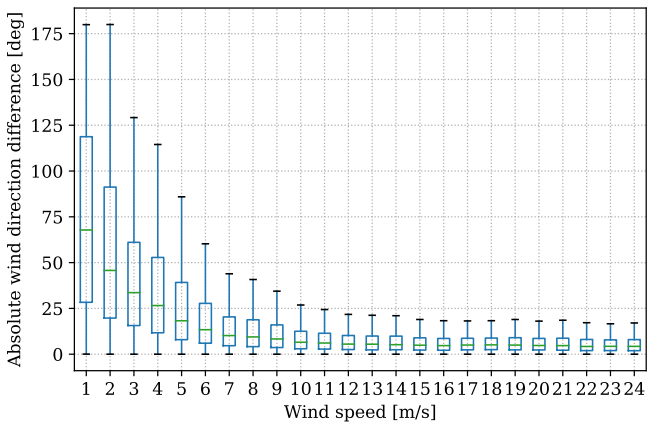

Fig. 11. Distribution wind speed versus wind direction error

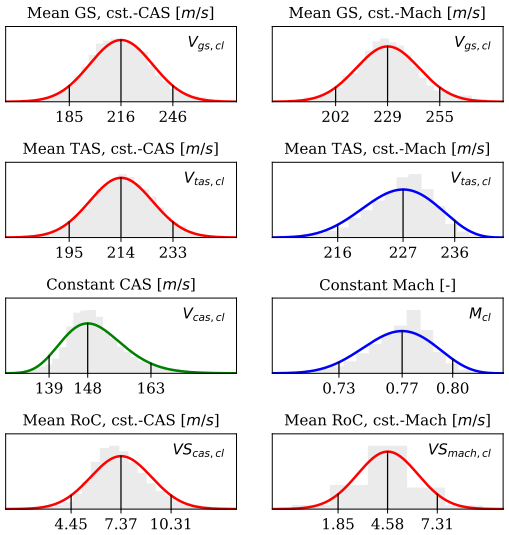

Fig. 12. Climb parameters

ADS-B/Mode S receiver installed at the Faculty of Aerospace Engineering at the Delft University of Technology, signals are received from aircraft up to 400 km around the location of the receiver. ADS-B and Mode S signals are decoded with the Python *pyModeS* library, which has been actively developed during this research. Decoding Mode S was a challenging task, due to the closed character of Mode S signals. Unlike ADS-B, no information is present in a Mode S signal that indicates which content it contains and from which aircraft it originates. A method has been proposed to identify the Mode S content (BDS register) and the interrogated aircraft (its ICAO address). Due to the limited range of our receiver, not all types of BDS registers that could be interrogated have been received, for example, Mode S MRAR. Some of these non-interrogated registers are implemented in *pyModeS*, but

TABLE X
OPTIMAL PERFORMANCE PARAMETERS FOR VARIOUS AIRCRAFT TYPES (SPEEDS IN M/S, MACH NUMBER DIMENSIONLESS)

Phase	Parameter	A319	A320	A321	A332	A333	A388	B737	B738	B739	B744	B752	B763	B77W	B788	B789	E190
CL, CAS	V_{GS}	214	216	221	223	221	240	212	215	219	238	223	226	238	240	240	201
	V_{TAS}	214	214	218	229	220	236	213	215	217	242	224	228	234	242	240	203
	V_{CAS}	148	148	153	153	156	162	147	149	156	169	155	159	163	155	164	140
	VS	8.38	7.37	6.65	6.38	6.22	6.06	10.32	8.88	8.60	8.27	8.99	8.23	7.49	6.77	7.12	8.25
CL, Mach	V_{GS}	229	229	231	238	237	252	228	228	234	249	230	232	250	254	251	224
	V_{TAS}	227	227	228	237	238	247	229	228	231	248	232	234	246	249	249	223
	M	0.77	0.77	0.77	0.80	0.81	0.84	0.78	0.77	0.78	0.84	0.79	0.79	0.83	0.84	0.84	0.76
	VS	4.79	4.58	4.40	3.85	3.33	4.44	4.49	4.52	3.64	4.42	5.97	5.58	6.25	4.27	4.44	4.53
CR	V_{GS}	226	228	228	239	240	249	229	227	229	248	232	237	245	249	249	229
	V_{TAS}	228	229	229	239	239	248	230	229	230	247	234	236	245	249	249	229
	V_{CAS}	129	132	138	132	134	138	126	130	137	144	133	140	150	135	140	135
	M	0.77	0.78	0.78	0.81	0.81	0.84	0.77	0.77	0.78	0.84	0.79	0.80	0.83	0.85	0.84	0.78
DE, Mach	V_{GS}	223	224	221	237	236	243	226	225	221	241	229	235	231	243	243	225
	V_{TAS}	226	227	225	238	236	245	227	227	227	243	232	233	236	245	245	225
	M	0.76	0.77	0.76	0.8	0.81	0.83	0.77	0.77	0.77	0.82	0.78	0.79	0.8	0.83	0.84	0.76
	VS	-6.39	-6.41	-7.27	-8.41	-9.03	-6.46	-7.37	-1.98	-6.78	-7.64	-4.70	-10.07	-7.46	-3.74	-8.96	-8.27
DE, CAS	V_{GS}	197	202	201	211	208	215	200	199	202	213	214	217	206	211	216	200
	V_{TAS}	199	203	199	218	213	223	201	203	205	214	217	223	213	213	224	201
	V_{CAS}	143	143	144	146	151	152	144	140	145	148	152	150	144	143	145	145
	VS	-8.53	-7.93	-8.17	-8.34	-8.50	-8.81	-7.95	-7.12	-7.40	-8.37	-9.18	-9.02	-8.23	-8.86	-8.91	-8.51

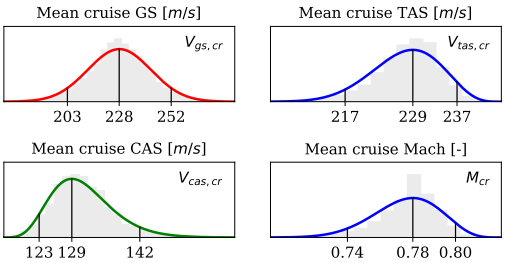

Fig. 13. Cruise parameters

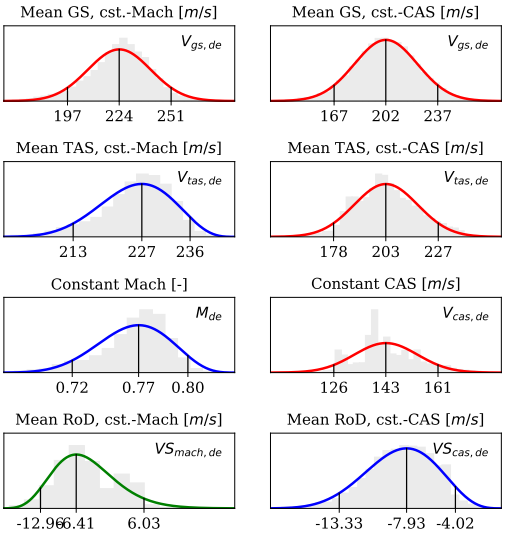

Fig. 14. Descent parameters

could not be validated. For three BDS registers, BDS 4,0, 5,0 and 6,0 (Mode S EHS), the BDS register identification was compared with ATC data. In 99.11% of the cases, the correct BDS register was identified, while in 0.025% of the cases the identification was incorrect and in 0.86% of the cases the BDS register was not identified due to missing fields. The interrogated aircraft can be identified only when the Mode S signal does not contain transmission errors. A method to detect corrupted signals has been developed with the additional information included in Mode S signals. For Mode S signals containing altitude, the altitude is compared with ADS-B and considered as correct when the altitude difference is below a certain threshold (250 ft). For Mode S signals containing the identity code (squawk code), the combinations of squawk code and ICAO addresses are counted. Signals are considered correct when a combination occurs more than ten times per five minutes.

Earlier research showed that the magnetic heading included in Mode S BDS 6,0 contain deviations. In this paper, a new method has been proposed to determine these deviations by using on-ground aircraft and runway/taxiway track angles. An ADS-B/Mode S receiver was installed at Amsterdam Airport Schiphol for half a year to record ground traffic. This data showed that there are deviations, but no trend could be seen between older and newer aircraft types. However, the deviations for aircraft in the same family type (for example the Boeing 737 series) are similar. A correction value has been determined based on the observed deviations. This correction was used to improve meteorological derivations. It should be noted that the magnetic declination at Amsterdam is small, +1.13 degrees. Using an airport with a larger magnetic deviation, for example, airports in the Western United States or Canada, that have a magnetic declination of about +15 degrees, the differences should become more clear. During this analysis has been assumed that aircraft are exactly aligned with the centerline

of the runway/taxiways, which is dependent on how well the pilots keep to the centerline. Due to the manual interactions by pilots, the aircraft will deviate from the centerline, but it has been assumed that this deviation will be cancelled-out by the corrections made by pilots. The use of runway exits also contributes to the number of outliers, because aircraft will turn on the runway but still satisfy the 15 m requirement from the centerline.

By using the Meteo-Particle model (MP model), wind and temperature are derived from ADS-B and Mode S signals. For each measurement, particles are created that propagate and decay over time. Due to the propagation of the particles, meteorological conditions can be computed in areas with fewer aircraft. The results of the MP model have been validated with on-board data of the Delft University of Technology research aircraft Cessna Citation II, as well as a numerical weather prediction model, the European Centre for Medium-Range Weather Forecasts (ECMWF) model.

Comparing the MP model with raw wind and temperature derivations to on-board data show that the MP model reduces the mean absolute error (MAE). The MAE for wind is 2.24 m/s, for wind direction 9.62 degrees and for temperature 1.89 K. This is an MAE reduction of 34% for wind speed, 25% for wind direction and 43% for temperature. Using magnetic heading corrections and limiting the roll angle up to 5 degrees, improvements up to 11% for wind speed, 13% for wind direction and 2% for temperature were found.

A 7-day ADS-B and Mode S dataset is processed with the MP model and validated with the ECMWF model. The MAE of the MP model with corrections and limiting roll angle compared to the ECMWF model are 2.73 m/s, 7.73 degrees and 1.32 K for wind speed, wind direction and temperature respectively. The reduction in MAE due to corrections are 5%, 10% and 1% for wind speed, wind direction and temperature respectively. It can be seen that the additional corrections reduce the MAE for wind speed and wind direction up to 13%. At low wind speeds, the MAE of wind direction is larger than at higher wind speeds. Wind speeds up to 5 m/s have a median of wind direction difference larger than 20 degrees, while wind speeds higher than 10 m/s have a median of wind direction difference smaller than 10 degrees.

Using one month of ADS-B and Mode S data from our receiver and the MP model, aircraft performance models have been derived in climb, cruise and descent phases. These flight phases were chosen since our receiver has limited coverage for low-altitudes, due to the line-of-sight characteristics of the signals. Comparing the ground speed and true airspeed, a narrower 90% confidence interval for true airspeed is shown. The difference between the mean ground speed and mean true airspeed was small.

Due to the limited range of our receiver, the number of single flights that contains all of these flight phases are limited. One month of flights is enough to determine the performance of aircraft operating short distances (narrow-body), while for aircraft operating long distance (wide-body) this period is too short. To improve the aircraft performance further, a larger scale ADS-B/Mode S network and a longer period are required for wide-body aircraft.

VII. Conclusion

This paper shows that with a simple receiver ADS-B and Mode S signals from aircraft can be received by everyone. With ADS-B and Mode S, meteorological conditions (wind and temperature) can be derived accurately. These meteorological conditions can be used for various applications, for example in air traffic management, trajectory planning, etc. and its application is not limited to aviation.

The decoding of Mode S is a challenge that has been tackled in this paper. No information is included on which content is included in the signal or which aircraft is the sender. A probabilistic method has been designed for identifying the content for Mode S Enhanced Surveillance. Using SSR data from Air Traffic Control the Netherlands, it has been shown that our ADS-B/Mode S decoding library *pyModeS* is able to identify the correct content in 99.11% of the Mode S EHS signals (BDS 4,0, BDS 5,0 and BDS 6,0). To determine the ICAO address, a method has been designed to filter out Mode S signals that contain transmission errors. From error-free signals, the ICAO address has been determined by applying a 'reverse parity' to the signal.

Using the Meteo-Particle model (MP model), wind speed, wind direction and temperature from ADS-B and Mode S are derived and validated using the European Centre for Medium-Range Weather Forecasts (ECMWF) model. For Mode S magnetic heading an additional correction has been determined by using on-ground traffic at Amsterdam Airport Schiphol. For 27 aircraft types, a heading correction has been applied before wind derivation in the MP model. Comparing the MP model meteorological derivations to the ECMWF model, strong correlations ($R > 0.90$, $p < 0.01$) have been shown for wind speed, wind direction and temperature. The mean absolute error with corrections compared to the ECMWF model are 2.73 m/s, 7.73 degrees and 1.32 K for wind speed, wind direction and temperature respectively. These meteorological conditions have been used to derive aircraft performance parameters for 16 aircraft types for the climb, cruise and descent flight phase. These results are summarized in this paper.

Acknowledgements

We would like to thank Air Traffic Control the Netherlands (LVNL) for providing us with a dataset containing Mode S interrogations for validations in this paper. We would also like to thank Royal Schiphol Group for the possibility of installing an ADS-B/Mode S receiver at their head office to track on-ground traffic at Amsterdam Airport Schiphol.

References

[1] Airbus, "Global Market Forecast 2017-2036," http://www.aircraft.airbus.com/market/global-market-forecast-2017-2036/, Accessed: 27 Jun 2017.

[2] Boeing, "Traffic and market outlook," http://www.boeing.com/commercial/market/long-term-market/traffic-and-market-outlook/, Accessed: 27 Jun 2017.

[3] EUROCONTROL, "Aircraft Equipage Requirements in the European Commission IRs 1207/2011, 1028/2014 and 2017/386," http://www.eurocontrol.int/spi-ir, Accessed: 13 Sep 2017.

[4] Federal Aviation Administration, "ADS-B Frequently Asked Questions (FAQs)," https://www.faa.gov/nextgen/programs/adsb/faq/#o2, Accessed: 13 Sep 2017.

[5] Orlando, V. A., "The Mode S Beacon Radar System," *The Lincoln Laboratory Journal*, Vol. 2, No. 3, 1989, pp. 345–362.

[6] Schäfer, M., Strohmeier, M., Lenders, V., Martinovic, I., and Wilhelm, M., "Bringing up OpenSky: A large-scale ADS-B sensor network for research," *IPSN-14 Proceedings of the 13th International Symposium on Information Processing in Sensor Networks*, IEEE Press, April 2014, pp. 83–94.

[7] GitHub, "The Python Decoder for ADS-B (DF17) and Mode-S Comm-B (DF20/21)," https://github.com/junzis/pyModeS, Accessed: 01 Sep 2017.

[8] Hoekstra, J. and Ellerbroek, J., "BlueSky ATC Simulator Project an Open Data and Open Source Approach," *7th International Conference on Research in Air Transportation (ICRAT)*, 2016.

[9] Legrand, K., Rabut, C., and Delahaye, D., "Wind and Temperature Networking Applied to Aircraft Trajectory Prediction," *7th International Conference for Research in Air Transportation*, 2016.

[10] Weitz, P., "Determination and visualization of uncertainties in 4D-trajectory prediction," *2013 Integrated Communications, Navigation and Surveillance Conference (ICNS)*, April 2013, pp. 1–9.

[11] Sun, J., Ellerbroek, J., and Hoekstra, J., "Modeling Aircraft Performance Parameters with Open ADS-B Data," *Twelfth USA/Europe Air Traffic Management Research and Development Seminar (ATM2017)*, 2017.

[12] Sun, J., Ellerbroek, J., and Hoekstra, J., "Large-Scale Flight Phase Identification from ADS-B Data Using Machine Learning Methods," *7th International Conference on Research in Air Transportation*, 2016.

[13] Sun, J., Ellerbroek, J., and Hoekstra, J., "Flight Phase Identification and Machine Learning for Mining ADS-B and Meteorological Data," Unpublished.

[14] Sun, J., Ellerbroek, J., and Hoekstra, J., "Modeling and Inferring Aircraft Takeoff Mass from Runway ADS-B Data," *7th International Conference on Research in Air Transportation*, 2016.

[15] Gloudemans, T., *Aircraft Performance Parameter Estimation using Global ADS-B and Open Data*, Master's thesis, Delft University of Technology, 2016.

[16] World Meteorological Organization, *Aircraft Meteorological Data Relay (AMDAR) Reference Manual*, World Meteorological Organization, 2003.

[17] Strajnar, B., "Validation of Mode-S Meteorological Routine Air Report aircraft observations," *Journal of Geophysical Research: Atmospheres*, Vol. 117, No. D23, Dec. 2012.

[18] de Haan, S., "High-resolution wind and temperature observations from aircraft tracked by Mode-S air traffic control radar," *Journal of Geophysical Research: Atmospheres*, Vol. 116, No. D10, 2011.

[19] de Haan, S., de Haij, M., and Sondij, J., "The use of a commercial ADS-B receiver to derive upper air wind and temperature observations from Mode-S EHS information in The Netherlands," Technical report, Royal Netherlands Meteorological Institute (KNMI), 2013.

[20] de Haan, S., "Quality assessment of high resolution wind and temperature observations from Mode-S: revised edition," Technical report, Royal Netherlands Meteorological Institute (KNMI), 2009.

[21] de Haan, S. and Stoffelen, A., "Assimilation of High-Resolution Mode-S Wind and Temperature Observations in a Regional NWP Model for Nowcasting Applications," *Weather and Forecasting*, Vol. 27, No. 4, 2012, pp. 918–937.

[22] de Leege, A., van Paassen, M., and Mulder, M., "Using Automatic Dependent Surveillance-Broadcast for Meteorological Monitoring," *Journal of Aircraft*, Vol. 50, No. 1, Jan. 2013.

[23] Stone, E. K. and Pearce, G., "A Network of Mode-S Receivers for Routine Acquisition of Aircraft-Derived Meteorological Data," *Journal of Atmospheric and Oceanic Technology*, Vol. 33, No. 4, 04 2016, pp. 757–768.

[24] de Haan, S., "An improved correction method for high quality wind and temperature observations derived from Mode-S EHS," Technical report, Royal Netherlands Meteorological Institute (KNMI), 2013.

[25] Mirza, A. K., Ballard, S. P., Dance, S. L., Maisey, P., Rooney, G. G., and Stone, E. K., "Comparison of aircraft-derived observations with in situ research aircraft measurements," *Quarterly Journal of the Royal Meteorological Society*, Vol. 142, No. 701, 2016, pp. 2949–2967.

[26] Hrastovec, M. and Solina, F., "Obtaining meteorological data from aircraft with Mode-S radars," *IEEE Aerospace and Electronic Systems Magazine*, Vol. 28, No. 12, Dec 2013, pp. 12–24.

[27] Strajnar, B. and Trojáková, A., "Analysis and preprocessing of Czech Mode-S observations," Technical report, Czech Hydrometeorological Institute, 2015.

[28] de Haan, S., "Availability and quality of Mode-S MRAR (BDS4.4) in the MUAC area: a first study," Technical report, Royal Netherlands Meteorological Institute (KNMI), 2014.

[29] Hollister, W. M., Bradford, E. R., and Welch., J. D., "Using aircraft radar tracks to estimate wind aloft," *The Lincoln Laboratory Journal*, Vol. 2, No. 3, 1989, pp. 555–565.

[30] Delahaye, D. and Puechmorel, S., "TAS and wind estimation from radar data," *2009 IEEE/AIAA 28th Digital Avionics Systems Conference*, Oct 2009, pp. 2.B.5–1–2.B.5–16.

[31] Hurter, C., Alligier, R., Gianazza, D., Puechmorel, S., Andrienko, G., and Andrienko, N., "Wind parameters extraction from aircraft trajectories," *Computers, Environment and Urban Systems*, Vol. 47, 09 2014, pp. 28 – 43.

[32] International Civil Aviation Organization, *ICAO Annex 10: Aeronautical Telecommunications Volume III - Communication Systems*, Vol. ICAO Annex 10 Volume III, International Civil Aviation Organization, 2007.

[33] International Civil Aviation Organization, *Technical Provisions for Mode S Services and Extended Squitter*, Vol. ICAO 9871 AN464, International Civil Aviation Organization, 1st ed., 2008.

[34] Boeing, "Correcting the effects of Magnetic Variation," https://www.boeing.com/commercial/aeromagazine/articles/qtr_04_09/pdfs/AERO_Q409_article04.pdf, 2009, Accessed: 18 Feb 2018.

[35] AIS the Netherlands, "Integrated Aeronautical Information Package," http://www.ais-netherlands.nl/aim/index.html, Accessed: 30 Jan 2018.

[36] Sun, J., Vû, H., Ellerbroek, J., and Hoekstra, J., "Ground-based Wind Field Construction from Mode-S and ADS-B Data with a Novel Gas Particle Model," *Proceedings of the Seventh SESAR Innovation Days*, 2017.

[37] EUROCONTROL, "EUROCONTROL Standard Document for Surveillance Data Exchange Part 4: Category 048," https://www.eurocontrol.int/sites/default/files/service/content/documents/nm/asterix/cat048-asterix-tmtr-part4-v1.21-20120701.pdf, July 2012, Accessed: 18 Mar 2018.

[38] GitHub - Croatia Control Ltd., "asterix," https://github.com/CroatiaControlLtd/asterix, Accessed: 18 Mar 2018.

Part II

Scientific Paper Appendix

Appendix A

Magnetic heading analysis

A.1 Mode S distribution at Amsterdam Airport Schiphol

In the distribution of Mode S signals of on-ground aircraft in table A.1, it is clearly visible that in almost half of all interrogations, the aircraft identification (callsign in BDS 2,0) is interrogated.

Table A.1: Distribution of Mode S BDS registers from aircraft with on-ground status at Amsterdam Airport Schiphol between 22 November 2017 and 19 April 2018

BDS Register	# Signals	Percentage
BDS 1,7	90,157	1%
BDS 2,0	2,813,347	41%
BDS 4,0	1,241,077	18%
BDS 5,0	832,191	12%
BDS 6,0	729,452	11%
Not identified	1,072,749	16%
Total	6,779,271	100%

A.2 Used runways and taxiways for magnetic heading analysis

Table A.2: Set of runways and taxiways at Amsterdam Airport Schiphol used for analysis

Name	Type	Lat1	Lon1	Lat2	Lon2	True track
36L18R	Runway	52.362400	4.711943	52.329765	4.708951	3.20
36C18C	Runway	52.330482	4.739969	52.301977	4.737351	3.22
Quebec	Taxiway	52.303393	4.742741	52.298153	4.752476	131.42
Victor (East-West)	Taxiway	52.326589	4.725537	52.320531	4.734050	139.32
Victor-Sierra (South)	Taxiway	52.333194	4.710760	52.328486	4.719500	131.36
Victor-Sierra (North)	Taxiway	52.331306	4.716842	52.327225	4.724408	131.36
2406	Runway	52.303980	4.775931	52.288041	4.734418	57.95
Zulu-Yankee	Taxiway	52.333972	4.736010	52.300206	4.732911	3.22
Delta-Bravo	Taxiway	52.330376	4.742879	52.304062	4.740468	3.22
Charlie-Alpha	Taxiway	52.333699	4.744620	52.302995	4.741799	3.22
Romeo	Taxiway	52.293448	4.741966	52.297372	4.752185	57.95
Whisky-5	Taxiway	52.320589	4.734874	52.320331	4.742386	93.23
Yankee (North)	Taxiway	52.334894	4.737585	52.334703	4.743060	93.23
Sierra	Taxiway	52.296930	4.752906	52.294585	4.755312	147.84
Bravo	Taxiway	52.314786	4.743984	52.316092	4.782016	86.78
Alpha	Taxiway	52.313878	4.742012	52.314866	4.770744	86.78
0927	Runway	52.316707	4.747895	52.318317	4.794818	86.78
Victor-1	Taxiway	52.343431	4.710999	52.341573	4.712509	153.63
Victor-2	Taxiway	52.337986	4.710545	52.336154	4.712046	153.31
Victor-4	Taxiway	52.330567	4.713801	52.328984	4.711512	41.24
Victor (North-South)	Taxiway	52.332980	4.712073	52.340706	4.712783	3.20
Whisky-6	Taxiway	52.316911	4.739614	52.314998	4.741181	153.34
Whisky-7	Taxiway	52.312161	4.738907	52.309895	4.740766	153.28

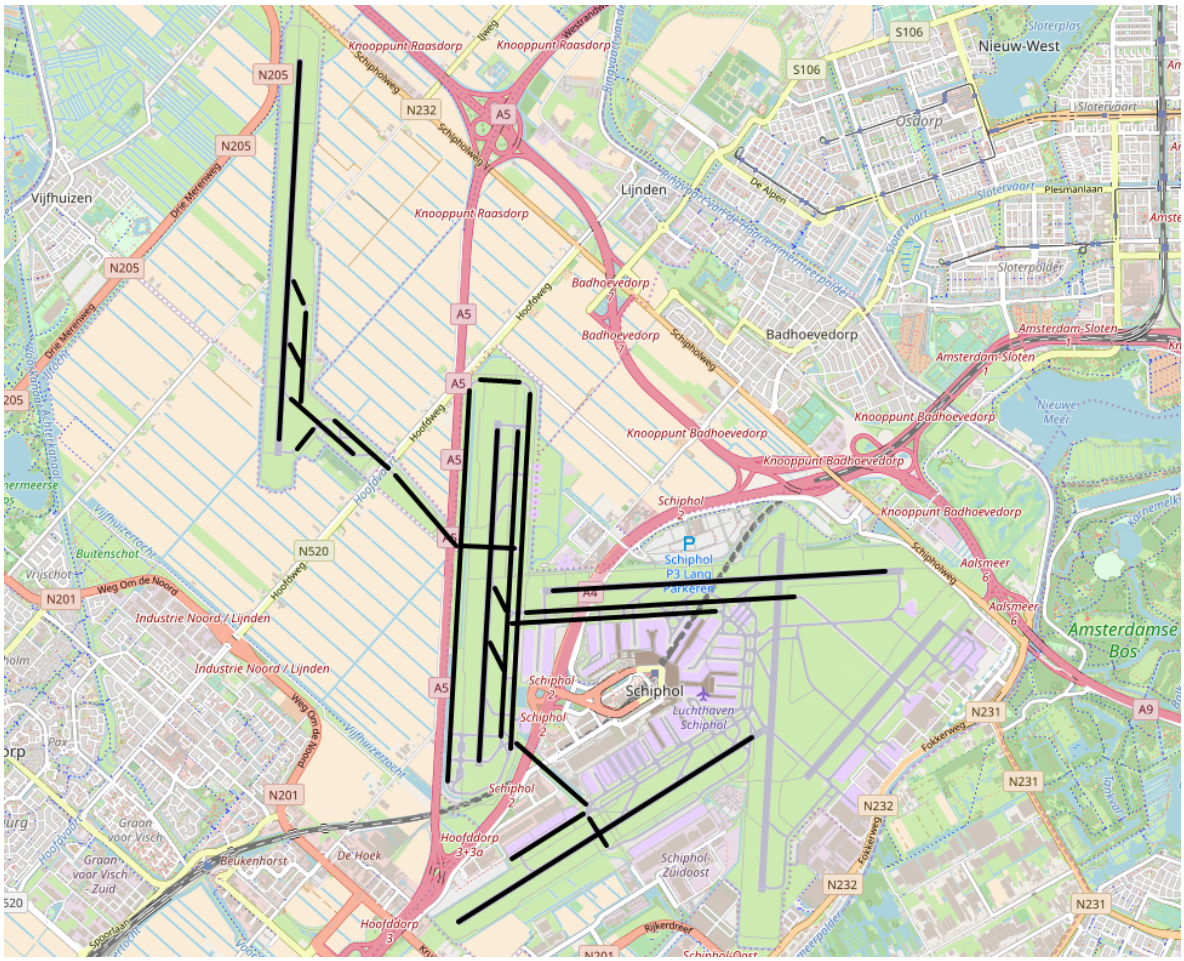

Figure A.1: Illustrated set of runways and taxiways at Amsterdam Airport Schiphol used for analysis

A.3 Runway track and BDS 5,0 track angle

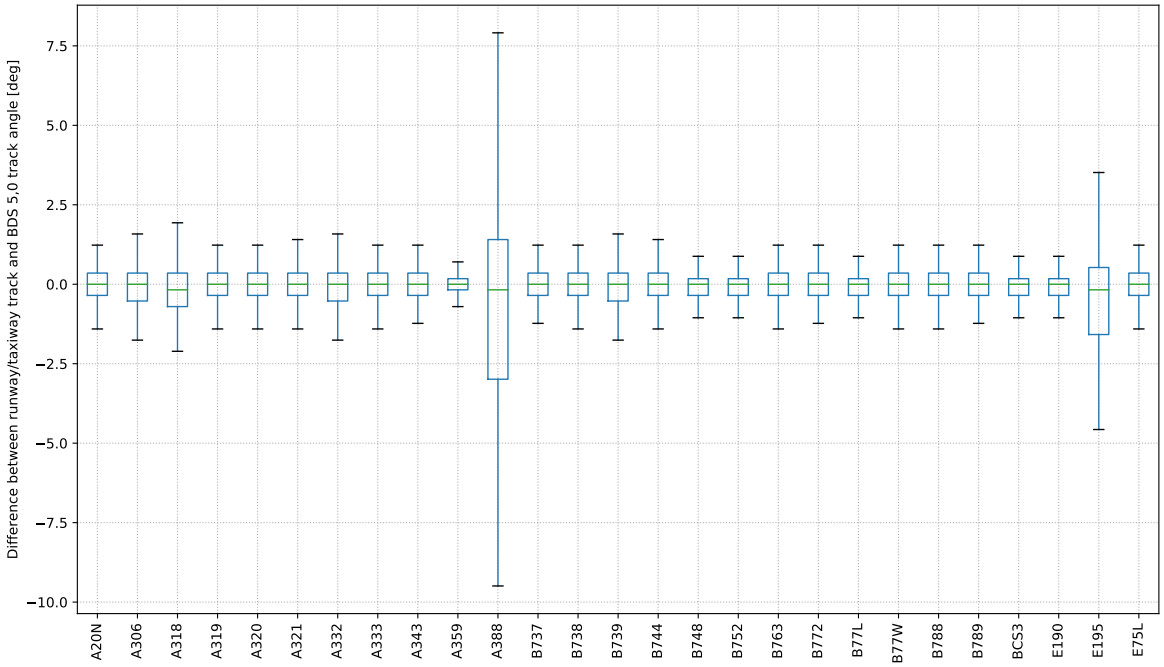

Figure A.2: Boxplots showing the difference between runway track and BDS 5,0 track angle per aircraft type

A.4 Runway track and BDS 6,0 magnetic heading

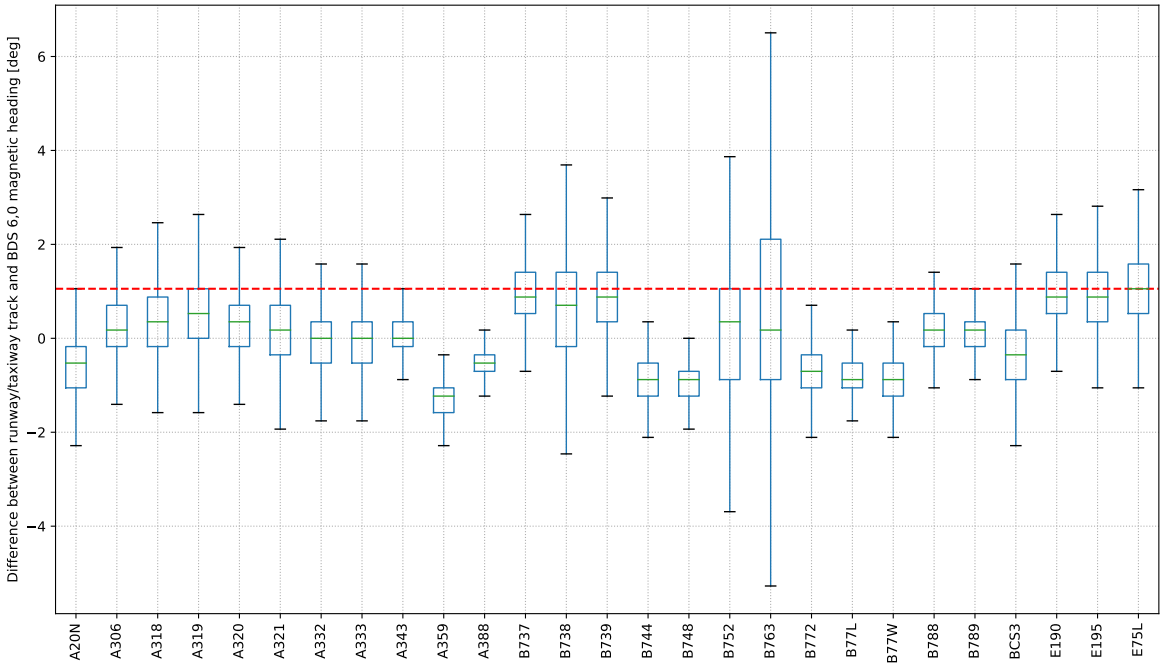

Figure A.3: Boxplots showing the difference between runway track and BDS 6,0 magnetic heading per aircraft type

A.5 BDS 5,0 track angle and BDS 6,0 magnetic heading

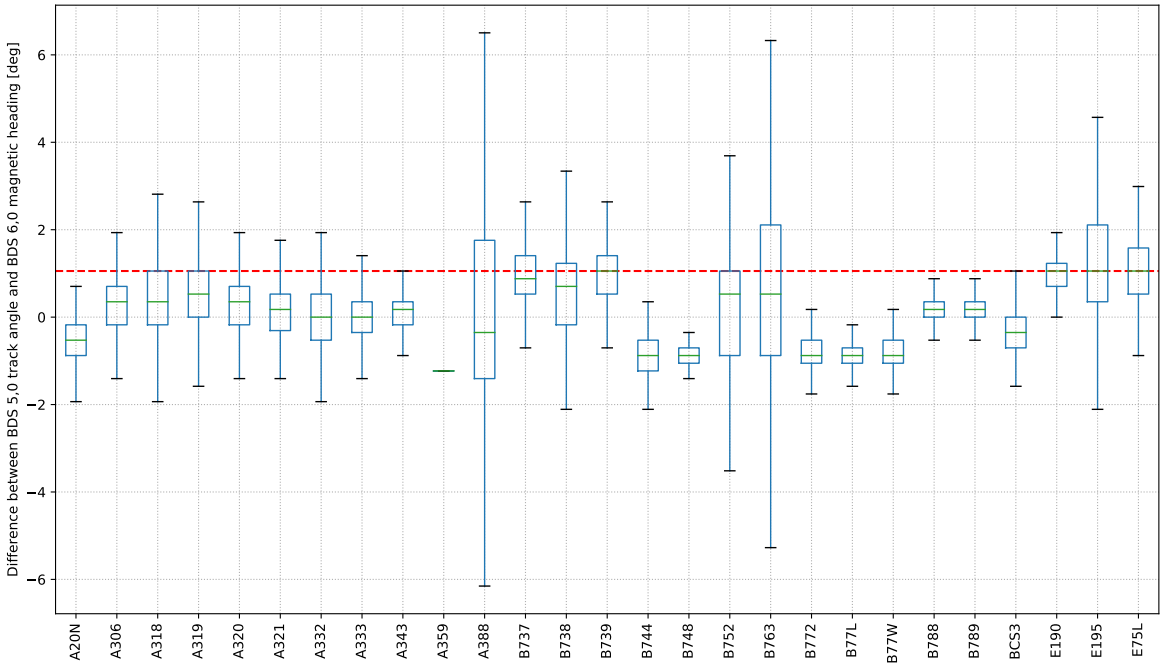

Figure A.4: Boxplots showing the difference between BDS 5,0 track angle and BDS 6,0 magnetic heading per aircraft type

A.6 Magnetic declination over time for a specific aircraft

Figure A.5 shows the boxplots for the difference between the runway track angle and the magnetic heading in BDS 6,0 per day for the aircraft with the highest number of BDS 6,0 signals (aircraft with ICAO address `484B92`, a B737 owned by KLM). Between 13 January and 19 April 2018, in total 4022 Mode S BDS 6,0 signals are received from this aircraft. Data before 13 January is not used, due to the low number of signals per day.

As can be seen in figure A.5, the daily median fluctuates around the magnetic declination, however the overall median of `484B92` is 1.055 degrees.

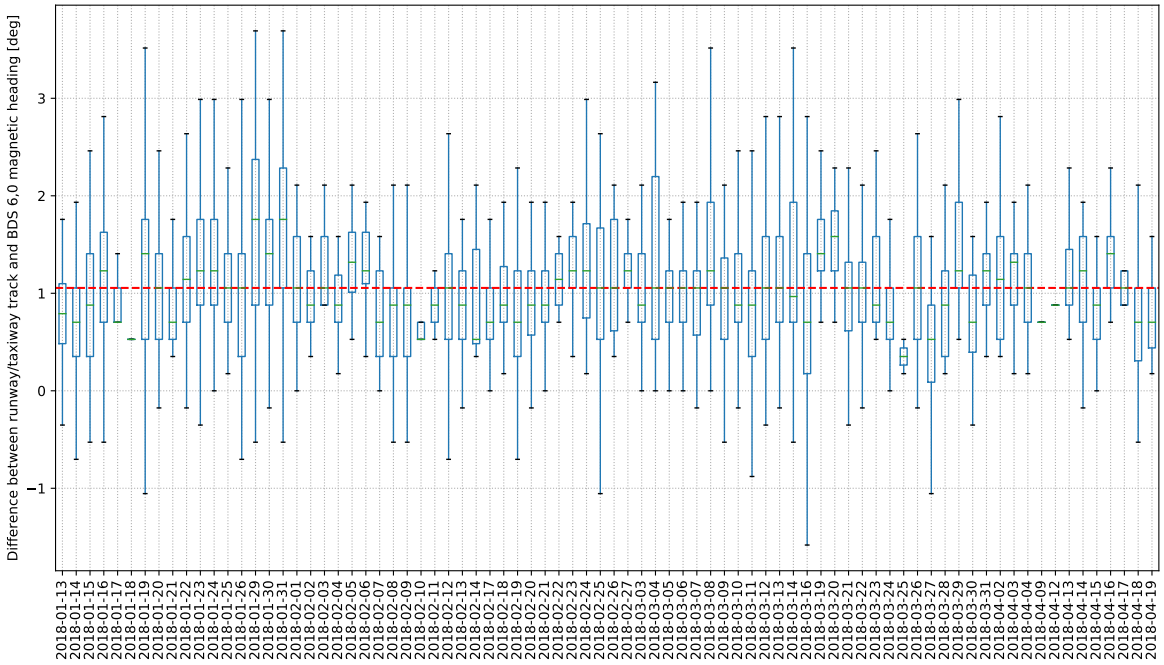

Figure A.5: Boxplots showing the difference between runway track angle and BDS 6,0 magnetic heading for ICAO address 484B92

Appendix B

Validation

B.1 On-board data and transmitted Mode S data

Received Mode S signals can contain errors due to aircraft measurements or transmissions and are compared with on-board data for BDS 5,0 and BDS 6,0 registers that are relevant for weather derivations. In table B.1, the mean error (ME), mean absolute error (MAE) and the mean squared error (MSE) are shown. The MAE for all parameters, except magnetic heading, are smaller than half the transmitted resolution in Mode S, which indicate that those parameters are the same as on-board instruments.

The transmitted magnetic heading in Mode S does not correspond with the value of the magnetic heading (from AHRS), neither the true heading (from FMS) or the true heading with magnetic variation (GPS) on-board.

Table B.1: Error in Mode S compared with Cessna on-board data

	ME	MAE	RMSE
True airspeed [kts]	0.11	0.69	3.66
Ground speed [kts]	0.21	0.70	3.54
Magnetic heading [deg]	0.25	0.77	5.28
Indicated airspeed [kts]	0.10	0.48	2.39
Mach number [-]	-0.000040	0.001217	0.005488

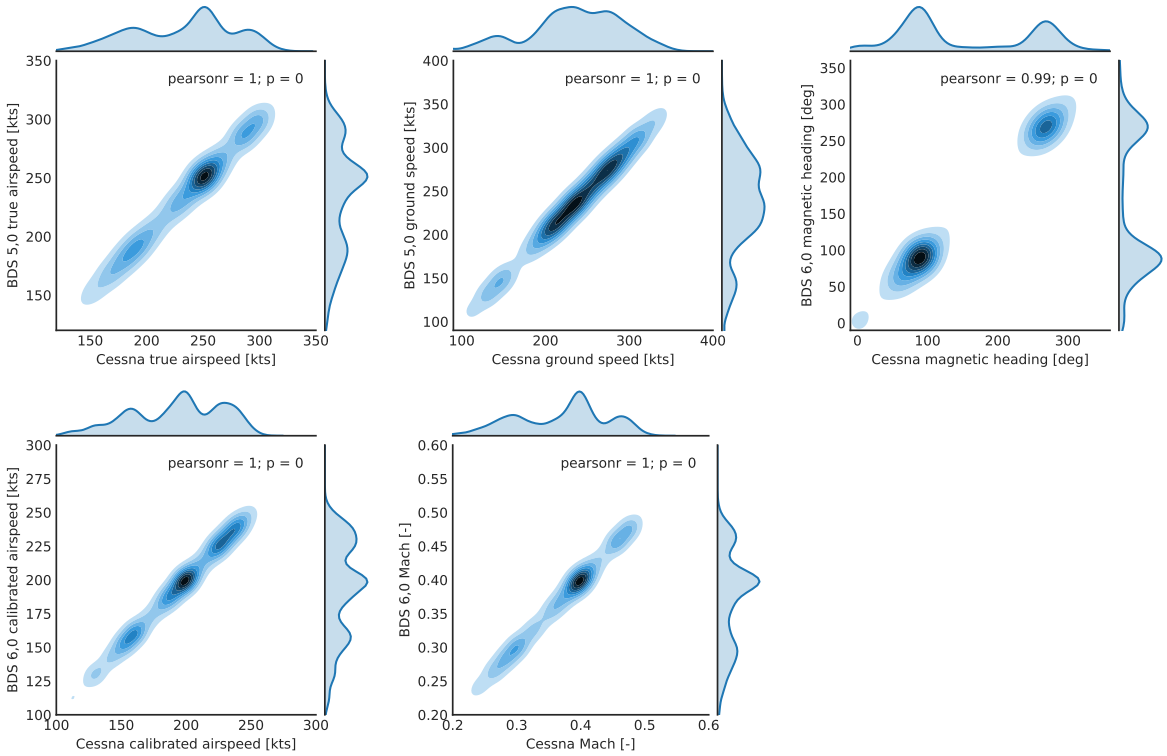

Figure B.1: Correlation plots Cessna versus Mode S

B.2 Correlation plots Cessna versus raw weather derivations (with corrections)

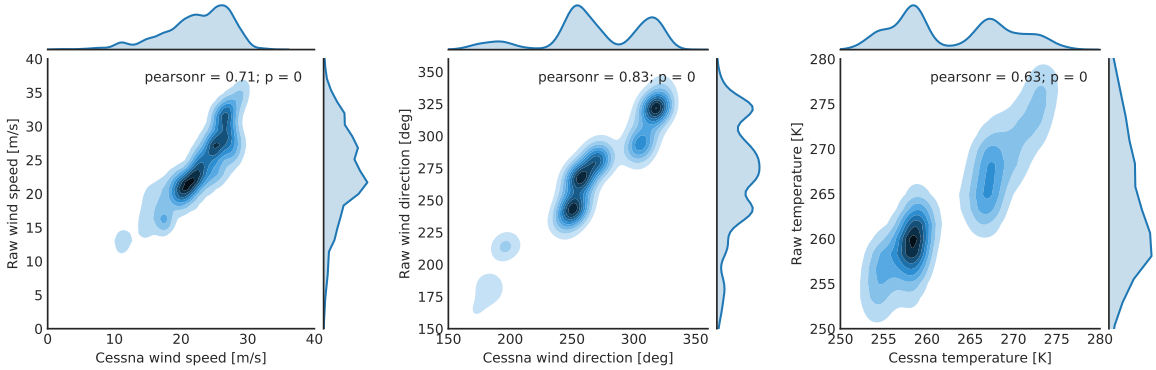

Figure B.2: Correlation plots Cessna versus raw weather derivations

B.3 Correlation plots Cessna versus MP model

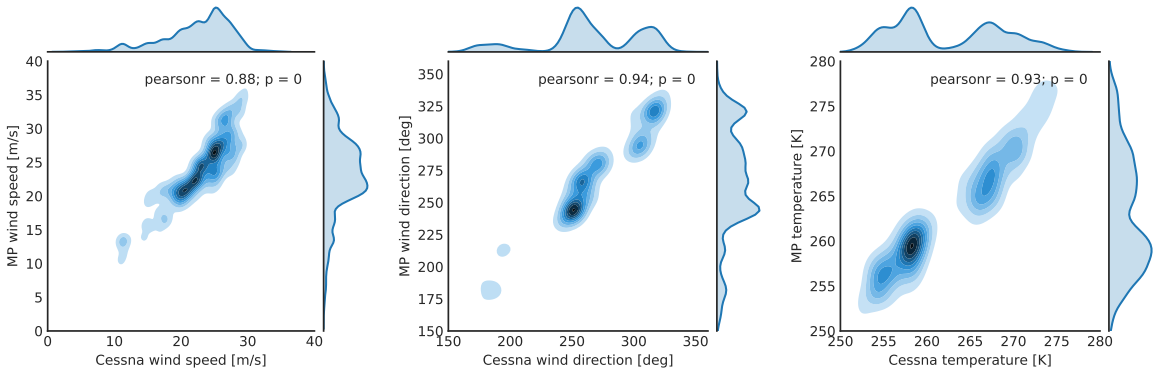

Figure B.3: Correlation plots NWP model versus MP model

B.4 Correlation plots NWP model versus MP model (with corrections)

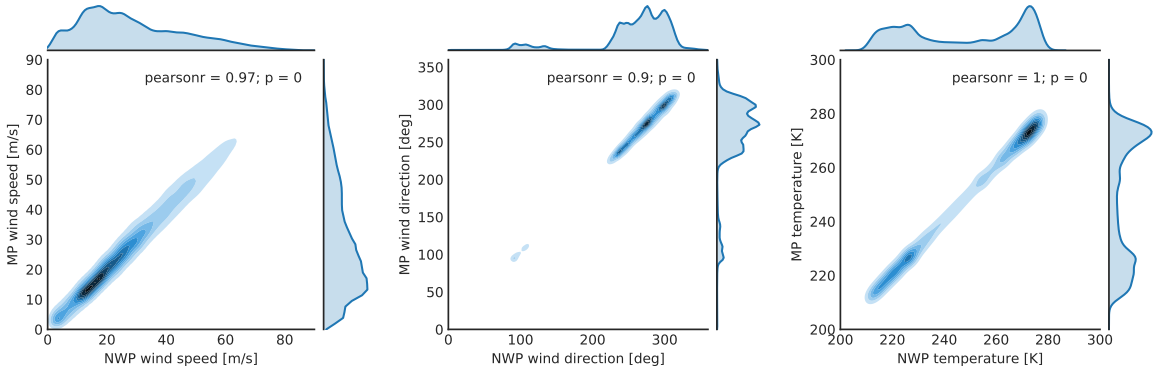

Figure B.4: Correlation plots NWP model versus MP model

B.5 NWP model vs MP mean error per altitude

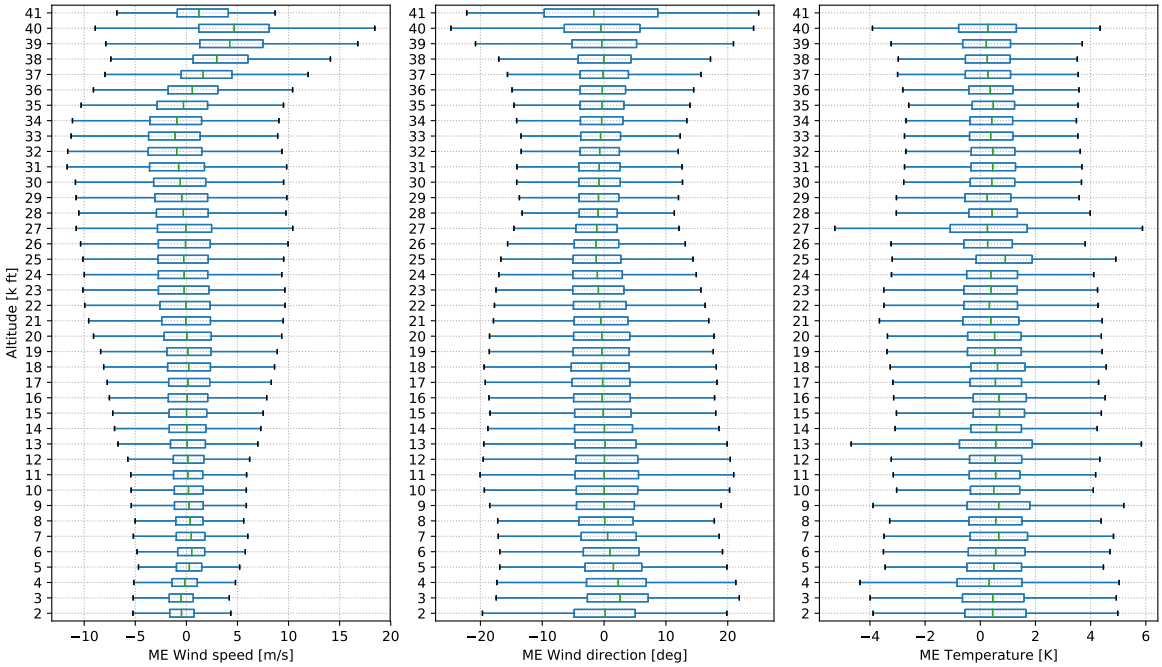

Appendix C

Aircraft Performance Parameters

Table C.1: Aircraft performance parameters A319 (speeds in m/s, Mach number dimensionless)

Phase	Parameter	Optimum	Min	Max	Distribution	Distr. parameters
CL, CAS	V_{GS}	214	183	246	norm	215 | 18
	V_{TAS}	214	194	234	norm	214 | 12
	V_{CAS}	148	136	160	norm	148 | 7
CL, Mach	V_{GS}	229	204	253	norm	229 | 14
	V_{TAS}	227	218	236	norm	227 | 5
	M	0.77	0.74	0.8	norm	0.77 | 0.02
CR	V_{GS}	226	202	250	norm	226 | 14
	V_{TAS}	228	215	237	beta	9 | 5 | 191 | 56
	V_{CAS}	127	121	140	gamma	6 | 114 | 2
	M	0.77	0.73	0.8	beta	10.59 | 5.40 | 0.64 | 0.19
DE, Mach	V_{GS}	223	196	250	norm	223 | 16
	V_{TAS}	226	211	236	beta	8 | 4 | 185 | 60
	M	0.76	0.72	0.8	beta	9.47 | 5.51 | 0.63 | 0.21
DE, CAS	V_{GS}	197	162	232	norm	197 | 21
	V_{TAS}	199	174	225	norm	199 | 15
	V_{CAS}	143	125	161	norm	143 | 10

Table C.2: Aircraft performance parameters A320 (speeds in m/s, Mach number dimensionless)

Phase	Parameter	Optimum	Min	Max	Distribution	Distr. parameters
CL, CAS	V_{GS}	216	185	246	norm	216 | 18
	V_{TAS}	214	195	233	norm	214 | 11
	V_{CAS}	148	139	163	gamma	15 | 121 | 1
CL, Mach	V_{GS}	229	202	255	norm	229 | 15
	V_{TAS}	227	216	236	beta	8 | 5 | 199 | 46
	M	0.77	0.73	0.8	beta	9.53 | 6.37 | 0.67 | 0.16
CR	V_{GS}	228	203	252	norm	228 | 14
	V_{TAS}	229	217	237	beta	11 | 5 | 192 | 53
	V_{CAS}	129	123	142	gamma	7 | 115 | 2
	M	0.78	0.74	0.8	beta	13.91 | 5.90 | 0.64 | 0.18
DE, Mach	V_{GS}	224	197	251	norm	224 | 16
	V_{TAS}	227	213	236	beta	8 | 4 | 191 | 53
	M	0.77	0.72	0.8	beta	8.77 | 5.30 | 0.65 | 0.18
DE, CAS	V_{GS}	202	167	237	norm	202 | 21
	V_{TAS}	203	178	227	norm	203 | 14
	V_{CAS}	143	126	161	norm	143 | 10

Table C.3: Aircraft performance parameters A321 (speeds in m/s, Mach number dimensionless)

Phase	Parameter	Optimum	Min	Max	Distribution	Distr. parameters
CL, CAS	V_{GS}	221	192	250	norm	221 | 17
	V_{TAS}	218	199	237	norm	218 | 11
	V_{CAS}	153	142	165	norm	153 | 6
CL, Mach	V_{GS}	231	205	258	norm	231 | 16
	V_{TAS}	228	221	236	norm	228 | 4
	M	0.77	0.75	0.8	norm	0.77 | 0.02
CR	V_{GS}	228	202	255	norm	228 | 15
	V_{TAS}	229	221	236	norm	229 | 4
	V_{CAS}	135	127	144	norm	136 | 5
	M	0.78	0.75	0.8	norm	0.78 | 0.01
DE, Mach	V_{GS}	221	190	252	norm	221 | 18
	V_{TAS}	225	212	237	norm	225 | 7
	M	0.76	0.71	0.8	beta	4.95 | 3.16 | 0.66 | 0.16
DE, CAS	V_{GS}	201	164	238	norm	201 | 22
	V_{TAS}	199	181	235	gamma	9 | 154 | 5
	V_{CAS}	144	126	162	norm	144 | 10

Table C.4: Aircraft performance parameters A332 (speeds in m/s, Mach number dimensionless)

Phase	Parameter	Optimum	Min	Max	Distribution	Distr. parameters
CL, CAS	V_{GS}	223	192	253	norm	223 | 18
	V_{TAS}	229	195	240	beta	5 | 1 | 155 | 89
	V_{CAS}	153	143	163	norm	153 | 6
CL, Mach	V_{GS}	238	214	262	norm	238 | 14
	V_{TAS}	237	228	247	norm	237 | 5
	M	0.8	0.78	0.83	norm	0.81 | 0.02
CR	V_{GS}	239	216	262	norm	239 | 13
	V_{TAS}	239	230	248	norm	239 | 5
	V_{CAS}	130	123	148	gamma	4 | 117 | 3
	M	0.81	0.78	0.84	norm	0.81 | 0.02
DE, Mach	V_{GS}	237	212	262	norm	237 | 15
	V_{TAS}	238	228	248	norm	238 | 6
	M	0.8	0.77	0.84	norm	0.80 | 0.02
DE, CAS	V_{GS}	211	177	245	norm	211 | 20
	V_{TAS}	218	186	235	beta	3 | 2 | 160 | 82
	V_{CAS}	146	131	160	norm	146 | 8

Table C.5: Aircraft performance parameters A333 (speeds in m/s, Mach number dimensionless)

Phase	Parameter	Optimum	Min	Max	Distribution	Distr. parameters
CL, CAS	V_{GS}	221	193	248	norm	221 | 16
	V_{TAS}	220	202	239	norm	220 | 11
	V_{CAS}	156	146	166	norm	156 | 5
CL, Mach	V_{GS}	237	212	261	norm	237 | 14
	V_{TAS}	238	229	247	norm	238 | 5
	M	0.81	0.78	0.83	norm	0.81 | 0.02
CR	V_{GS}	240	217	263	norm	240 | 14
	V_{TAS}	239	231	248	norm	239 | 5
	V_{CAS}	131	124	149	gamma	4 | 118 | 3
	M	0.81	0.79	0.83	norm	0.81 | 0.01
DE, Mach	V_{GS}	236	208	265	norm	237 | 17
	V_{TAS}	236	223	249	norm	236 | 7
	M	0.81	0.75	0.83	beta	4.58 | 2.16 | 0.69 | 0.15
DE, CAS	V_{GS}	208	172	245	norm	209 | 22
	V_{TAS}	213	181	234	beta	3 | 2 | 155 | 90
	V_{CAS}	151	125	161	beta	2 | 1 | 110 | 54

Table C.6: Aircraft performance parameters A388 (speeds in m/s, Mach number dimensionless)

Phase	Parameter	Optimum	Min	Max	Distribution	Distr. parameters
CL, CAS	V_{GS}	240	214	267	norm	240 | 16
	V_{TAS}	236	223	250	norm	236 | 8
	V_{CAS}	162	155	168	norm	162 | 3
CL, Mach	V_{GS}	252	229	275	norm	252 | 14
	V_{TAS}	247	240	253	norm	247 | 3
	M	0.84	0.82	0.85	norm	0.84 | 0.01
CR	V_{GS}	249	225	272	norm	249 | 14
	V_{TAS}	248	240	257	norm	249 | 5
	V_{CAS}	134	128	154	gamma	3 | 122 | 4
	M	0.84	0.82	0.86	norm	0.84 | 0.02
DE, Mach	V_{GS}	243	216	269	norm	243 | 15
	V_{TAS}	245	232	258	norm	245 | 7
	M	0.83	0.79	0.87	norm	0.83 | 0.03
DE, CAS	V_{GS}	215	177	254	norm	215 | 23
	V_{TAS}	223	191	247	beta	2 | 2 | 172 | 85
	V_{CAS}	152	126	165	beta	2 | 1 | 115 | 53

Table C.7: Aircraft performance parameters B737 (speeds in m/s, Mach number dimensionless)

Phase	Parameter	Optimum	Min	Max	Distribution	Distr. parameters
CL, CAS	V_{GS}	212	187	237	norm	212 | 15
	V_{TAS}	213	196	230	norm	213 | 10
	V_{CAS}	147	138	164	gamma	11 | 122 | 2
CL, Mach	V_{GS}	228	206	250	norm	228 | 13
	V_{TAS}	229	221	237	norm	229 | 4
	M	0.78	0.75	0.8	norm	0.78 | 0.01
CR	V_{GS}	229	206	252	norm	229 | 14
	V_{TAS}	230	217	240	beta	9 | 4 | 192 | 56
	V_{CAS}	124	116	142	gamma	5 | 109 | 3
	M	0.77	0.74	0.81	norm	0.77 | 0.02
DE, Mach	V_{GS}	226	201	252	norm	226 | 15
	V_{TAS}	227	216	239	norm	227 | 6
	M	0.77	0.73	0.8	beta	10.62 | 4.05 | 0.62 | 0.21
DE, CAS	V_{GS}	200	166	234	norm	200 | 20
	V_{TAS}	201	175	226	norm	201 | 15
	V_{CAS}	144	126	162	norm	144 | 11

Table C.8: Aircraft performance parameters B738 (speeds in m/s, Mach number dimensionless)

Phase	Parameter	Optimum	Min	Max	Distribution	Distr. parameters
CL, CAS	V_{GS}	215	187	242	norm	215 | 16
	V_{TAS}	215	198	232	norm	215 | 10
	V_{CAS}	149	139	159	norm	149 | 6
CL, Mach	V_{GS}	228	204	253	norm	228 | 14
	V_{TAS}	228	220	236	norm	228 | 5
	M	0.77	0.75	0.8	norm	0.77 | 0.02
CR	V_{GS}	227	204	250	norm	227 | 14
	V_{TAS}	229	216	237	beta	10 | 4 | 190 | 54
	V_{CAS}	127	121	139	gamma	8 | 114 | 1
	M	0.77	0.73	0.8	beta	12.51 | 5.38 | 0.64 | 0.19
DE, Mach	V_{GS}	225	198	251	norm	225 | 16
	V_{TAS}	227	211	237	beta	6 | 3 | 191 | 54
	M	0.77	0.72	0.8	beta	6.93 | 4.15 | 0.65 | 0.18
DE, CAS	V_{GS}	199	163	236	norm	199 | 22
	V_{TAS}	203	173	227	beta	4 | 3 | 146 | 96
	V_{CAS}	140	121	158	beta	3 | 3 | 107 | 65

Table C.9: Aircraft performance parameters B739 (speeds in m/s, Mach number dimensionless)

Phase	Parameter	Optimum	Min	Max	Distribution	Distr. parameters
CL, CAS	V_{GS}	219	194	245	norm	219 | 15
	V_{TAS}	217	200	233	norm	217 | 10
	V_{CAS}	156	144	168	norm	156 | 7
CL, Mach	V_{GS}	234	208	260	norm	234 | 15
	V_{TAS}	231	223	239	norm	231 | 4
	M	0.78	0.76	0.81	norm	0.78 | 0.02
CR	V_{GS}	229	201	257	norm	229 | 17
	V_{TAS}	230	222	238	norm	230 | 4
	V_{CAS}	135	124	145	norm	135 | 6
	M	0.78	0.76	0.8	norm	0.78 | 0.01
DE, Mach	V_{GS}	221	192	250	norm	221 | 17
	V_{TAS}	227	215	239	norm	227 | 7
	M	0.77	0.73	0.81	norm	0.77 | 0.02
DE, CAS	V_{GS}	202	167	237	norm	202 | 21
	V_{TAS}	205	179	232	norm	205 | 16
	V_{CAS}	145	125	164	norm	145 | 11

Table C.10: Aircraft performance parameters B744 (speeds in m/s, Mach number dimensionless)

Phase	Parameter	Optimum	Min	Max	Distribution	Distr. parameters
CL, CAS	V_{GS}	238	214	263	norm	238 | 14
	V_{TAS}	242	218	254	beta	5 | 2 | 188 | 73
	V_{CAS}	169	159	180	norm	169 | 6
CL, Mach	V_{GS}	249	224	274	norm	249 | 14
	V_{TAS}	248	241	256	norm	248 | 4
	M	0.84	0.82	0.86	norm	0.84 | 0.01
CR	V_{GS}	248	223	272	norm	248 | 14
	V_{TAS}	247	238	257	norm	247 | 6
	V_{CAS}	141	132	165	gamma	5 | 122 | 4
	M	0.84	0.81	0.87	norm	0.84 | 0.02
DE, Mach	V_{GS}	241	210	271	norm	241 | 18
	V_{TAS}	243	222	258	beta	2 | 2 | 210 | 54
	M	0.82	0.75	0.87	beta	2.67 | 2.10 | 0.72 | 0.17
DE, CAS	V_{GS}	213	177	250	norm	213 | 22
	V_{TAS}	214	189	239	norm	214 | 15
	V_{CAS}	148	130	166	norm	148 | 10

Table C.11: Aircraft performance parameters B752 (speeds in m/s, Mach number dimensionless)

Phase	Parameter	Optimum	Min	Max	Distribution	Distr. parameters
CL, CAS	V_{GS}	223	194	252	norm	223 | 17
	V_{TAS}	224	207	240	norm	224 | 10
	V_{CAS}	155	143	166	norm	155 | 6
CL, Mach	V_{GS}	230	204	257	norm	230 | 15
	V_{TAS}	232	223	242	norm	232 | 5
	M	0.79	0.76	0.82	norm	0.79 | 0.02
CR	V_{GS}	232	208	256	norm	232 | 14
	V_{TAS}	234	225	243	norm	234 | 5
	V_{CAS}	131	123	149	gamma	5 | 115 | 3
	M	0.79	0.76	0.82	norm	0.79 | 0.02
DE, Mach	V_{GS}	229	203	256	norm	229 | 16
	V_{TAS}	232	221	243	norm	232 | 6
	M	0.78	0.75	0.82	norm	0.78 | 0.02
DE, CAS	V_{GS}	214	181	248	norm	214 | 20
	V_{TAS}	217	195	238	norm	217 | 13
	V_{CAS}	152	135	169	norm	152 | 10

Table C.12: Aircraft performance parameters B763 (speeds in m/s, Mach number dimensionless)

Phase	Parameter	Optimum	Min	Max	Distribution	Distr. parameters
CL, CAS	V_{GS}	226	199	253	norm	226 | 16
	V_{TAS}	228	214	242	norm	228 | 8
	V_{CAS}	159	150	169	norm	159 | 5
CL, Mach	V_{GS}	232	205	259	norm	232 | 16
	V_{TAS}	234	226	243	norm	235 | 4
	M	0.79	0.77	0.82	norm	0.79 | 0.02
CR	V_{GS}	237	211	262	norm	237 | 15
	V_{TAS}	236	227	245	norm	236 | 5
	V_{CAS}	137	127	159	gamma	6 | 115 | 3
	M	0.8	0.77	0.83	norm	0.80 | 0.02
DE, Mach	V_{GS}	235	206	265	norm	235 | 17
	V_{TAS}	233	221	246	norm	233 | 7
	M	0.79	0.75	0.83	norm	0.79 | 0.02
DE, CAS	V_{GS}	217	180	254	norm	217 | 22
	V_{TAS}	223	185	238	beta	3 | 1 | 154 | 90
	V_{CAS}	150	132	168	norm	150 | 10

Table C.13: Aircraft performance parameters B77W (speeds in m/s, Mach number dimensionless)

Phase	Parameter	Optimum	Min	Max	Distribution	Distr. parameters
CL, CAS	V_{GS}	238	212	264	norm	238 | 15
	V_{TAS}	234	223	245	norm	234 | 6
	V_{CAS}	163	157	168	beta	12 | 5 | 141 | 31
CL, Mach	V_{GS}	250	224	277	norm	250 | 16
	V_{TAS}	246	240	252	norm	246 | 3
	M	0.83	0.82	0.85	norm	0.83 | 0.01
CR	V_{GS}	245	218	272	norm	245 | 16
	V_{TAS}	245	237	253	norm	245 | 4
	V_{CAS}	148	134	163	beta	2 | 3 | 126 | 46
	M	0.83	0.8	0.85	beta	17.14 | 7.05 | 0.72 | 0.16
DE, Mach	V_{GS}	231	200	262	norm	231 | 18
	V_{TAS}	236	219	253	norm	236 | 10
	M	0.8	0.74	0.86	norm	0.80 | 0.04
DE, CAS	V_{GS}	206	170	242	norm	206 | 21
	V_{TAS}	213	186	237	beta	2 | 2 | 170 | 79
	V_{CAS}	144	127	164	beta	2 | 2 | 121 | 51

Table C.14: Aircraft performance parameters B788 (speeds in m/s, Mach number dimensionless)

Phase	Parameter	Optimum	Min	Max	Distribution	Distr. parameters
CL, CAS	V_{GS}	240	209	270	norm	240 | 18
	V_{TAS}	242	214	251	beta	4 | 1 | 188 | 67
	V_{CAS}	155	147	164	norm	155 | 5
CL, Mach	V_{GS}	254	234	274	norm	254 | 12
	V_{TAS}	249	243	255	norm	249 | 3
	M	0.84	0.83	0.86	norm	0.84 | 0.01
CR	V_{GS}	249	226	272	norm	249 | 14
	V_{TAS}	249	240	258	norm	249 | 5
	V_{CAS}	133	127	149	gamma	4 | 121 | 3
	M	0.85	0.81	0.87	beta	10.82 | 3.86 | 0.72 | 0.16
DE, Mach	V_{GS}	243	215	272	norm	243 | 17
	V_{TAS}	245	231	259	norm	245 | 8
	M	0.83	0.77	0.87	beta	4.50 | 2.52 | 0.72 | 0.17
DE, CAS	V_{GS}	211	175	247	norm	211 | 22
	V_{TAS}	213	191	243	beta	1 | 1 | 184 | 69
	V_{CAS}	143	125	162	beta	1 | 1 | 118 | 50

Table C.15: Aircraft performance parameters B789 (speeds in m/s, Mach number dimensionless)

Phase	Parameter	Optimum	Min	Max	Distribution	Distr. parameters
CL, CAS	V_{GS}	240	212	267	norm	240 | 16
	V_{TAS}	240	216	252	beta	3 | 1 | 201 | 54
	V_{CAS}	164	153	176	norm	164 | 7
CL, Mach	V_{GS}	251	227	275	norm	251 | 14
	V_{TAS}	249	242	255	norm	249 | 3
	M	0.84	0.82	0.86	norm	0.84 | 0.01
CR	V_{GS}	249	226	272	norm	249 | 14
	V_{TAS}	249	240	258	norm	249 | 5
	V_{CAS}	141	128	154	norm	141 | 7
	M	0.84	0.82	0.87	norm	0.84 | 0.02
DE, Mach	V_{GS}	243	217	270	norm	243 | 16
	V_{TAS}	245	232	258	norm	245 | 8
	M	0.84	0.78	0.87	beta	3.58 | 2.03 | 0.74 | 0.15
DE, CAS	V_{GS}	216	179	253	norm	216 | 22
	V_{TAS}	224	191	246	beta	1 | 1 | 180 | 73
	V_{CAS}	145	126	167	beta	1 | 1 | 120 | 54

Table C.16: Aircraft performance parameters E190 (speeds in m/s, Mach number dimensionless)

Phase	Parameter	Optimum	Min	Max	Distribution	Distr. parameters
CL, CAS	V_{GS}	201	166	236	norm	201 | 21
	V_{TAS}	203	175	227	beta	2 | 2 | 158 | 80
	V_{CAS}	140	134	156	gamma	5 | 128 | 2
CL, Mach	V_{GS}	224	198	250	norm	224 | 15
	V_{TAS}	223	213	233	norm	223 | 6
	M	0.76	0.72	0.79	norm	0.76 | 0.02
CR	V_{GS}	229	204	253	norm	229 | 15
	V_{TAS}	229	221	237	norm	229 | 5
	V_{CAS}	133	120	146	norm	133 | 7
	M	0.78	0.75	0.8	norm	0.78 | 0.02
DE, Mach	V_{GS}	225	198	252	norm	225 | 16
	V_{TAS}	225	215	235	norm	225 | 5
	M	0.76	0.73	0.79	norm	0.76 | 0.02
DE, CAS	V_{GS}	200	169	231	norm	200 | 18
	V_{TAS}	201	179	223	norm	201 | 13
	V_{CAS}	145	132	159	norm	145 | 8

Part III

Preliminary Report

Chapter 1

Introduction

Air traffic increased over the past years and Airbus and Boeing are expecting a growth in air traffic of almost five percent a year for the coming twenty years [2, 3]. To increase efficiency in Air Traffic Management (ATM), EUROCONTROL and the Federal Aviation Administration (FAA) has setup the programs SESAR and NextGen respectively. To increase surveillance, all commercial aircraft are required to have transponders onboard in Europe and the United States by 2020 [4, 5]. With the transponder, aircraft can transmit information, periodically via Automatic Dependent Surveillance - Broadcast (ADS-B) or on request (interrogation) by Air Traffic Control (ATC) with the Secondary Surveillance Radar (SSR) via Mode A/C/S. ADS-B is nowadays already implemented in the majority of aircraft. Via ADS-B, position, altitude, ground speed, heading and vertical velocity are broadcasted. Next to ADS-B, ATC can interrogate aircraft with Mode A/C for identification and altitude information. Via Mode S (selective) the SSR can interrogate for Downlink Aircraft Parameters (DAP) from individual aircraft [6]. These DAPs contain, for example, aircraft state and intent data, which are called Mode S Enhanced Surveillance (EHS). Mode S EHS includes for example selected altitude, indicated airspeed, roll angle and track angle/rate. With Mode S it is also possible to obtain direct weather information measured onboard via Meteorological Routine Air Report (MRAR).

ADS-B and Mode S signals transmitted by aircraft can be received by everyone within line-of-sight with low-cost hardware receivers and can therefore be considered as 'open data' [7]. Popular online flight trackers, like FlightRadar24, use these signals to show real-time aircraft location and information.

For trajectory planning, meteorological conditions (temperature and wind), aircraft performance (weight and thrust, aerodynamics) and navigation performance (aircraft intent, pilot skills) are important variables [8, 9].

For the BlueSky simulator [10], developed by C&S/ATM section of Aerospace Engineering of the Delft University of Technology, ADS-B data has been used to build a database with aircraft performance parameters [11–15], because aircraft performance parameters are usually kept confidential by aircraft manufacturers and airlines. Since only ground speed is broadcast with ADS-B, an accurate method for determining True airspeed (TAS) should be developed. TAS is considered as one of the most influencing factors for deriving aircraft performance parameters.

The goal of this thesis project is to improve aircraft performance parameters, that already have been obtained in earlier research for BlueSky [10], by using additional Mode S EHS and MRAR data to construct meteorological models, as well as using the results to derive the TAS of aircraft.

1.1 Thesis objective and research questions

The objective of this research is: *Using ADS-B and Mode S signals to build accurate meteorological models and using these models to improve aircraft performance models.*

1.1.1 Research questions

The following sub-questions should help towards the research objective:

1. With which aircraft does the Mode S signal originate?
2. What is the location of the aircraft?
3. What is the quality of the received Mode S signals?
   (a) What percentage of the signals is corrupt?
   (b) What percentage of the signals is not decodable?
4. What is the quality of Mode S signals in comparison to ADS-B?
5. What is the content in the received Mode S signal?
6. What is the availability of Mode S signals?
7. How can Mode S signals be used to build meteorological models (temperature and wind speed/direction)?
8. How can a meteorological model improve aircraft performance parameters?

1.2 Methodology

At the roof of the Delft University of Technology Aerospace Engineering faculty an ADS-B/Mode S receiver is installed that is capable of receiving signals from aircraft in line-of-sight. This receiver is running continuously and the raw data is stored daily on a server. ADS-B and Mode S signals are stored in separate files.

The research can be divided in four parts: signal pre-processing, signal analysis, building the meteorological model and application of the model.

1.2.1 Signal pre-processing

In Mode S, no information is included about the position of the aircraft because with the primary radar, the position can be determined. This information is not available during this research, and therefore ADS-B data will be used instead. The interval between received ADS-B positions is irregular, and therefore ADS-B data will be interpolated (resampled) first.

Since the SSR expects a reply from a certain aircraft, the parity (data check) in the reply contains (partly) the ICAO address of that aircraft. An initial guess of the aircraft will be done based on the parity of the received Mode S signal. However, when the signal contains transmission errors, this will lead to a wrong ICAO address. Therefore, Mode S will be combined with ADS-B to develop an alternative method to check whether the signal contains transmission errors. This should result in signals without transmission errors with correct ICAO address.

1.2.2 Signal analysis

The next step will be determining the content of a Mode S signal. In the signal is also not included what information it contains and therefore a solid method will be developed to determine the correct parameters. Because from signal pre-processing only signals will be used that are considered as error free, determining the content will be easier.

Knowing the signal is correct, the parameters can still contain errors due to measurements onboard. These errors should be detected, improved and verified.

1.2.3 Meteorological model

When the information in Mode S is verified, meteorological derivations will be applied and a meteorological model will be built.

To assess the quality of the received signals and the developed meteorological interpolation model, flight data from the TU Delft/NLR aircraft PH-LAB Cessna Citation II with aircraft parameters and wind information will be used when available. Since the flight data of the TU Delft aircraft is limited and very local, the meteorological model will also be compared to a numerical weather prediction (NWP) model.

1.2.4 Apply meteorological model

The meteorological model will be used to obtain the true airspeed of aircraft and to improve aircraft performance parameters.

1.3 Thesis overview

In figure 1.1, a flowchart is shown with all steps that should be taken from RAW ADS-B and Mode S data to an application of the meteorological model. The dotted lines from literature review indicate in which parts it is used.

1.4 Outline of the report

This report is built-up as follows: in chapter 2 and 3 Mode A, Mode C and Mode S will be explained. Before deriving meteorological conditions, first the International Standard Atmosphere and different airspeeds will be discussed in chapter 4. Chapter 5 contains a literature review of research that has been conducted on meteorological derivations from aircraft data. In chapter 6 a start is given to processing the signals.

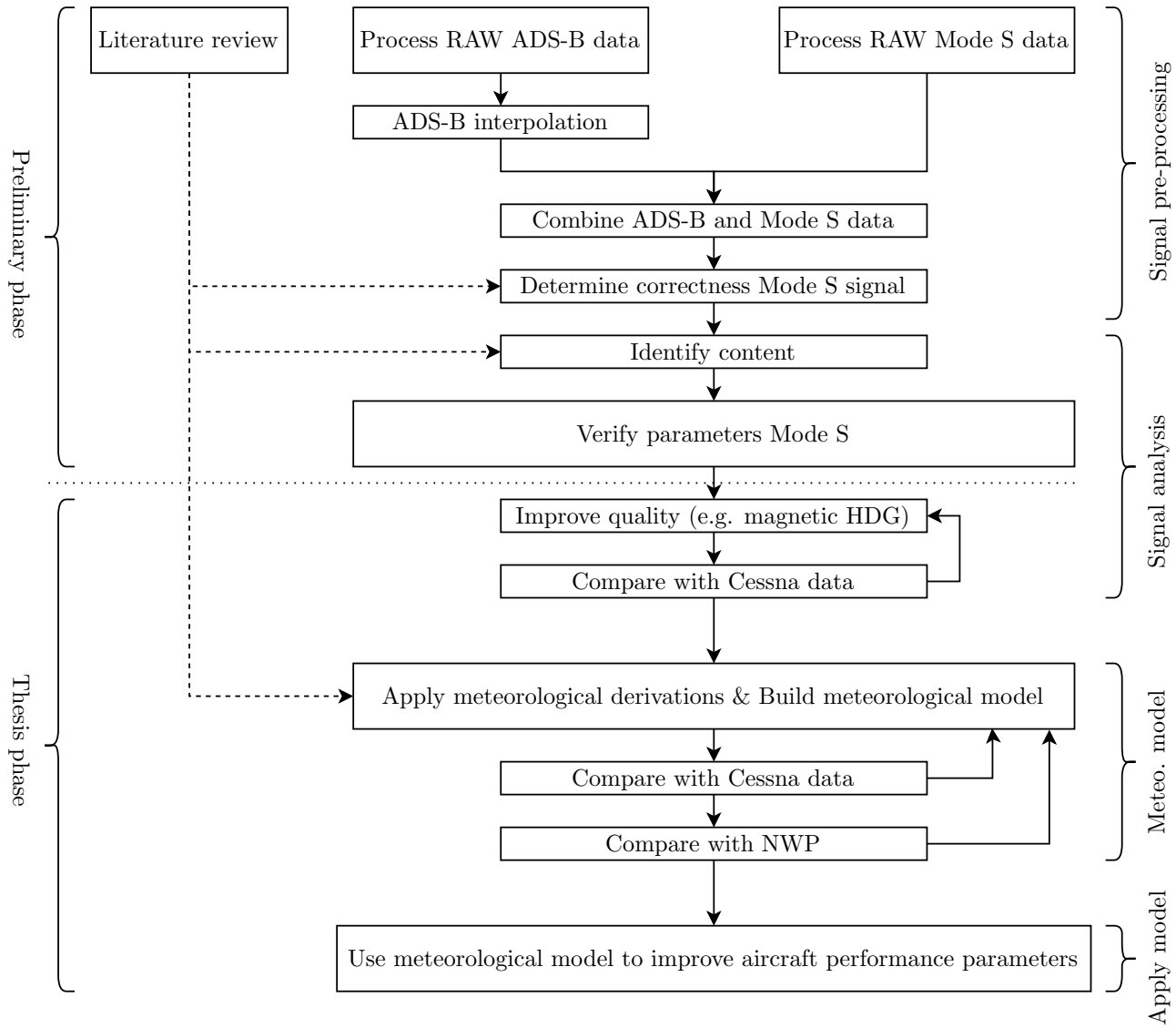

Figure 1.1: Flowchart showing process from RAW data to application

Chapter 2

Mode A, Mode C and Mode S

Nowadays air traffic surveillance is done with a Primary Surveillance Radar (PR) and a secondary surveillance radar (SSR). A primary radar works with passive echoes [16]: the radar transmits an electromagnetic wave and measures the direction and the time between the transmitted and reflected signal from aircraft. Primary radars determine the presence, slant distance and azimuth of aircraft, but are not able to obtain the identity. To obtain the identity of the aircraft, the SSR is used. Usually an SSR is mounted on top of a PR and has a horizontal beam width of 2 to 3 degrees [6]. The SSR is a cooperative surveillance method, which requires aircraft to be equipped with a transponder (transmitter and responder), while the PR is non-cooperative (independent), it does not require the installation of aircraft transponders. The SSR can interrogate aircraft by three modes: Mode A, Mode C and Mode S.

2.1 Mode A/C

In Mode A, aircraft reply with four-digit octal codes for aircraft identification purpose (squawk code), which is assigned by ATC and set in the cockpit by the pilot. The squawk code consists of 12 bits and therefore 4096 squawk codes are possible (2^{12}). Some identity codes are reserved for indicating emergency conditions (set by International Civil Aviation Organization (ICAO) worldwide), for instance 7500 for aircraft hijacking (unlawful interference), 7600 for radio failure/lost communication and 7700 for emergency. In Mode A, a special position identification (SPI) may be transmitted on ATC request to further aid in identification of an individual aircraft.

Mode C provide pressure-altitude reporting, encoded with 100 ft resolution.

Mode A/C interrogations are unaddressed, which means that all aircraft in the main beam of the SSR shall reply. In high traffic areas, the SSR can receive too many replies, and result in FRUIT and garbling.

2.1.1 Limitations of Mode A/C

Mode A/C has some limitations in its use. These are FRUIT, garbling, over-interrogation and limited aircraft identification [6].

FRUIT is an acronym of False Replies Unsynchronized in Time or False Replies Unsynchronised to Interrogator Transmission. These are unwanted replies received by an interrogator that have been interrogated by another SSR [1]. This happens in areas covered by multiple SSRs. FRUIT can be detected because SSRs have different Pulse repetition frequencies (PRT), which is the number of pulses transmitted per second by an SSR.

ICAO defines garbling as the overlapping in range and/or azimuth of two or more SSR replies so that the pulse positions of one reply fall close to or overlap the pulse positions of another reply, making the decoding resulting of the reply resulting in error [1]. Garbling occurs when two aircraft are within about 3 degree in azimuth and when the slant range is less than 1.64 nm [6]. There are three different types of garbling:

- Synchronous garbling: the signal meets all specification in time and amplitude, and can appear as a new reply which no aircraft have sent. The two signals are indistinguishable and cannot be recovered
- Asynchronous garbling: the resulting signal does not meet the necessary time scales and therefore do not appear as ghost codes. These signals are potentially distinguishable and can be recovered
- Multipath, the echo has a lower amplitude than the direct signal, which can be detected and the original signal can be recovered

Other problems with Mode A/C are over-interrogation and the number of possible Mode A codes. In an area with many SSR, it is possible that the transponder receives a high rate of interrogations and is unable to reply in time for all interrogation. In Mode A only 4096 squawk codes are available. With increasing air traffic, these combinations are insufficient for unique aircraft identifications.

In selective addressing, FRUIT, garbling, over-interrogation and insufficient identification codes are reduced or eliminated.

2.2 Mode S

In Mode S, the SSR selectively interogates an aircraft by its 24-bit ICAO address. A Mode S reply can contain some or all of the following information, which is dependent on the level of the transponder. Except the first two items, they are available from all transponders [1]:

- The unique Mode S address of the aircraft: the 24-bit ICAO address
- Aircraft 'on ground' status
- Aircraft identification (squawk code)
- Aircraft pressure-altitude with 25 ft resolution
- Other information through use of the Mode-S data link, including Mode-S specific services

Mode S is entirely compatible with SSR Modes A and C. Since in Mode S only one specific aircraft is interrogated at a time, garbling can be avoided and FRUIT is eliminated. This is because a reply from an aircraft that is not interrogated can be discarded. More information about the content in Mode S is given in chapter 3.

2.3 Mode A/C/S interrogation and reply

To interrogate an aircraft, a uplink frequency of 1030 MHz is used, while the replies from the aircraft transponder are sent on the 1090 MHz downlink frequency.

2.3.1 Interrogation

Depending on the mode, the interrogation can consist of six pulses, P_1 to P_6.

For Mode A/C interrogation, pulses P_1, P_2 and P_3 are used. The time between pulse P_1 and P_3 (8 μs or 21 μs) determines whether Mode A or Mode C is interrogated respectively. Pulse P_2 is a control pulse that is sent by the omnidirectional transmitter to ensure the aircraft is not in one of the side lobes of the SSR (Sidelobe suppression (SLS)). The signal strength of P_2 should be smaller than P_1 and P_3, otherwise the

aircraft should ignore the interrogation. All pulses are 0.8 μs long. Mode S responders will reply like Mode A/C transponders. When pulse P_4 (0.8 μs long) is also transmitted by the SSR, only Mode A/C transponders will reply and Mode S transponders will ignore this interrogation.

In case that P_4 is 1.6 μs long and P_6 is transmitted (which includes the interrogator code), all Mode A/C transponders reply normally. But because of the duration of P_4, Mode S transponders will reply its ICAO address and will be locked-out (see section 2.4).

For Mode S only, pulse P_2 will be sent by the directional transmitter at full strength to suppress Mode A/C replies. There is no P_4 pulse transmitted. Instead pulses P_5 and P_6 are transmitted. P_5 is transmitted at the same time as P_6, but at a weaker strength. It has the same function as P_2 in Mode A/C. P_6 contains the addressed aircraft ICAO address and information that is requested (see chapter 3 for what information can be requested).

2.3.2 Reply

When aircraft transponders receive a valid interrogation, they will reply 128 μs after the reception.

In a Mode A or Mode C reply is not indicated what information it contains. The interrogator expects a reply to its latest interrogation. The reply lasts 20.3 μs and can contain up to 15 pulses of 0.45 μs. Two pulses indicate the start and end, and one is the center pulse. 12 pulses are used to transmit the squawk code or altitude code.

In Mode S, the signal contains a preamble with four pulses of 0.5 μs per pulse over a period of 8 μs. After the preamble a data block is included that consist of 56 bits (56 μs) or 112 bits (112 μs).

2.4 Mode A/C/S aircraft acquisition

Since Mode A/C and Mode S are working on the same uplink frequency, the uplink frequency is divided into an 'all-call' and 'roll-call' period as shown in figure 2.1. During the all-call period, the SSR interrogates Mode A/C/S transponders and acquires the ICAO addresses of all aircraft. When the SSR has acquired the ICAO addresses of aircraft, it can start with selective interrogation. During the roll-call period, only selective interrogation (Mode S) are sent to aircraft.

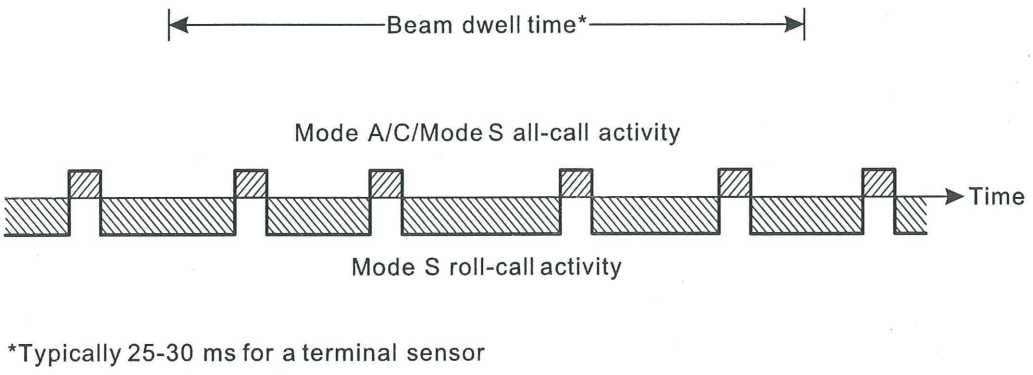

Figure 2.1: All-call and roll-call periods [1]

The ICAO addresses of acquired aircraft can be obtained as follows:

- Mode A/C/S all-call interrogation and/or
- Mode S only all call interrogation, followed by Mode A/C interrogation.

When the aircraft is in range of multiple SSRs, the second approach must be used since in the interrogation the interrogator/SSR (interrogator code) is included.

The Interrogator code (IC) of the interrogating site consists of two types:

- Interrogator identifier (II) code is used for multisite surveillance.
- Surveillance identifier (SI) code is used *only* for multisite surveillance.

In Europe, IC allocation is coordinated by EUROCONTROL to avoid overlapping areas with the same IC. However if multiple SSRs are part of a cluster, they will have the same IC. ICs allocated by EUROCONTROL can be found in [17].

2.4.1 Stochastic interrogation & Lock-out

To avoid garbling during the all-call period from closely spaced aircraft, the all-call interrogations can be sent with a probability of reply weighting. The following probabilities are possible: 1, 1/2, 1/4, 1/8 or 1/16. For example two aircraft (AC1 and AC2) are closely spaced, but at different height, receive an all-call interrogation with a probability of 1/2. The acquisition of an aircraft will happen as follow [18]:

1. AC1 and AC2 both decide to reply: garbling occurs and no aircraft will be acquired.
2. AC1 decides not to reply (0.5 probability) and AC2 replies. AC2 will be selectively interrogated and locked-out.
3. AC2 is locked out and will not reply. AC1 decides again not to reply. No replies sent.
4. AC2 is locked out and will not reply. AC1 decides to reply. AC1 will be selectively interrogated and locked-out. Both targets are now locked out to the ground interrogator.

When the ICAO address is obtained by the SSR, the aircraft will be 'locked-out' and will not reply to all-call interrogations from that or other SSR interrogators with the same IC for a period of 18 seconds. This timer will be reset with selective interrogations. It will only reply to all-call interrogations from other interrogators with a different IC and keeps replying to Mode A/C. However, an interrogator is able to override the lock-out of a transponder. The benefit of locking-out is to reduce FRUIT.

The interrogations during the roll-call period are scheduled for each SSR rotation. First, the furthest aircraft will be interrogated, and the expected arrival time of the reply is calculated. During this period a listening period is provided. The next aircraft will be scheduled in sequence based on the interrogation time and the reply listening period.

2.4.2 All-call lock-out example

In figure 2.2 and 2.3, the all-call replies for a two-hour period (21 May 2017, 12 UTC-14 UTC) are shown from II code 07 and II code 08 respectively. II code 07 is a cluster from the Royal Netherlands Air Force (RNLAF) that consist of five Mode S interrogators (Leeuwarden, Soesterberg, Twenthe, Volkel and Woensdrecht). II code 08 is the Mode S interrogator located at Brussels Airport. As can be seen, aircraft that are within the operating area of an interrogator will usually not reply to an all-call interrogation with this II code. In figure 2.3, aircraft above Brussels airport respond to all-calls because the aircraft is in the 'cone of silence' of the interrogator and therefore not locked-out. Mode S interrogations take place in the region where no all-call replies are received from that interrogator.

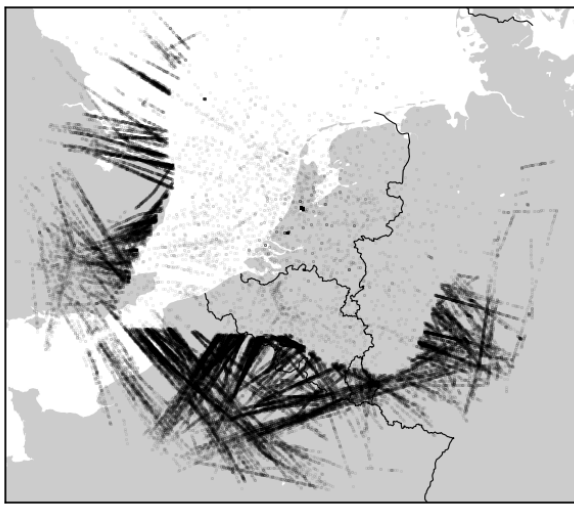

Figure 2.2: All-call replies II code 07

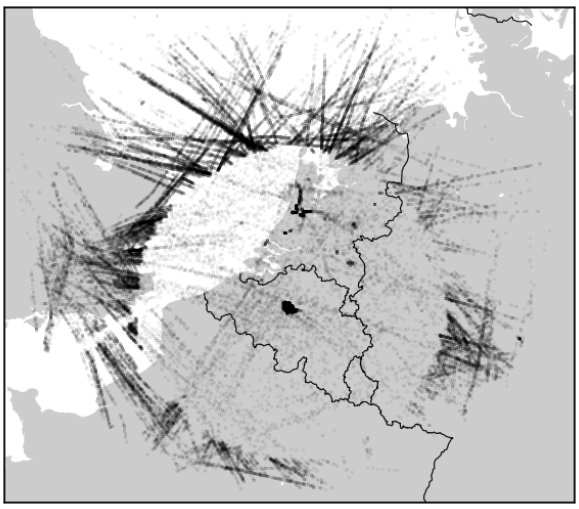

Figure 2.3: All-call replies II code 08

Chapter 3

Mode S

In this chapter, different (downlink) formats of Mode S signals will be discussed. Next, two specific formats will be discussed in more detail. These formats (20 and 21) contain different registers with specific aircraft information. Finally, the error detection method included in Mode S will be explained.

3.1 Downlink formats

Via 25 different Downlink formats (DF), a variety of aircraft states and intent information can be requested. The downlink formats are listed below and the bold downlink formats will be used in this thesis.

- DF00: Short air-air surveillance (ACAS)
- DF04: Surveillance, altitude reply
- DF05: Surveillance, identity reply
- DF11: All-call reply
- DF16: Long air-air surveillance (ACAS)
- **DF17 and DF18: Extended squitter (ADS-B)**
- DF19: Military extended squitter
- **DF20: Comm-B, altitude reply**
- **DF21: Comm-B, identity reply**
- DF24: Comm-D, ELM (extended length message)

Via DF20 and DF21, Mode S EHS/MRAR registers are transmitted. The format of DF20 and DF21 are given below, with on the top row the `starting bit`, on the center row `field:bit length` and on the bottom row the `ending bit`.

	1	6	9	14	20	33	89
Downlink format 20	DF: 5	FS: 3	DR: 5	UM: 6	AC: 13	MB: 56	AP/DP: 24
	5	8	13	19	32	88	112

As shown in the previous diagrams, the only difference between DF20 and DF21 are bits 20 to 32, which represent either the altitude code or identity respectively.

	1	6	9	14	20	33	89
Downlink format 21	DF: 5	FS: 3	DR: 5	UM: 6	ID: 13	MB: 56	AP/DP: 24
	5	8	13	19	32	88	112

- The downlink format (DF) indicates the DF of the signal
- Flight status (FS) indicates whether the aircraft is airborne or on ground, Mode A code alert (change) or special position indicator
- Downlink request (DR) contains requests to downlink information
- Utility message (UM) contains the transponder communication status
- The Altitude code (AC) field contains encoded altitude of the aircraft. It encodes values between -1000 ft and +50175 ft in either 25 ft increments or 100 ft increment
- The Identity code (ID) contains the aircraft identity code, which is identical to Mode A codes (squawk code)
- The message, Comm-B (MB) is a 56-bit field that contains the BDS registers (section 3.2)
- At the end the signal an address parity (AP) or data parity (DP) is included. This parity can be used to check whether the signal is contains bit errors and is explained in more detail in section 3.3.1

3.2 Binary Data Store registers

The Mode S transponder can maintain 255 different 56-bit wide Comm-B Data Selector (BDS) registers that can be interrogated by ATC [19]. These BDS registers contain a variety of aircraft states and intent information, as well as Airborne Separation Assurance Systems (ASAS).

BDS registers will be updated with a minimum interval specified in ICAO Doc 9871 [20] and will be cleared by the transponder if the register is not updated within this interval. The BDS registers are indicated by two-digit hexadecimal numbers and the most common are listed below:

- BDS 2,0: Aircraft identification (call sign)
- BDS 2,1: Aircraft and airline registration markings
- BDS 3,0: ACAS active resolution advisory
- **BDS 4,0: Selected vertical intention (EHS)**
- **BDS 4,4: Meteorological routine air report (MRAR)**
- BDS 4,5: Meteorological hazard report
- **BDS 5,0: Track and turn report (EHS)**
- BDS 5,3: Air-referenced state vector
- **BDS 6,0: Heading and speed report (EHS)**

The bold registers will be used in this thesis (if available). The register fields of BDS 4,0, 5,0, 6,0 and 4,4 are given in table 3.1, 3.2, 3.3 and 3.4 respectively. The status bit indicates whether the register field is available or not. If the register field is not available, the sign, status and content bits should be zero. When a value is signed (sign bit = 1), the two's complement representation will be used and the bit following the status bit shall be the sign bit. Reserved fields do not contain information and these bits are set to zeros.

Table 3.1: BDS 4,0: Selected vertical intention

Content	Status bit	Sign bit	Content bits	Range	Resolution
MCP/FCU selected altitude	1		2-13	[0, 65520] ft	16 ft
FMS Selected altitude	14		15-26	[0, 65520] ft	16 ft
Barometric pressure setting	27		28-39	[800, 1210] hPa	10 Pa
Reserved			40-47		
MCP/FCU mode	48		49-51		
Reserved			52-53		
Target altitude source	54		55-56		

Table 3.2: BDS 5,0: Track and turn report

Content	Status bit	Sign bit	Content bits	Range	Resolution
Roll angle	1	2	3-11	[-90, 90] deg	0.1758 deg
True track angle	12	13	14-23	[-180, 180] deg	0.1758 deg
Ground speed	24		25-34	[0, 2046] kts	2 kts
Track angle rate	35	36	37-45	[-16, 16] deg/s	0.03125 deg/s
True airspeed	46		47-56	[0, 2046] kts	2 kts

Table 3.3: BDS 6,0: Heading and speed report

Content	Status bit	Sign bit	Content bits	Range	Resolution
Magnetic heading	1	2	3-12	[0, 360] deg	0.1758 deg
Indicated air speed	13		14-23	[0, 1023] kts	1 kts
Mach	24		25-34	[0, 4.092] M	0.004 M
Barometric altitude rate	35	36	37-45	[-16384, +16352] fpm	32 fpm
Intertial vertical velocity	46	47	48-56	[-16384, +16352] fpm	32 fpm

Table 3.4: BDS 4,4: Meteorological routine air report

Content	Status bit	Sign bit	Content bits	Range	Resolution
FOM/Source			1-4		
Wind speed	5		6-14	[0, 511] kts	1 kts
Wind direction (True)			15-23	[0, 360] deg	0.703125 deg
Static air temperature		24	25-34	[-128, 128] °C	0.25 °C
Average static pressure	35		36-46		
Turbulence	47		48-49		
Humidity	50		51-56	[0, 100] %	1.5625 %

3.3 Signal parity

All uplink and downlink signals contain a parity of 24 bits at the end. This parity is used to check whether the signal contains errors or not.

3.3.1 Parity generation

The parity is overlaid with additional information: the aircraft ICAO address (Address parity (AP)), AA field information (Data parity (DP)) or the interrogator code (Interrogator parity (PI)). Interrogator parity is only used for DF11 (all-call replies). DF20 and DF21 contain either an address parity or data parity while all other DFs use address parity. AP and DP will be explained in sections 3.3.2 and 3.3.3 respectively.

Cyclic polynomial methods are used to detect errors in the transmitted message. In some cases, they can also correct transmissions errors. The parity is generated by a modulo-2 division of the message by the generator $G(x)$ in equation 3.1. The remainder (parity) overlaid with information is added to the end of the signal as shown in figure 3.1.

$$G(x) = x^{24} + x^{23} + x^{22} + x^{21} + x^{20} + x^{19} + x^{18} + x^{17} + x^{16} + x^{15} + x^{14} + x^{13} + x^{12} + x^{10} + x^3 + 1 \quad (3.1)$$

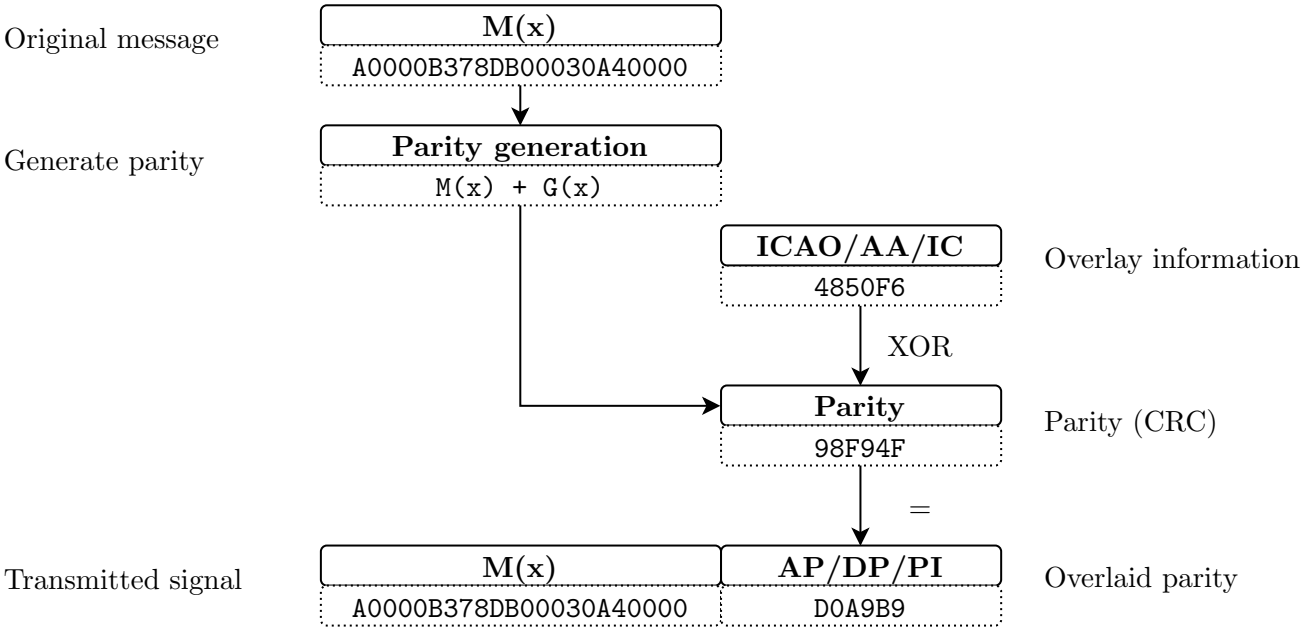

Figure 3.1: Parity generation and overlay

3.3.2 Address parity

In address parity, the parity is overlaid with the ICAO address of the aircraft.

3.3.3 Data parity

In data parity, the parity is overlaid on a modified AA field, established by performing a modulo-2 addition of the discrete address most significant 8 bits with BDS1 and BDS2 (first two hexadecimal characters of BDS register) that is specified by the Reply request (RR) and Reply request subfield (RRS) field in the uplink by the interrogator. An example of data parity is shown below, with BDS 6,0 as BDS register. With the reversed parity as described, the address `CAAAAA` will be obtained, while the correct address is `AAAAAA`.

As shown in the previous example, only the first two hexadecimal digits will be changed in data data parity. Hence, in case of a correct signal, the last four characters of the ICAO address should always be correct, regardless of whether AP or DP is used.

```
Discrete address   =   AA AA AA Hex     1010 1010 1010 1010 1010 1010
BDS1, BDS2         =   60 00 00 Hex     0110 0000 0000 0000 0000 0000
Discrete address   ⊕   BDS1, BDS2 Hex   0110 0000 1010 1010 1010 1010

Modified AA        =   CA AA AA Hex     1100 0101 1010 1010 1010 1010
```

3.3.4 Parity check and correction

Since the SSR knows what is interrogated, it knows what kind of parity is replied back in the signal. The received signal is similarly divided by the generator polynomial. If no errors occurred, an all-zero remainder will result. In some cases, errors can be identified and corrected. If a particular added pattern is expected, then the corresponding error-free remainder can be predicted. Error-correction cannot normally be used in these cases unless the added pattern is invariant or at least known to the receiver. With the parity, the ground station can perform a limited amount of error-correction.

Two types of bit errors can be considered: single bit-errors or burst errors. In single bit-errors, only one bit is incorrect (flipped from 0 to 1 or vice versa). When more than one bit is flipped, the error is called a burst error. The length of the burst is measured from the first corrupted bit to the last corrupted bit, however not all bits in between have to flipped. In Mode S, interference with Mode A/C is the main source of corrupt signals, which mainly leads to burst errors [21]. Interference from simultaneously-received Mode A/C replies that causes burst-errors can mostly be corrected. The error detection of Mode S provide an undetected error rate of 1 in 10^7 messages [1].

The generator in equation 3.1 was discovered by Kasami [22] and is able to correct any single 12-bit error burst or less in code length of 72 bits (or it can correct any two erasure burst each of 12 bits or less). This code also guarantees detection (correction) of any single 24-bit error (erasure) burst over any length [23].

Chapter 4

Atmospheric relationships & Meteorological derivations

In this chapter, the ICAO International Standard Atmosphere will be discussed, as well as its relation with aircraft airspeeds. Next, it is explained that how ADS-B and Mode S data can contribute to meteorological conditions derivations.

4.1 International Standard Atmosphere

The International Standard Atmosphere (ISA) is used for calculations in aircraft design to compare test results of aircraft and their components under identical conditions. ISA is also recommended in the processing of data from geophysical and meteorological observations [24].

Temperature

In ISA, the temperature is a function of altitude and can be calculated with equation 4.1. The temperature at an altitude h can be calculated with the temperature gradient λ ($\lambda = dT/dH$), the base temperature (T_b) and the difference in altitude with the base altitude (h_b) of a layer. The base values for the first three atmosphere layers are given in table 4.1. Commercial aircraft fly up to 14 km, so the first two layers are sufficient for calculations.

$$T = T_b + \lambda(h - h_b) \tag{4.1}$$

Air pressure

Air pressure is an exponential function of altitude and can be calculated with equation 4.2 when $\lambda \neq 0$ or with equation 4.3 when $\lambda = 0$. p_b is the base air pressure of that layer. g_0 is the gravitational acceleration and is 9.80665 m/s^2.

$$p = p_b \left[1 + \frac{\lambda(h - h_b)}{T_b}\right]^{\frac{-g_0}{\lambda R}} \tag{4.2}$$

$$p = p_b \exp\left[-\frac{g_0(h - h_b)}{RT}\right] \tag{4.3}$$

Air density

The air density ρ can be calculated with the perfect gas law given in equation 4.4, knowing the air pressure p, the temperature T and the ideal gas constant $R = 287.05$ J/(kg·K).

$$\rho = \frac{p}{RT} \tag{4.4}$$

Speed of sound

The speed of sound a is a function of temperature and is given by equation 4.5, with specific heat constant $\gamma = 1.4$

$$a = \sqrt{\gamma RT} \tag{4.5}$$

Table 4.1: International Standard Atmosphere layers

	h_b [m]	T_b [K]	λ [K/km]	p_b [Pa]	ρ [kg/m^3]
Troposphere	0	288.15	-6.5	101,325	1.25
Tropopause	11,000	216.65	0	22,632	0.3639
Stratosphere	20,000	216.65	+1.0	5,475	0.088

4.2 Airspeeds

Different types of airspeeds are used in aviation. The Indicated airspeed (IAS) is the speed that is measured by the pitot tubes mounted outside of the aircraft. The IAS is measured by the difference between the total pressure and the static pressure in the airflow. Measurements can contain errors due to the instrument, its installation or its position. The Calibrated airspeed (CAS) is the IAS corrected for these errors. Normally, the difference between IAS and CAS is not large.

The CAS contain errors due to air compressibility and variations from standard air density (effect of altitude and temperature). The Equivalent airspeed (EAS) will correct for these errors. At sea level, the EAS is equal to CAS, but the difference will increase as altitude increases.

The true airspeed (TAS) is equal to CAS at sea level. However at higher altitudes, TAS takes into account that the air density and temperature are different than at sea level. TAS is the speed of the aircraft relative to the air and is the true measure of aircraft performance in cruise.

The Ground speed (GS) is the speed of the aircraft relative to the ground. GS is equal to TAS when no wind is present.

The Mach number M is defined as the ratio between TAS and the speed of sound (and therefore a function of air temperature) as given in equation 4.6:

$$M = \frac{V_{TAS}}{a} = \frac{V_{TAS}}{\sqrt{\gamma RT}} \tag{4.6}$$

4.3 Meteorological derivations

To obtain the actual air temperature, the Mach number and the true airspeed should be known. To determine the wind, the true airspeed and ground speed should be known. These parameters can be obtained from ADS-B and Mode S data. In table 4.2, the relevant variables from ADS-B and Mode-S are given for later meteorological derivations.

Table 4.2: Usable information from ADS-B and Mode S

ADS-B	BDS 5,0	BDS 6,0	BDS 4,4 (MRAR)
True track angle	True track angle	Magnetic heading	Wind speed
Ground speed	Ground speed	Indicated airspeed	Wind direction (True)
Position (lat, lon)	True airspeed	Mach number	Static air temperature
Pressure altitude			Average static pressure
Geometric altitude			

As shown in table 4.2, ADS-B and BDS 5,0 are similar, except that ADS-B contains position and altitude information. BDS 6,0 contains magnetic heading information which is essential in calculating wind.

4.3.1 Temperature

To calculate the temperature, equations 4.5 and 4.6 are combined and rewritten to compute T as shown in equation 4.7. This information is available in BDS 5,0 combined with BDS 6,0.

$$T = \frac{V_{TAS}^2}{\gamma R M^2} \tag{4.7}$$

ADS-B data contains the pressure altitude and the difference to the geometric altitude from Global Navigation Satellite System (GNSS). Stone and Kitchen [25] used the difference between these values to determine the temperature of a layer in the atmosphere as given in equation 4.8:

$$\bar{T} = \frac{\left[(h_{p1} + a_1) - (h_{p2} + a_2)\right] g_0}{5.2561 R \left(\ln\left[p_0\left(1 + \lambda \frac{h_{p1}}{T_0}\right)\right] - \ln\left[p_0\left(1 + \lambda \frac{h_{p2}}{T_0}\right)\right]\right)} \tag{4.8}$$

h_p is the pressure altitude in meters from ISA. a is the difference between GNSS altitude and pressure altitude. For this method, two aircraft are required or an ascending/descending aircraft to determine the temperature of a layer.

4.3.2 Wind

In figure 4.1 the relation between TAS, GS and wind is shown. The ground speed vector ($\boldsymbol{V_{GS}}$) is the sum of the true airspeed vector ($\boldsymbol{V_{TAS}}$) and wind vector ($\boldsymbol{W}$) as shown in equation 4.9. χ_g, χ_a and χ_w are the ground speed vector angle (track angle), airspeed vector angle (heading) and wind vector angle w.r.t to true north respectively.

$$\boldsymbol{V_g} = \boldsymbol{V_{TAS}} + \boldsymbol{W} \tag{4.9}$$

To simplify calculations in equation 4.9, the vectors $\boldsymbol{V_{GS}}$, $\boldsymbol{V_{TAS}}$ and $\boldsymbol{W}$ will be decomposed into a west-east component V_x and an south-north component V_y. Decomposing a vector in x and y components can be done with equations 4.10 and 4.11 respectively.

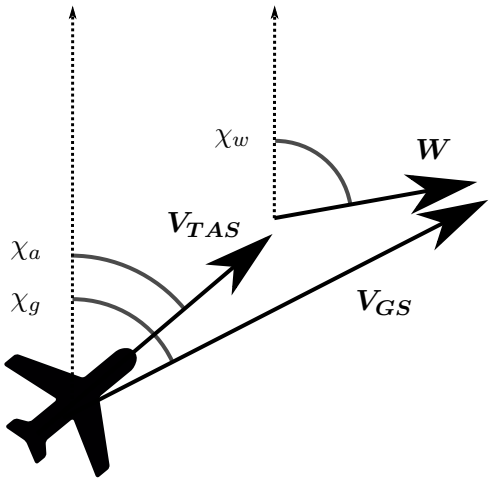

Figure 4.1: Relation between true airspeed, ground speed and wind vector

$$V_x = \boldsymbol{V} \sin(\chi) \tag{4.10}$$
$$V_y = \boldsymbol{V} \cos(\chi) \tag{4.11}$$

Wind components can then be calculated with equations 4.12 and 4.13.

$$W_x = V_{GS_x} - V_{TAS_x} \tag{4.12}$$
$$W_y = V_{GS_y} - V_{TAS_y} \tag{4.13}$$

To calculate the wind vector, the airspeed vector and ground speed vector should be determined, which can be done with ADS-B and Mode S data. In table 4.2, the variables from ADS-B and Mode S are shown that can be used to obtain these vectors.

The wind vector can than be determined as follows:

- In BDS 5,0, the GS, TAS and track angle are available. GS and the track angle results in the ground speed vector, but for determining the airspeed vector, the heading is required. The heading can be obtained via BDS 6,0. However this is the magnetic heading and should be corrected to true north. The magnetic declination in The Netherlands is around 1 degree.
- In BDS 6,0 the IAS is available. Assuming that IAS is equal to CAS, the TAS can be calculated with equation 4.14.

$$V_{TAS} = \sqrt{\frac{2\gamma}{\gamma-1}\frac{p}{\rho}\left[\left[1+\frac{p_0}{p}\left[\left(1+\frac{\gamma-1}{2\gamma}\frac{\rho_0}{p_0}V_{CAS}^2\right)^{\frac{\gamma}{\gamma-1}}-1\right]\right]^{\frac{\gamma-1}{\gamma}}-1\right]} \tag{4.14}$$

  BDS 6,0 also contains the Mach number. In combination with IAS, the TAS can also be derived with the relation in equations 4.15 and 4.16.

$$V_{TAS} = \frac{V_{CAS}}{f(p,M)}\sqrt{\frac{\rho_0}{\rho}} \tag{4.15}$$

$$f(p,M) = 1 + \frac{1}{8}\left(1-\frac{p}{p_0}\right)M^2 + \frac{3}{640}\left(1-10\frac{p}{p_0}+9\frac{p^2}{p_0^2}\right)M^4 \tag{4.16}$$

  The airspeed vector can then be found with the magnetic heading that is also included in BDS 6,0. Together with the ADS-B ground speed vector, the wind vector can finally be calculated.
- BDS 4,4 (MRAR) contains direct meteorological information and no derivations are required.

Chapter 5

Obtaining meteorological conditions

In this chapter a literature review is given from research that has been conducted on obtaining and deriving meteorological conditions from aircraft. First, in section 5.2 multiple sources for meteorological conditions are presented. In section 5.3, Mode S EHS is used for deriving meteorological information. Mode S Meteorological Routine Air Report is used in section 5.4 and in section 5.5, aircraft flight trajectories are used for estimation. In section 5.6, research conducted with an own ADS-B receiver are presented.

5.1 Trajectory optimisation and aircraft performance parameters

Wind is an important parameter in aviation. To improve efficiency in air traffic and to reduce emission and pollution by aircraft, accurate trajectory predictions are required. For these predictions, accurate aircraft performance parameters are required.

5.1.1 Trajectory optimisation

For trajectory planning meteorological conditions (temperature and wind), aircraft performance (weight and thrust, aerodynamics) and navigation performance (aircraft intent, pilot skills) are important variables [8, 9]. Ground speed and cumulative along-track error can occur when no accurate wind estimations are available [8]. Tang et al. [26] processed derived meteorological data onboard (AMDAR) for wind estimations and used this for strategic 4D trajectory estimation. Legrand [8] tried improving trajectory prediction by simulating sharing the wind and temperature information among aircraft. Gonzalez-Arribas [27] used meteorological ensemble probabilistic forecasting to determine a wind-based robust trajectory optimisation. Assaad [28] proposed an optimisation model that is achieving minimum fuel trajectories by making use of high-speed winds. Aircraft are allowed to divert from fixed airways and still meet on-time arrival schedules. Reducing fuel consumption will lead to a reduction in emissions and pollution [29].

5.1.2 Aircraft Performance Parameters

For the BlueSky simulator [10], developed by C&S/ATM section of Aerospace Engineering of the Delft University of Technology, ADS-B data has been used to build a database with aircraft performance parameters. Gloudemans [11] used ADS-B data to determine the operational flight envelope (operational limits like maximum altitude, minimum and maximum rate of climbs and minimum turn radius) and obtained estimations

for lift and drag coefficients for seven flight phases. However, in this research, strong assumptions were made in terms of wind and flight strategies.

Sun [12] extracted a set of more than thirty aircraft performance parameters from seven distinct flight phases for common commercial aircraft. Using machine learning methods and ADS-B data, it is possible to identify flight phases [13] and to extract relevant properties. All parametric models were combined to describe a complete flight that includes take-off, initial climb, climb, cruise, descent, final approach and landing. However, wind effects are ignored in this research [12]. In [14] meteorological data from the Global Forecast System (GFS) is integrated to obtain the true airspeed of an aircraft at any given location.

The lift, thrust, fuel consumption and climb/descent rates are influenced by the aircraft mass. ADS-B data was used by Sun et al. [15] to infer the mass of an aircraft at its take-off phase with two separate methods. Aggregated Meteorological Aerodrome Report (METAR) data at observed airports and ground speed is used to estimate the TAS of aircraft during take-off.

5.2 Sources for meteorological conditions

There are different methods to obtain meteorological information. The first method is using a Numerical Weather Prediction (NWP) model which uses mathematical models to predict weather based on current conditions (obtained data from satellites, ground stations, weather balloons, etc.). Starting with the current conditions, a forecast is generated by integration in time. Two commonly used global NWPs are the Global Forecast System (GFS) and the European Centre for Medium-Range Weather Forecasts (ECMWF).

The second method, uses the aircraft as a 'meteorological sensor'. Aircraft Meteorological Data Relay (AMDAR) is reporting meteorological information to ground stations via the Aircraft Communications Addressing and Reporting System (ACARS). However this information is not publicly available. The frequency of AMDAR observations depends on the flight phase (ascent, level or descent) [30] and therefore has a typical average resolution of few tens of kilometers [31]. In AMDAR, data from different aircraft sensors are smoothed over a period of ten seconds during ascent/descent phase and 30 seconds during level above FL200. Smoothing is applied to ensure consistency between observations from different sensors and different onboard computer systems [30].

In Mode S EHS, for example selected altitude, indicated airspeed, roll/track angle/rate and airspeeds are transmitted. With this information it is possible to derive the wind vector (speed and direction) and temperature information by using atmospheric relationships, as described in section 4.3. Mode S can also contain direct meteorological observations (wind, temperature and humidity) in Meteorological Routine Air Report (MRAR), which is publicly available like other Mode S signals, in contrast to AMDAR. Despite information for AMDAR and Mode S are coming from the same instruments, Mode S has a much higher frequency. They also have no smoothing or pre-processing and can be requested at each rotation of the SSR.

The third method uses aircraft track/flight information to derive meteorological information. This information is available from the primary radar or from ADS-B data, which contains position information (latitude, longitude and altitude), ground speed and track angle.

The last method uses radiosondes or weather balloons. Radiosondes are equipped with a temperature sensor and humidity sensor. To determine the geopotential altitude, a pressure sensor and/or GPS receiver is installed. The wind speed is derived from the ground track of the balloon during its ascent.

In this chapter a literature review will be conducted on ADS-B and Mode S (EHS and MRAR) meteorological derivations.

5.3 Mode S Enhanced Surveillance

5.3.1 Deriving meteorological parameters from Mode S EHS

De Haan from the Royal Netherlands Meteorological Institute (KNMI) conducted a lot of researches on Mode S EHS meteorological observations between 2009 and 2014 [32–35]. Air Traffic Control the Netherlands (LVNL)

provided Mode S EHS data from the tracking and ranging (TAR) radar at Schiphol. A check was done to ensure data quality, which consist of checking the minimum and maximum values of flight parameters, such as the Mach number, GS, TAS and roll. To deal with jumps in values, data for M and V_{TAS} are smoothed. To compute wind, it is important to have the true north instead of magnetic heading for aircraft TAS, so a heading correction is applied.

From research it was concluded that after the correction of magnetic deviation, aircraft still had a heading error of several degrees. An additional heading correction is determined with landing aircraft, whereby the runway heading is used as correction factor over a period of twelve months. The disadvantage of this method is that many aircraft are enroute over The Netherlands instead of landing (at Amsterdam Schiphol Airport).

In 2009, De Haan [34] compared the quality of Mode S with three sources: an NWP model, AMDAR observations and radiosonde observations. EHS temperature observations (even with corrections) were bad, the AMDAR root mean square (RMS) was twice two time larger than compared to an NWP (HIRLAM by KNMI). This could be caused by the resolution of the Mach number and TAS. The quality of wind (after magnetic heading correction and aircraft dependent corrections) was good. It was comparable to AMDAR, but slightly worse than radiosonde. Mode S temperature observations are less accurate than AMDAR and radiosonde. The NWP mean difference was almost the same of AMDAR and radiosonde, but the RMS was twice as large.

In 2013 an improved method for deriving wind and temperature was proposed [36]. For temperature within a certain flight phase, time dependent and aircraft specific temperature corrections are applied. A lookup table for correction was built with the differences of EHS derived temperature and NWP temperature.

An additional heading correction is proposed to determine the correct heading by using additional wind information, for example from NWP or AMDAR. A time dependent heading correction is used, because over the time the heading correction changes for individual aircraft. For a period of one year, a constant heading correction will be good enough. Also the effect of outdated magnetic variance tables were investigated. For the Mode S coverage over The Netherlands, the difference would be 0.2 degrees when a ten-year old magnetic variance table was used. The author concluded that this effect can be neglected. But for other regions, it should be taken into account.

To improve TAS, a correction method has been developed to remove biases from aircraft winds. This results in a correction based on a linear relationship between the measured TAS and the estimated TAS from the ground vector and additional wind data, which is stored in a lookup table for each aircraft. This correction consists of the difference between the measured TAS and estimated TAS from the ground speed vector, as well as additional wind information.

The results of these additional corrections were compared to an NWP (ECMWF) and AMDAR. It was shown that the corrections had positive effects on the quality of Mode S observations. Compared to the NWP, the temperature bias was reduced over the entire atmospheric profile and had almost a zero bias. The wind speed error reduced by 5% in the direction of flight and was almost zero due to airspeed correction. The heading correction reduced the bias and standard deviation in the transversal direction.

5.3.2 Precision of Mode S EHS signals and its influence on derivations

As mentioned by De Haan [34], the resolution of Mode S has an influence on the precision of the derived meteorological values. Mode S EHS reduces the precision of the state vector from 16-bit to 10-bit binary representation (quantization error). Mirza et al. [37] investigated the observation errors due to the reduced precision of Mode S EHS signals by comparing it to in-situ research aircraft measurements.

Due to reduction in accuracy, the data increment for TAS is 2 knots and 0.004 for Mach number (see tables 3.1-3.4 for other parameters). The standard deviation for the quantization error ranges from 2.5 to 1.25 °C for a pressure altitude from 0 to 10 km respectively. The wind speed had a standard deviation of 0.25 to 0.40 m/s and 0.25 m/s for west-east and south-north components respectively. However, the differences in the wind components can also be caused by a systemic error that is directionally dependent. Quantifying the statistical error due to Mode S EHS processing may be assisted with data assimilation of the derived observations.

5.4 Mode S Meteorological Routine Air Report

Strajnar [31] and Hrastovec [38] collected MRAR data from the TAR radar at Ljubljana airport (LJU, Slovenia), moreover Strajnar [39] also did a similar study in the Czech airspace using three Czech radars, one German radar and one Slovakian radar. De Haan [40] obtained MRAR information from Maastricht Upper Area Control (MUAC).

5.4.1 Availability of MRAR

Since MRAR is not a mandatory Mode S register, MRAR messages are only sent by a small number of aircraft [31, 38–40]. In Slovenia only around 6.3% of all interrogated aircraft reported temperature and 5.1% wind observations [31,38]. In the area controlled by Maastricht Upper Air Control (MUAC), which covers The Netherlands, Belgium, Luxembourg and north-west Germany, only MRAR interrogations from Copenhagen, Denmark were received in 2014 [40]. Only 16% of the aircraft responded with MRAR information. This 16%, however, contains 26% and 32% of the total wind and temperature observations via Mode-S EHS and MRAR. The reason for this is that MRAR contains direct information while EHS has indirect information and requires further processing (and filtering). Another observation is that aircraft from Airbus and Boeing, do not or barely send MRAR information. Other commercial passenger aircraft that do transmit MRAR are ATR, Bombardier and Canadair [31, 38–40].

5.4.2 Quality of MRAR

The quality of MRAR has been compared to other sources: AMDAR, NWP, Mode S EHS and radiosonde data. Hrastovec [38] and De Haan [40] compared MRAR with an NWP. De Haan did not mention any data processing in the report, but Hrastovec uses a Kalman filter to smooth the data and to take the measurement errors into account. The results can be seen in table 5.1. The biases for all parameters are low, but the standard deviation for wind direction can be high. Hrastovec mentioned that this deviation can be caused by inaccurate measurement, misprediction of the NWP, or locally bounded atmosphere anomalies that are reflected in the measured data.

De Haan compared MRAR with Mode S EHS. The bias in temperature was concluded to be caused by the resolution of the Mach report in Mode S EHS. Wind speed and direction show negative biases with respect to Mode S EHS.

Strajnar [31, 39] compared direct observations of Slovenian and Czech MRAR with AMDAR. It can be seen in table 5.1 that there is a negative bias of MRAR compared to AMDAR. The bias for wind speed is almost zero, but the biggest bias occurs in wind direction. also, wind direction has the highest standard deviation. Strajnar concluded that the quality of MRAR observations is equivalent to AMDAR.

A comparison by Strajnar [31] with a radiosonde and with smoothed MRAR observations showed negative basis for all MRAR observations. The standard deviation for direction is still high, however, the values are reasonable and comparable to other studies that compared aircraft observations to radiosondes.

5.4.3 Applications of MRAR

In terms of applications of MRAR, not many researches are conducted. Strajnar [41] evaluated the MRAR observations in a mesoscale NWP. It has shown that there is a clear improvement for short forecast range, that is between one and three hours. Strajnar concluded that MRAR had a significant potential for mesoscale NWP and could improve data assimilation modelling.

Table 5.1: MRAR quality comparison

	NWP [40]		NWP [38]		Radiosonde [31]	
	Bias	Std. dev.	Bias	Std. dev.	Bias	Std. dev.
Temperature [K]	0.34	0.82	0.4	2.1	-0.27	1.7
Speed [m/s]	0.11	2.5	0.3	5.6	-0.34	3
Direction [deg]	0.15	12.69	0	41	-3.1	23

	AMDAR [31]		AMDAR [39]		EHS [40]	
	Bias	Std. dev.	Bias	Std. dev.	Bias	Std. dev.
Temperature [K]	-0.14	0.39	-0.09	0.32	0.4	0.6
Speed [m/s]	0.01	0.83	0	0.7	-0.2	1.5
Direction [deg]	0.57	7.2	0.43	6.81	-1.3	9.9

5.5 Estimating meteorological conditions from aircraft flight trajectories

Wind observations can also be derived from aircraft flight trajectories. This data can be obtained from surveillance radars or ADS-B.

5.5.1 Aircraft flight trajectories from radar with downlinked TAS

Hollister et al. proposed a method to derive wind speed from aircraft tracks during a turn [42]. Delahaye [43] uses the same method including downlinked TAS data to estimate wind. When onboard TAS measurements are available, wind estimations are obtained from a linear model solved with a Kalman filter. However, when only aircraft tracks are available, wind is estimated from one or two turns, depending on the number of aircraft in a certain airspace. In case only one track is available, wind is derived only after two asymmetric turns (three straight lines separated by two turns). When two aircraft are available, one turn for both trajectory is enough to estimate wind. Finally vector spline interpolations are used to generate wind maps from these local wind estimations.

5.5.2 Aircraft flight trajectories from ADS-B

De Leege et al. [44] used ADS-B data to estimating wind, air pressure and temperature. From single or multiple aircraft, the velocity vector information was used. The wind is recursively estimated, by a modified Kalman filter, from an aircraft in a turn, assuming that the aircraft flies at constant altitude with constant TAS in all directions. With a constant wind vector, this results in a nonlinear least-square problem that is solved using the Kalman filter. Pressure is estimated by the difference between the pressure altitude and the GNSS altitude. The temperature can then be derived from ISA.

Compared with the GFS model, the authors concluded that the ADS-B system can be used for meteorological monitoring. No correlation between the wind estimate error and the forecast wind was found. The direction estimate was negatively correlated with the forecast wind speed. The wind direction was more sensitive at lower wind speeds due to errors in the derived wind components. The RMS for wind speed and direction estimates were 12.9 kts and 31.5 degrees respectively.

5.5.3 Aircraft flight trajectories from radar

Hurter et al. [45] used aircraft trajectories of aircraft flying in different directions to estimate the wind speed and direction with a least squares approximation. The idea is that when ground speeds are plotted from equal aircraft sizes, sinusoidal shapes will emerge, which is a result of wind. For location, head and tail wind will have a phase of 180 degrees in a sine. The wind direction can be obtained from the sine angle shift (headwind results in a lower ground speed), and the amplitude gives the wind speed. The results were compared with Météo France data and Mode S EHS wind observations, and the results were almost similar in airspace volumes with sufficient data.

5.6 Using Mode S signals with a ADS-B receiver

The KNMI [44] and the Meteorological Office (Met Office) [46] from the United Kingdom, also installed an own ADS-B receiver to obtain ADS-B and Mode S signals. This section describes how the signals are decoded and its quality for meteorological derivations.

5.6.1 KNMI and LVNL EHS data

The KNMI installed one receiver in De Bilt and Met Office installed five receivers to receive ADS-B and Mode-S signals. The KNMI considered a valid Mode-S EHS observation when ADS-B and BDS registers 4,0, 5,0 and 6,0 were received from a specific aircraft (no time span), while Met Office considered an observation when ADS-B and BDS registers 5,0 and 6,0 are received within ten seconds from a specific aircraft (because of the SSR rotation time). The ADS-B signal was used to obtain the location and ground movement vector. Smoothing of aircraft data was not applied at any stage.

In both cases, the received Mode-S signals were decoded by checking the status bits and content as given in section 3.2. Also additional validity and consistency checks for TAS/IAS/GS, V/S, heading and track angle were applied. Met Office considered this not as sufficient and a comparison to a table of error conditions is made. This table was built over time when gross errors were identified and investigated.

Quality of KNMI EHS derivations

The KNMI compared their decoded signals with a dataset from LVNL. The comparison was done with one full year (2012) of received signals, with some interruptions from both sources. The number of observations from KNMI were around 9% of the EHS messages from LVNL. The reason given for this was the decoding algorithm. During night-time, this percentage was higher due to the lower number of overlapping messages that resulted in a higher percentage of decoded signals.

Also a distribution was made with the time difference between subsequent observations from the same aircraft. LVNL showed that 98% of the valid observations had a time difference for 4.2 seconds (which is the rotation time of Schiphol TAR). Data from the KNMI showed that only 20% was within 4 seconds and 10% between 5 to 8 seconds. A valid observation is when all EHS registers were filled, so a delay in one register causes a delay in an observation.

In a comparison with almost 2.5 million decoded EHS signals and LVNL data, it has shown that the Mach number was similar from both sources with few outliers. TAS observations showed a similar behaviour, only outliers show a clear signal, which could be caused by the BDS identification. IAS, magnetic heading and GS comparison were very good and no extreme outliers were seen.

Track angle comparison was good, except track angles around 210 degrees. No explanation was given why there were many outliers at 210 degrees. By removing these outliers, the outliers in TAS, GS and IAS also disappeared.

From the dataset of KNMI and LVNL, meteorological conditions were derived and compared. For temperature the mean difference was 0.00 °C, however the standard deviation is almost 2 °C. This is due to the method

on how temperature is derived, which uses Mach number and TAS. Wind directions were only calculated when wind speeds were higher 4 m/s, since low wind speeds result in inaccurate wind directions, which would increase scatter. The mean difference for wind speed and direction were 0.04 m/s and 0.0 degrees respectively. The standard deviation was 1.15 m/s for speed and 4.64 degree for direction.

Some trends were visible in the comparison, temperature higher than -20 °C was very noisy and the reason for this is corrupted signals or wrong decoding. For wind there was no trend was visible, however a large part of the wind had a direction of around 270 degrees which corresponds with a westerly wind. Furthermore a comparison was made with AMDAR, however the reader is referred to [44] for these results.

Quality of Met Office derivations

Met Office compared the Mode S derivations with their own NWP. The results were similar to researches from De Haan [32], where also no smoothing or correction has been applied. Temperature showed a mean bias in the range from -3 °C to 2 °C. The RMS was the highest at low altitudes. The wind vector was split into a u-component (west-east) and v-component (south-north). The RMS for the u-component was between 0.5 and 5 m/s and 0.75 and 10 m/s for the v-component. The RMS of the wind component showed a better result for u-component, which is due to the higher number of flights in east-west direction (or vice versa) over the United Kingdom. The wind component that is orthogonal to the direction for air movement vector showed a larger uncertainty because a heading correction was required, which affected the v-component more than the u-component.

Assuming the wind vector, ground movement vector and TAS were correct, the heading was found for each observation. The heading correction is applied by calculating the difference between observed and calculated heading. The heading differences were then averaged for each aircraft and defined as the heading correction. The corrections were not distributed around zero and found to have three peaks. These peaks could be caused by the magnetic lookup tables onboard.

The overall quality of the wind observations are similar to the AMDAR observations. Therefore, it has adequate quality for NWP and aviation forecasting. However wind observations could be improved significantly by heading corrections.

5.7 Validation of Downlink Aircraft Parameters

Grappel et al. [47] evaluated the avionics configuration and status information of Mode S Elementary Surveillance (ELS) and EHS. 22 tests were developed for validating the aircraft configuration and flight status. 21 tests were developed for BDS 2,0-6,0 validation. These tests were mainly checking the status and content bits and comparing the values with the thresholds derived from primary radar to determine the accuracy of these parameters.

Puntin et al. [48] continued on the work of Grappel and validated downlink aircraft parameters by comparing it to an estimate of the parameter derived from other data sources (e.g. PR or SSR derived azimuth). Smoothing and wind estimation are an integral part of this validation and is applied to BDS 5,0 and BDS 6,0. Data from the PR is smoothed to increase the precision of the aircraft track. The difference between the estimated and downlinked parameter is considered as error. A downlink parameter is considered as validated when the error magnitude is smaller than a predetermined threshold. Over the entire flight track the DAP is tested and an overall validation percentage is calculated.

Chapter 6

Signal pre-processing

For decoding ADS-B and Mode S data, the open source library pyModeS [49] for Python and ICAO documents [1, 20, 50] are used.

6.1 ADS-B signal processing

RAW ADS-B data is processed with pyModeS [49]. The output will be a file with ICAO address, ground speed, track angle, altitude and call-sign. ADS-B data is re-sampled with a resolution of 1.0 second and interpolated. For position, a spline is used, while for altitude and ground speed a linear interpolation is applied. Altitude is rounded to the nearest 25-feet increment.

6.2 ICAO address retrieval

In order to obtain the location of the origin of a signal, the transmitting aircraft should be determined first. Since it is not known whether an AP or DP is used for message parity, a correct message shall produce an full ICAO address (AP) or the last four hexadecimals digits of the ICAO address (DP).

Retrieval of the ICAO address is done as follows and shown in figure 6.1.

1. The parity of the first 88 bits (without overlay) is calculated with the generator as explained in section 3.3.1.
2. A modulo-2 addition is applied on the parity with the last 24 bits of the received signal (the overlaid parity). This will result the ICAO address or the modified AA field (see subsection: 3.3.3). This method is for now called the 'reversed parity'.

When checking the parity with the method mentioned above, the check will result in two cases:

- Possible ICAO address[1], and the signal is
  - correct

[1] A possible ICAO address is defined when it is in a block of allocated addresses for countries (blocks in sizes of 2^{10}, 2^{12}, 2^{15}, 2^{18} or 2^{20} addresses) as stated in ICAO Annex 10 Aeronautical Telecommunications [19].

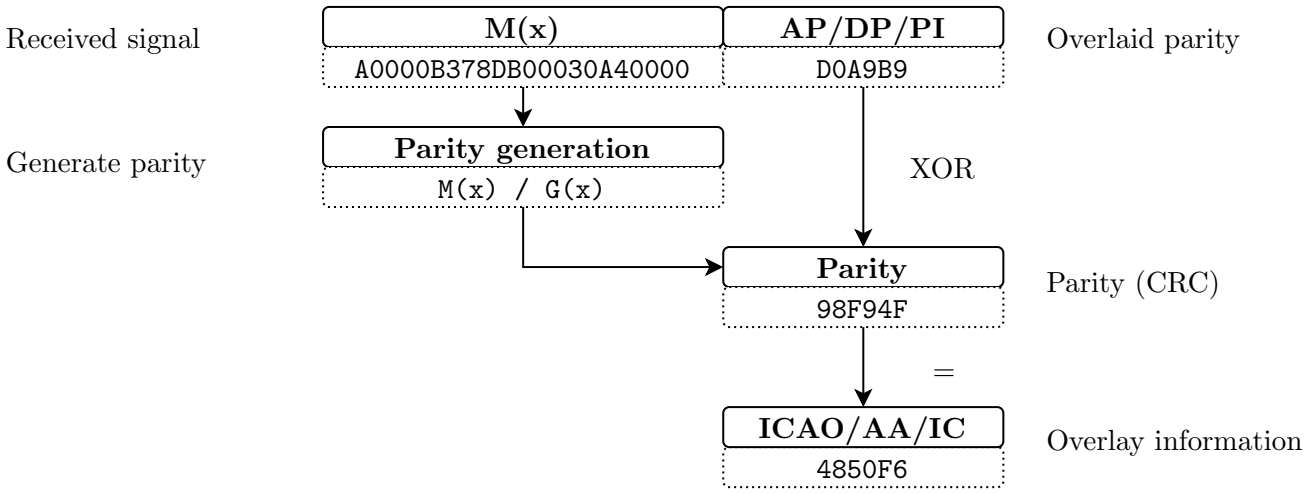

Figure 6.1: Reversed parity

  - corrupt, but resulting in a possible ICAO address
- Impossible ICAO address, which indicates that the signal is
  - overlaid by DP (last four hexadecimal digits should be correct)
  - corrupt

A small error in the signal can result in another possible ICAO address. If, for example, a single bit flipped, the parity may result in a slightly different ICAO address. Since ICAO addresses are usually allocated in sequence (within the allocated country block), this error can result in an existing ICAO address of a subsequent aircraft. In table 6.1 an example is shown where only the last two characters of the ICAO address change.

Table 6.1: ICAO addresses of some KLM aircraft

ICAO address	Aircraft registration	ICAO aircraft code
484368	PH-BQA	B772
484369	PH-BQB	B772
48436A	PH-BQC	B772
48436B	PH-BQD	B772
48436C	PH-BQE	B772
48436D	PH-BQF	B772
48436E	PH-BQG	B772
48436F	PH-BQH	B772
484370	PH-BQI	B772
484371	PH-BQK	B772

6.3 Error detection of downlink formats 20 and 21 signals

The SSR expects a specific type of reply from a certain aircraft. Hence, the SSR can determine the correctness of Mode S signals. Since in this research it is not known which aircraft is interrogated, another method should be developed to check whether the signal contains errors or not.

6.3.1 Correctness of downlink format 21 signals

For determining the correctness of DF21 signals, the encoded squawk code is used. For each squawk code, 'found' ICAO addresses are linked. This gives a distribution of addresses that are found for each squawk code. Addresses that occurs more than a certain times for a given squawk code are assumed to be correct.

Squawk codes 1000 (general code for IFR) and 7000 (general code for VFR) are not unique, so the allocation method will be more difficult in these cases. Since squawk codes will be re-used, looking over a longer period will not lead to unique combinations. With additional flight status information in the signal (see section 3.1), it can be determined when an aircraft changes squawk code.

Since then the correct address is known for a squawk code, it is possible to allocate slightly different addresses to the correct address[2] or to apply error correction. The difference between the addresses is determined by the number of hexadecimal digits that are different from the correct ICAO address. An algorithm that calculates this difference is the Hamming distance.

In this research, only signals will be used that are overlaid by address parity, so slightly different ICAO addresses are not allocated to the correct address. This is because for data parity it can not be determined whether the message is correct.

With this method, also a list of airborne aircraft addresses will be build. This could be used to identify aircraft that do not transmit ADS-B signals.

Example

In table 6.2, it can be seen that squawk code 2137 is most likely assigned to aircraft 484165 (KLM B738, PH-BXM). In the last column is shown how many hexadecimal digits of the ICAO address are different to 484165.

In most of the groups, the ICAO addresses are possible, which only have one or two hexadecimal digits different. It is almost certain that these groups have a small error and also belong to aircraft 484165. The ICAO of groups 2, 14, and 15 are not possible. However the first character is different, which indicates it could be overlaid with data parity or still contains a transmission error.

The ICAO addresses of group 8 and 9 are also transmitting ADS-B. When only a check was done whether from that aircraft ADS-B signals were received, this corrupt signal would be linked to the wrong aircraft and result in an outlier in later calculations.

6.3.2 Correctness of downlink format 20 signals

Determining the correctness of DF20 signals is more difficult than DF21, since DF20 does not contain a unique parameter like the squawk code. DF20 contains the encoded altitude, which is not unique. These signals are combined with ADS-B data that have the same ICAO code and same timestamp. The correctness of DF20 is determined by comparing the Mode S altitude with ADS-B altitude. When the difference is below a certain threshold, the message is considered as correct.

Aircraft without ADS-B

Since not all aircraft are transmitting ADS-B, the ICAO address list of DF21 can be used to determine whether an ICAO address is possible. However, for meteorological derivations, the position of an aircraft is required. Thus Mode S signals with an ICAO address that does not transmit ADS-B cannot be used. Therefore these messages will be left out for analysis in this research.

[2]For example, if the first two digits of an ICAO address are different, it can be overlaid with DP

Table 6.2: Squawk code 2137 (subset over a period of 15 minutes)

Group	Squawk	ICAO	Occurrences	ICAO possible	ADS-B seen	Hamming dist.
1	2137	084165	2	True	False	2
2	2137	284165	2	False	False	2
3	2137	404165	1	True	False	2
4	2137	484125	4	True	False	1
5	2137	48412D	1	True	False	2
6	2137	484145	5	True	False	1
7	2137	484147	1	True	False	2
8	2137	484161	2	True	True	1
9	2137	484164	6	True	True	1
10	**2137**	**484165**	**1065**	**True**	**True**	**0**
11	2137	484167	5	True	False	1
12	2137	48416D	1	True	False	1
13	2137	48417D	1	True	False	1
14	2137	584165	1	False	False	1
15	2137	584965	1	False	False	2

6.4 BDS register identification

Except for BDS registers 1,0, 2,0 and 3,0, in the signal is no information included about the BDS register that is transmitted. Since the interrogator requests a certain BDS register, this would not be a problem for the interrogator itself. To identify the BDS register, the following method is applied. Most of the BDS versions have a status bit and content bits (and in some cases a sign bit, for example vertical rate). If the status bit is zero (register field not available), the sign bits and all content bits of that field should contain zeros. If the status bit is equal to one, the content bits will contain a value. All reserved fields should contain zeros. It is possible that signals will match with multiple BDS registers with this method, for example registers BDS 5,0 and BDS 6,0 have the status, sign and content bits on almost exactly the same position (except first two register fields).

To identify the most likely BDS register, a probabilistic approach is used. Several normally distributed probability density functions (PDF) are designed to compute the likelihood of each BDS register.

6.4.1 BDS 4,0

In BDS 4,0 the selected MCP/FCU/FMS altitude and/or the barometric pressure is transmitted.

From analysis it showed that if a signal is identified as BDS 4,0, it will be almost certain BDS 4,0, irrespectively matches with other BDS registers. However, a small additional check is applied. The modulo 100 is calculated of the value of MCP/FCU or FMS selected altitude. Modulo 100 is chosen because usually the selected altitude can be changed by increments of 100 ft or 1000 ft. Due to the resolution of the MCP/FCU or FMS selected altitude (which is 16 ft, see section 3.2), precision errors can occur (for example, 33008 ft instead of 33000 ft). If the remainder is smaller than 8 ft or larger than 92 ft, it will be accepted as BDS 4,0. When MCP/FCU or FMS selective altitude is not available, a check is done on the barometric setting (QNH, atmospheric pressure adjusted to mean sea level). If the barometric setting is in range of 1013.25 ± 25 hPa, it will be accepted as BDS 4,0 either.

6.4.2 Probability density function BDS 5,0 and BDS 6,0

In BDS 5,0, the ground speed, track angle (rate) and true airspeed are included. BDS 6,0 contains Mach number, indicated airspeed and vertical rate.

To identify the most likely BDS register, a multivariate normal distribution $\mathcal{N}(\boldsymbol{\mu}, \boldsymbol{\Sigma})$ is used with the mean $\boldsymbol{\mu}$ (equation 6.1) and variance $\boldsymbol{\Sigma}$ (equation 6.2) of the decomposed ground speed vector from 20 ADS-B measurements with the closest timestamps (earlier and later) from the same ICAO address.

$$\boldsymbol{\mu} = \begin{bmatrix} \mu_{V_x} & \mu_{V_y} \end{bmatrix} \tag{6.1}$$

Since there is no covariance between V_x and V_y, the covariance matrix will be as given in equation 6.2

$$\boldsymbol{\Sigma} = \begin{bmatrix} \sigma^2_{V_x} & 0 \\ 0 & \sigma^2_{V_y} \end{bmatrix} \tag{6.2}$$

In BDS 5,0 the ground speed is decomposed in a V_x and V_y component with the track angle, while in BDS 6,0 the Mach is converted to TAS (with ISA) and decomposed with the magnetic heading. The track angle and heading angle is usually small and therefore considered as comparable.

The BDS version is identified by the highest probability density function as given in equation 6.3.

$$f(\boldsymbol{x}) = \frac{1}{\sqrt{(2\pi)^k \det \boldsymbol{\Sigma}}} \exp\left(-\frac{1}{2}(\boldsymbol{x}-\boldsymbol{\mu})^T \boldsymbol{\Sigma}^{-1} (\boldsymbol{x}-\boldsymbol{\mu})\right) \tag{6.3}$$

Example

In this section two signals from the same aircraft at the same timestamp are received and it can be either BDS 5,0 or BDS 6,0.

- ICAO address: `C0054A`
- Altitude: 3850 ft
- Timestamp: 1507371046 (10/07/2017 @ 10:10:46 UTC)
- Signal #1: `A000031189BADF1A214C7B79E86D`
- Signal #2: `A0000311DAB9D317A12C2541C664`

The signals are combined with ADS-B ground speed (GS) and track angle (TRK). The GS and TRK are an average of 20 ADS-B signals as explained earlier. The register fields of BDS 5,0 and BDS 6,0 are given in table 6.3.

Table 6.3: Decoded signals

#	ADS-B		BDS 5,0					BDS 6,0		
	$\mu_{V_{GS}}$ [kts]	μ_{TRK} [deg]	Roll angle [deg]	TRK rate [deg/s]	GS [kts]	TRK [deg]	TAS [kts]	HDG [deg]	IAS [kts]	M [-]
1	208.7	245.7	13.5	1.28	208	245	246	27	367	0.416
2	208.7	245.7	-52.6	1.16	188	221	74	255	233	0.376

In table 6.4, the decomposed speed vectors are shown, with the calculated PDF for each register (with equation 6.3). At the moment, the ISA is used for Mach to TAS calculation. However, due this assumption, the derived TAS can differ a lot from reality. Further, due to wind, the TAS will be different than GS. Therefore a high variance of 20 (kts) is chosen, but the variance will only scale the distributions. In the last column of table 6.4 is shown which BDS register is allocated to signal. These PDFs are visualised in figures 6.2 and 6.3.

Table 6.4: BDS register probability calculation

#	ADS-B		BDS 5,0		BDS 6,0		P(BDS 5,0)	P(BDS 6,0)	Accepted as
	V_x [kts]	V_y [kts]	V_x [kts]	V_y [kts]	V_x [kts]	V_y [kts]			
1	-190.5	-84.6	-190.2	-84.6	124.1	241.5	3.82E-04	1.39E-115	BDS 5,0
2	-190.5	-84.6	-123.3	-141.9	-237.2	-63.1	2.37E-08	1.46E-05	BDS 6,0

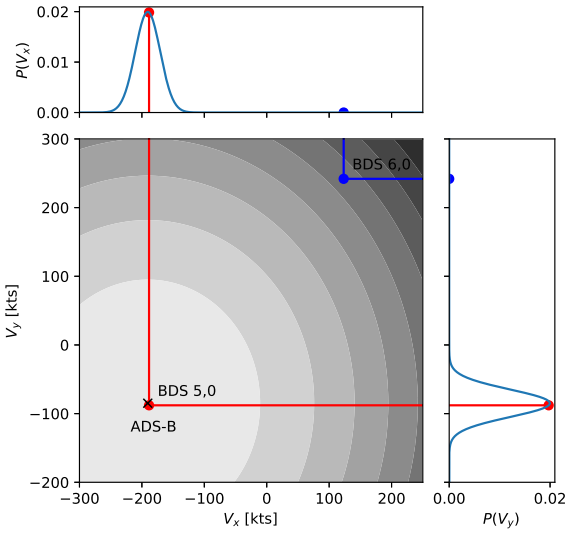

Figure 6.2: PDF of signal #1

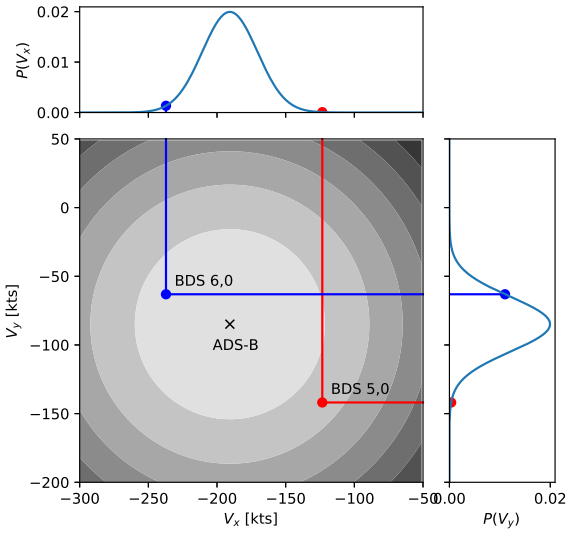

Figure 6.3: PDF of signal #2

Chapter 7

Conclusion

In this report, the research objective, the working principles of Mode A, Mode C and Mode S, atmospheric relations, how to derive meteorological parameters and a literature study are given. In the end, a start with processing Mode S EHS data is shown.

The research objective of this research is: using ADS-B and Mode S data to build accurate meteorological models and using these models to improve aircraft performance models. ADS-B and Mode S data can be obtained from aircraft in line-of-sight with a low-cost receiver by everyone.

Previously conducted research that used ADS-B and Mode S data to derive temperature and wind, showed that accurate meteorological derivations can be obtained when corrections are applied to Mode S data. In Mode S, the magnetic heading is included. This should be converted to true north with the magnetic declination at that location. However, the magnetic heading is obtained via a lookup table onboard. Therefore an additional aircraft specific correction should be applied for conversion to true north. Earlier research used runway heading and/or additional wind information to obtain these corrections.

To build accurate meteorological models, the parameters in Mode S should be accurate. However, transmission errors can occur. Mode S contains a check for transmission errors, but this requires the interrogated aircraft to be known. In the pre-processing phase, a method is developed to detect transmission errors. After omitting signals that contain transmission errors, a probabilistic method is used to determine the content of Mode S.

Bibliography

[1] International Civil Aviation Organization, *Manual of the Secondary Surveillance Radar (SSR) Systems*, Vol. ICAO 9684-AN/951/3, International Civil Aviation Organization, 2004.

[2] Airbus, "Global Market Forecast 2017-2036," `http://www.aircraft.airbus.com/market/global-market-forecast-2017-2036/`, Accessed: 27 Jun 2017.

[3] Boeing, "Traffic and market outlook," `http://www.boeing.com/commercial/market/long-term-market/traffic-and-market-outlook/`, Accessed: 27 Jun 2017.

[4] EUROCONTROL, "Aircraft Equipage Requirements in the European Commission IRs 1207/2011, 1028/2014 and 2017/386," `http://www.eurocontrol.int/spi-ir`, Accessed: 13 Sep 2017.

[5] Federal Aviation Administration, "ADS-B Frequently Asked Questions (FAQs)," `https://www.faa.gov/nextgen/programs/adsb/faq/#o2`, Accessed: 13 Sep 2017.

[6] Orlando, V. A., "The Mode S Beacon Radar System," *The Lincoln Laboratory Journal*, Vol. 2, No. 3, 1989, pp. 345–362.

[7] Schäfer, M., Strohmeier, M., Lenders, V., Martinovic, I., and Wilhelm, M., "Bringing up OpenSky: A large-scale ADS-B sensor network for research," *IPSN-14 Proceedings of the 13th International Symposium on Information Processing in Sensor Networks*, IEEE Press, April 2014, pp. 83–94.

[8] Legrand, K., Rabut, C., and Delahaye, D., "Wind and Temperature Networking Applied to Aircraft Trajectory Prediction," *7th International Conference for Research in Air Transportation*, 2016.

[9] Weitz, P., "Determination and visualization of uncertainties in 4D-trajectory prediction," *2013 Integrated Communications, Navigation and Surveillance Conference (ICNS)*, April 2013, pp. 1–9.

[10] Hoekstra, J. and Ellerbroek, J., "BlueSky ATC Simulator Project an Open Data and Open Source Approach," *7th International Conference on Research in Air Transportation (ICRAT)*, 2016.

[11] Gloudemans, T., *Aircraft Performance Parameter Estimation using Global ADS-B and Open Data*, Master's thesis, Delft University of Technology, 2016.

[12] Sun, J., Ellerbroek, J., and Hoekstra, J., "Modeling Aircraft Performance Parameters with Open ADS-B Data," *Twelfth USA/Europe Air Traffic Management Research and Development Seminar (ATM2017)*, 2017.

[13] Sun, J., Ellerbroek, J., and Hoekstra, J., "Large-Scale Flight Phase Identification from ADS-B Data Using Machine Learning Methods," *7th International Conference on Research in Air Transportation*, 2016.

[14] Sun, J., Ellerbroek, J., and Hoekstra, J., "Flight Phase Identification and Machine Learning for Mining ADS-B and Meteorological Data," Unpublished.

[15] Sun, J., Ellerbroek, J., and Hoekstra, J., "Modeling and Inferring Aircraft Takeoff Mass from Runway ADS-B Data," *7th International Conference on Research in Air Transportation*, 2016.

[16] Radartutorial, "Primary Surveillance Radar (PSR) vs. Secondary Surveillance Radar (SSR)," `http://www.radartutorial.eu/02.basics/PSR%20vs.%20SSR.en.html`, Accessed: 29 Jun 2017.

[17] International Civil Aviation Organization, *Mode S Interrogator Code (IC) allocations for the ICAO EUR region*, EUR DOC 024 Attachment, International Civil Aviation Organization, 1st ed., 2017.

[18] EUROCONTROL, "Principles of Mode S Operation and Interrogator Codes," Technical report, EUROCONTROL, 2003.

[19] International Civil Aviation Organization, *ICAO Annex 10: Aeronautical Telecommunications Volume III - Communication Systems*, Vol. ICAO Annex 10 Volume III, International Civil Aviation Organization, 2007.

[20] International Civil Aviation Organization, *Technical Provisions for Mode S Services and Extended Squitter*, Vol. ICAO 9871 AN464, International Civil Aviation Organization, 1st ed., 2008.

[21] Gertz, J., "Fundamentals of Mode S Parity Coding," Technical report ATC-117, Lincoln Laboratory, M.I.T., 04 1984.

[22] Kasami, T. and Matoba, S., "Some efficient shortened cyclic codes for burst-error correction," *IEEE Transactions on Information Theory*, Vol. 10, No. 3, 07 1964, pp. 252–253.

[23] Barrows, J., "DABS Downlink Coding," Technical report ATC-48, Lincoln Laboratory, M.I.T., 09 1975.

[24] International Civil Aviation Organization, *Manual of the ICAO standard atmosphere*, Vol. Doc 7488/3, ICAO, 3rd ed., 1993.

[25] Stone, E. K. and Kitchen, M., "Introducing an Approach for Extracting Temperature from Aircraft GNSS and Pressure Altitude Reports in ADS-B Messages," *Journal of Atmospheric and Oceanic Technology*, Vol. 32, No. 4, apr 2015, pp. 736–743.

[26] Tang, X., Chen, P., and Zhang, Y., "4D trajectory estimation based on nominal flight profile extraction and airway meteorological forecast revision," *Aerospace Science and Technology*, Vol. 45, 2015, pp. 387 – 397.

[27] González-Arribas, D., Soler Arnedo, M. F., and Sanjurjo Rivo, M., "Wind-Based Robust Trajectory Optimization using Meteorological Ensemble Probabilistic Forecasts," *Proceedings of SESAR Innovation Days 2016*, 2016.

[28] Assaad, Z., Moore, M., Bil, C., and Eberhard, A., "Aircraft Trajectory Optimisation using Wind Forecasting Data," *56th AIAA/ASCE/AHS/ASC Structures, Structural Dynamics, and Materials Conference*, 2015.

[29] IATA, "Operational Fuel Efficiency," `http://www.iata.org/whatwedo/ops-infra/Pages/fuel-efficiency.aspx`, Accessed: 06 Jul 2017.

[30] World Meteorological Organization, *Aircraft Meteorological Data Relay (AMDAR) Reference Manual*, World Meteorological Organization, 2003.

[31] Strajnar, B., "Validation of Mode-S Meteorological Routine Air Report aircraft observations," *Journal of Geophysical Research: Atmospheres*, Vol. 117, No. D23, Dec. 2012.

[32] de Haan, S., "High-resolution wind and temperature observations from aircraft tracked by Mode-S air traffic control radar," *Journal of Geophysical Research: Atmospheres*, Vol. 116, No. D10, 2011.

[33] de Haan, S., de Haij, M., and Sondij, J., "The use of a commercial ADS-B receiver to derive upper air wind and temperature observations from Mode-S EHS information in The Netherlands," Technical report, Royal Netherlands Meteorological Institute (KNMI), 2013.

[34] de Haan, S., "Quality assessment of high resolution wind and temperature observations from Mode-S: revised edition," Technical report, Royal Netherlands Meteorological Institute (KNMI), 2009.

[35] de Haan, S. and Stoffelen, A., "Assimilation of High-Resolution Mode-S Wind and Temperature Observations in a Regional NWP Model for Nowcasting Applications," *Weather and Forecasting*, Vol. 27, No. 4, 2012, pp. 918–937.

[36] de Haan, S., "An improved correction method for high quality wind and temperature observations derived from Mode-S EHS," Technical report, Royal Netherlands Meteorological Institute (KNMI), 2013.

[37] Mirza, A. K., Ballard, S. P., Dance, S. L., Maisey, P., Rooney, G. G., and Stone, E. K., "Comparison of aircraft-derived observations with in situ research aircraft measurements," *Quarterly Journal of the Royal Meteorological Society*, Vol. 142, No. 701, 2016, pp. 2949–2967.

[38] Hrastovec, M. and Solina, F., "Obtaining meteorological data from aircraft with Mode-S radars," *IEEE Aerospace and Electronic Systems Magazine*, Vol. 28, No. 12, Dec 2013, pp. 12–24.

[39] Strajnar, B. and Trojáková, A., "Analysis and preprocessing of Czech Mode-S observations," Technical report, Czech Hydrometeorological Institute, 2015.

[40] de Haan, S., "Availability and quality of Mode-S MRAR (BDS4.4) in the MUAC area: a first study," Technical report, Royal Netherlands Meteorological Institute (KNMI), 2014.

[41] Strajnar, B., Žagar, N., and Berre, L., "Impact of new aircraft observations Mode-S MRAR in a mesoscale NWP model," *Journal of Geophysical Research: Atmospheres*, Vol. 120, No. 9, 2015, pp. 3920–3938.

[42] Hollister, W. M., Bradford, E. R., and Welch., J. D., "Using aircraft radar tracks to estimate wind aloft," *The Lincoln Laboratory Journal*, Vol. 2, No. 3, 1989, pp. 555–565.

[43] Delahaye, D. and Puechmorel, S., "TAS and wind estimation from radar data," *2009 IEEE/AIAA 28th Digital Avionics Systems Conference*, Oct 2009, pp. 2.B.5–1–2.B.5–16.

[44] de Leege, A., van Paassen, M., and Mulder, M., "Using Automatic Dependent Surveillance-Broadcast for Meteorological Monitoring," *Journal of Aircraft*, Vol. 50, No. 1, Jan. 2013.

[45] Hurter, C., Alligier, R., Gianazza, D., Puechmorel, S., Andrienko, G., and Andrienko, N., "Wind parameters extraction from aircraft trajectories," *Computers, Environment and Urban Systems*, Vol. 47, 09 2014, pp. 28 – 43.

[46] Stone, E. K. and Pearce, G., "A Network of Mode-S Receivers for Routine Acquisition of Aircraft-Derived Meteorological Data," *Journal of Atmospheric and Oceanic Technology*, Vol. 33, No. 4, 04 2016, pp. 757–768.

[47] Grappel, R., Harris, G., Kozar, M., and Wiken, R., "Elementary Surveillance (ELS) and Enhanced Surveillance (EHS) Validation via Mode S Secondary Radar Surveillance," Tech. Rep. ATC-337, Lincoln Laboratory, M.I.T., 2008.

[48] Puntin, B., Billingsley, T., Heinz, V., Orlando, V., and Wiken, R., "Aircraft Derived Data Validation Algorithms," Technical report, Lincoln Laboratory, Massachusetts Instutute of Technology, 2012.

[49] Sun, J., Vû, H., Ellerbroek, J., and Hoekstra, J., "pyModeS: The Python Mode-S Decoder," Sept. 2017.

[50] International Civil Aviation Organization, *ICAO Annex 10: Aeronautical Telecommunications Volume IV - Surveillance and Collision Avoidance Systems*, Vol. ICAO Annex 10 Volume IV, International Civil Aviation Organization, 5th ed., July 2014.